MOMENT - RESISTANT CONNECTIONS IN PRECAST CONCRETE

by

Emile Langlois

A thesis submitted to the Faculty of Graduate Studies and Research in partial fulfilment of the requirements for the degree of Master Engineering.

Department of Civil Engineering
McGill University
Montreal.

July, 1968

ABSTRACT

MOMENT - RESISTANT CONNECTIONS IN PRECAST CONCRETE

Emile Langlois
Master Engineering — Department of Civil Engineering

Tests are performed on two commercially available column-to-base connection arrangements. The structural characteristics of both systems are presented in the form of moment-rotation curves. A method by which these connections can be used in a practical design problem is proposed.

One type of moment-resistant beam-to-column connection for precast concrete is developed and tested in the laboratory. The structural characteristics of three different sizes of prototypes using the same arrangement are presented in the form of moment-rotation curves. The applicability to design of these connections is outlined through a brief theoretical study.

ACKNOWLEDGEMENTS

The author wishes to express his gratitude to: Joseph Nemec Jr., Assistant Professor of Civil Engineering, McGill University, under whose supervision this work was carried out.

A. A. Gyimesi, Chief Engineer, Francon of Canada Limited who gave valuable advice in the detailing of the connections.

B. Cockayne and his technical staff, for their consistent assistance throughout the experimental work.

Francon of Canada Limited who kindly supplied the concrete.

The financial assistance of the Technical Activities Committee on Research of the Canadian Prestressed Concrete Institute is gratefully acknowledged.

TABLE OF CONTENTS

Page

Page

CHAPTER I - INTRODUCTION

1.1 - Introduction

For the past few years, the North American industry of precast concrete has accomplished a great step forward. Especially in Canada, due to its climate, the use of prefabricated units has spread widely. This rather sudden expansion is explained by the fact that the choice of prefabricated reinforced concrete members as the structural material results in appreciable economy in certain types of buildings.

Along with the spread of a building material through the spheres of construction, design procedures and erection techniques pertaining to this material must be developed simultaneously, in order to insure safe and economical structures.

One of the most intricate and most difficult problems arising in both design and construction of precast concrete is the joining up of the elements. Until now the development of connections has been carried out by engineers and contractors in many countries strictly to meet the needs of a particular structure. This development work included a few tests, usually designed to check the adequacy of a specific arrangement subjected to a particular system of forces. But now that the precast concrete industry is undergoing expansion, more precise design standards must be established. It is recognized that only a systematic study of the most common types of connections

can provide the exhaustive test data needed to develop general design methods.

In precast reinforced concrete frames, the structural behavior depends largely on techniques of joining the individual members. On this continent, until recently, the joints used have been of a simple type, providing little or no other continuity than that developed by bond and friction. The evidence of catastrophic failures of structures exhibited in the earthquake in Anchorage[1] points out the clear need for moment rigid connections.

1.2 - Purpose of Investigation

A research program was initiated at McGill University during the summer of 1967 to deal with the problems pertaining to the development of various moment-resistant connections between precast concrete members. The objects of this study are to 1: - Investigate the moment-resistant properties of some commercially available column-to-base connections. 2: - Design a suitable moment-resistant beam-to-column connection and study its structural characteristics, by means of a laboratory study.

Two different column-to-base and five beam-to-column full-scale prototypes are tested to failure. The fixity properties of all the arrangements are presented in the form of moment-rotation curves. A comparison of the actual moment transmitted through the connection with the ultimate resisting moment of the connected member is also given.

CHAPTER II - PREVIOUS WORK

While numerous studies on semi-rigid connections in steel have been reported in the past, the literature survey on precast concrete joints yields few papers.

Eberbach[2] reports on results of testing square (6"x6") columns where the steel base plate thickness is used as test variable. Lafraugh and Magura[3] report on an extensive laboratory study of base plate connections of various types. Among the variables tested are the sizes and thicknesses of steel base plates, diameters of the anchor bolts and the ratio of M/P. Birkeland and Birkeland[4] discuss the design and use of the "knife connection" in the Washington State University dormitories. This type of joint consist essentially of one embedded steel plate protruding from the end of the beam and of two similar plates projecting out of the column. The beam blade slides between the two plates which form the column sheath and are tightened together by means of bolts. No test data is reported.

Holmes and Bond[5] present a laboratory study on the structural behavior of six concrete columns where load is applied through a vertically embedded steel plate. They were able to predict the load which cause tensile cracking of the column, by analogy with the Brazilian test of concrete cylinders.

In response to the need expressed by the members of the Prestressed Concrete Institute regarding studies in the area of

connections, a special Technical Committee on joints was initiated in January 1961. A comprehensive list of the most common connections in precast-prestressed concrete was collected and published as "Connections Details for Precast - Prestressed Concrete Buildings".[6] The details, applicable to buildings only are divided into four categories as follows: column-base, beam-to-column, beam-to-girders and bearing wall. However, no report on the actual testing of any of these connections is given.

The ACI - ASCE committee 512 gives suggestions for the design of connections between precast concrete members in: "Suggested Design of Joints and Connections in Precast Structural Concrete".[7] The report presents methods by which joints in precast concrete construction may be designed. No test data is given. Connection details most common in current Canadian practice are compiled in the "CPCI Handbook".[8] Characteristics of each connection are described and design guidelines are presented. No experimental data is presented.

This survey points out the scarcity of test data on moment-resistant connections in precast structural concrete. In an effort to participate to the development of this field, the present work aims at providing some experimental information on the structural behavior of some moment-rigid joint prototypes.

CHAPTER III - SCOPE OF WORK

3.1 - Requirements of Connection Design

The design of connections in precast concrete is usually based on the following desirable requirements:

a) Ease of fabrication and minimizing of total erection costs; (labour and equipment).

b) Economy of material.

c) Satisfaction of specified dimensional tolerances.

d) Speed of erection.

e) Elimination of cast-in-place concrete such that heated enclosures are omitted, during winter concreting.

Many precast concrete manufacturers believe that there is generally little or no appreciable saving of materials involved in precasting reinforced concrete beams and columns; any profit obtainable must therefore be realized on the formwork and labour; precasting is justified when the overall cost of casting, transportation, erection and joining is less than the cost of casting the members in place or where the time factor is considered as being the major consideration. In the light of these requirements, a few types of connections in precast reinforced concrete will be studied.

3.2 - Types of Connections Studied

a) Column-to-base

i) Fixity at the base

In commercial and residential buildings, partitions and exterior walls are frequently omitted in the first story to permit

an open ground floor for parking and other facilities. A somewhat similar situation arises in industrial buildings or in buildings of considerable length where in general no interior cross walls or bracing are feasible. In such circumstances the problem of lateral stability becomes predominant.

One currently used way of overcoming this difficulty is to fix the columns to their foundations such that they will resist the overturning moments produced by the lateral loads.

There exists many column-to-base joint arrangements capable of transferring moments. Types that require site concreting or bolting are used, depending on various local conditions. The "pocket type" connection, which requires cast-in-place concrete has been successfully used in the past and is mostly suitable for mild weather conditions. However when concreting has to be carried out during winter, as is currently done in Canada, the elimination of cast-in-place concrete and of heated enclosures is preferred. This requirement is easily met by using a bolted connection. Further advantages offered by this arrangement are reasonably low labor costs, economy of material, speed of erection and an unrestricted usability. PLACING is greatly facilitated by means of levelling nuts similar to those often used in steel construction. Grouting at the base, if necessary, may be postponed to summer time.

ii) Description of the connections

The connections studied in this thesis have been obtained from Francon of Canada Limited; they represent two of the types used

by this firm. The column is designed as part of a single story multi-bay industrial building following the ACI[9] and NBC[10] code recommendations. The connectors at the base are dimensioned so as to resist the stresses produced by an eccentrically applied ultimate load of 165 Kips.

The two connections differ in the arrangement of the base. Type I, shown in Figure 1, has cast-in hardware at the four corners. Each corner bar is welded to its respective box. The column is fastened to the base by anchor bolts projecting into the cross sectional area of the column. The hardware openings are then grouted to obtain a smooth surface. Type II, shown in Figure 2, has hardware in the form of brackets, projecting outwards. Each bracket is welded to an anchor bar and the whole arrangement is embedded in the corner of the column, as shown in Figure 2. Details of the reinforcement and of the base hardware embedment are presented in Figures 3, 4 and 5.

b) Beam-to-column

i) Reasons for rigid connections

While various moment-resistant column-base systems are commercially available, there exist few arrangements for beam-to-column that offer the characteristics of moment transfer capability. A survey carried among the local precast concrete fabricators in the Montreal area revealed that presently there exist only a few practical ways of

connecting beams and columns such that reasonable continuity is achieved. Both the PCI booklet on connection details[6] and the CPCI Handbook[8] present a collection of joint arrangements which can suit a variety of needs. Types most currently used in single and multi-story buildings are fully described. The designer dealing with a connection problem refers to either publications and selects the arrangement that suits his situation. In most joint arrangements, however, shoring of the beams and cast-in-place concrete have to be used. The elimination of these two costly operations motivates on the search for better arrangements.

On the whole, the increasing demand for precast reinforced concrete in the metropolitan surroundings and the fulfilment of various design requirements accentuate the need for more rational joining systems between beams and columns. Moreover, the fact that Montreal is classified in the most highly rated earthquake intensity zone (No. 3) clearly justifies the importance of obtaining moment-resisting connections.

The scarcity of information pertaining to this field has convinced the concrete research team of McGill University to concentrate their efforts on the development and study of some typical beam-to-column joint arrangements.

ii) Description of the connection

Past experience has shown that among the afore-mentioned requirements relating to connections in precast concrete, ease of

erection and structural continuity are the two chief conflicting requirements of the joints between beams and columns. Furthermore, it is often desired that continuity be achieved without recourse to cast-in-place concrete so as to eliminate the need for heated enclosures during the winter.

The crane time is the controlling item when estimating the erection cost. Therefore the connection must be such as to permit the crane to be freed immediately after the beam is placed. This requirement is met by providing steel angles cast into the column. The angles act as erection seats for the beams. The stability during erection is provided by bolts which do not have any influence on the strength of the connection. Once the beam has been set on the seat angles and the bolts tightened, the crane is freed and can proceed further. Continuity without recourse to cast-in-place concrete is obtained by site welding. Fixity on the tension side is made possible by site welding a loose plate to hardware embedded in the beam and in the face of the column. In the compression zone, the connection is fastened by site welding together the plate cast in the beam and the erection angle in the column. This summary description of the outside part of the connection is detailed on Figure 6.

iii) Internal arrangement

The internal anchoring device at the connection must be proportioned and arranged such that it can resist the loads transferred

by the outside hardware. Type B-C1a, which was first tested, had bars welded to the anchor plates and extending longitudinally in the section of the beam. The laboratory investigation revealed that the internal arrangement was insufficient and therefore was subsequently modified until testing showed that an adequate anchoring system had been obtained; a satisfactory design was achieved after the third trial, with prototype B-C1c. The successive modifications of the connection arrangements are illustrated in Figures 7 - 13.

At the same time, a brief study was made to examine the adverse effects brought about by the welding.

iv) Problems of welding

In the light of previous work on the damage due to welding of precast concrete units[11,12] an investigation was carried on three cubes with cast-in steel plates. Each cube was subjected to various degrees of welding exposure. Ultrasonic pulse tests were then performed on each, in order to detect any structural damage due to the heat developed by the welding. The results obtained indicated that no harmful cracks developed in the specimens and that the structural properties of the concrete were for all practical purposes, unaltered. This study is detailed in Appendix C.

Within the welding test program, tensile tests were conducted on a number of No. 6 deformed reinforcing bars subjected to variable exposures of welding. The results showed that the welded bars had an

ultimate strain equal to approximately 65% of the plain ones. No apparent differences between the yield or ultimate stresses were noticed. Stress-strain curves and structural properties of the specimens are presented in Appendix D.

This concluded the first step of the beam-to-column connection investigation program. Attention was now turned to the study of the other possible arrangements.

v) Alternate possibility

Having obtained a suitable arrangement where welding is the means through which continuity is achieved, efforts were oriented towards the development of a system where bolts could be used as fasteners. A thorough study of this alternate system was performed and many possible arrangements were discussed. For instance it was intended to maintain the dimensions of the sections unchanged; it was hoped that a suitable connection using bolts could be obtained and an interesting comparison between the two different arrangements be established. However the use of bolts as fasteners in connections between such prismatic members present serious problems; finally this approach was shown to be impractical and was then rejected for the following reasons:

a) First, as the dimensions of the sections were unchanged, it was found that the distance between the vertical face of beam to the edge of the column was too small to allow the elements to be

connected by bolts according to the specifications of the Canadian Standards Association[13] relating to edge distances for fasteners. Furthermore, even the minimum distance provided would not allow the impact wrench to firmly grip the head of the bolt.

b) Second, the loads acting at the connection had to be resisted by a number of 1" diameter bolts which extended beyond the leg of the seat angle.

c) Third, the face of the column which lies on the tension side of the connection has to be free of projecting hardware such that the beam may be inserted freely.

This study points out the practical impossibility of using bolts as fasteners in beam-to-column connections. In the light of this it was decided that the same arrangement, using welds, be investigated for smaller loads. Two more prototypes, BC-2 and BC-3 were designed and tested. The description and the design details are presented in Figures 14 to 19.

The experimental setup and instrumentation used are now discussed in detail.

CHAPTER IV - EXPERIMENTAL WORK

4.1 Column-to-Base Connection

a) Design and Fabrication of Test Specimen

The column was designed as a typical interior compression member of a standard 40'-0" x 40'-0" (each way) building frame. A 15 inch x 12 inch section reinforced with four No. 10 bars was selected. To accomodate the clearance of the testing machine, an overall height of 4'-0" was chosen. The configuration of a typical test specimen is shown in Figures 1, 2 and 3. The corbel bracket through which load was applied was similar for both specimens. Its design was based upon the findings of another study.[14] The main reinforcement was identical for both specimens. The hardware characterizing the base was designed such that it resists the stresses produced by the ultimate eccentric load acting on the column. Design recommendations of the ACI[9] and NBC[10] codes were followed.

The two prototypes were fabricated at the Francon precast concrete factory, using the following material specifications:

i) Concrete

Normal Type I Portland cement.

f'_c = 4500 psi at 28 days.

Maximum size aggregates = 3/4 inch.

Slump = 4 to 5 inches.

ii) Reinforcing steel

Deformed Intermediate Grade.

$f_y \geq 50000$ psi (nominal).

The two specimens were cast in steel forms and cured under a plastic cover for three days. They were then stored in a moist room for twenty days after which they were delivered to the structural laboratory.

b) Assembly of connections

Foundations for the two specimens consisted in two sections of standard beams connected together as shown on Figures 4 and 5. Due to the high load applied, the webs were stiffened in the fashion indicated. Each anchor bolt was then welded along one stiffening plate throughout the depth of the web. After the bolts were welded on, the two beams were aligned and attached together.

The columns were then set over the anchor bolts and were plumbed by adjusting the levelling nuts. The nuts on the anchor bolts inside the steel pockets were tightened such as to firmly attach the column to the beam support. A non-shrink grout was used as a bearing pad between the bed plate and the base of the column. This commercially available grout (brand name: Embeco) completely filled the space between the footing and the column base. At the same time, the recesses in type I were filled with the same mix in order to obtain a smooth surface. The pad was cured for at least four days prior to testing.

Compression test carried on three 3" x 6" grout cylinders at the day of testing showed that the desired f'_c (5000 psi) was obtained.

c) Instrumentation and test setup

Two SR-4 electrical strain gages were glued on the bolts of the tension side in order to have a continuous record of their elongation. This attempt was unsuccessful due to the deterioration of the gages. It is believed that the grouting operation, although performed with meticulous care, has damaged most of strain gages and rendered them inoperative, even though these were waterproofed.

Horizontal displacements of the specimens were measured at four locations on the tension side of the column by dial gages that had readings of 1/1000 inch. Gages No. 1 and No. 2, respectively situated at 4 inches and 24 inches from the column top gave a continuous record of the deflected shape of the column, under increasing load. Gages No. 3 and No. 4 both situated at 8 inches from the grout pad recorded the deflections used to compute the rotations of the connection. Gage No. 5 indicated any vertical movement of the supporting beams while No. 6 detected any transversal deflections. A typical arrangement of the dial gages is shown in Figure 20.

It was also of interest to know how the hardware would deform under increasing loads. Type 1 was provided with reference points on each of the upper and lower plates forming the pocket; readings were recorded from these punchmarks by means of spacers, at

every load increment. For type II, typical with its projecting brackets, no other information than the moment-rotation characteristics were obtained.

d) Test Procedure

A typical test setup is shown in Figure 33. The specimen is located directly beneath the Baldwin-Lima hydraulic testing machine and is accurately positioned so as to get the proper eccentricity. In order to prevent restraint of the column by the loading head of the press, a 4 inches roller-plate was placed between the head and a 2 inch x 1 inch flat resting on the corbel.

Prior to any application of load, all dial gages were zeroed. Subsequent application and removal of a 4 kips load was exerted on the specimen after which all the gages were set back to initial reading. Load was then applied in increments of 10 kips up to failure. At each increment, the press maintained the load while data was collected. During that constant load interval, all readings were recorded and cracks, if any, were located.

In both cases the column failed at a load greater than the ultimate design value of 165 kips. The failure mode was one of direct shear of the corbel, accompanied by severe deterioration of the connection hardware.

4.2 Beam-to-Column Connection

a) Design and Fabrication of Test Specimen

In this case the loads used for the design of the elements

were computed from a typical interior panel of a hotel floor. The span of the beams were 25 feet 0 inches, and the distance center to center of beams is 18 feet 0 inches. The calculated total ultimate load of 4.48 kips per linear foot acting on the beam developed a maximum negative moment of 200 kips.ft. and a maximum shear force of 50 kips. Using a maximum steel ratio of $0.18 \frac{f'_c}{f_y}$ and with the aid of design graphs, a 12 in. x 18.5 in. beam effective section reinforced in tension with 4 No. 8 bars was selected. To support the loads transmitted by the beams at the story considered, a 16 in. x 16 in. column section reinforced with 8 No. 8 was found to be adequate. After the dimensioning of the pieces was completed, the design of the connecting elements was initiated.

The proportioning of the connecting pieces and the design of welds were achieved by using the current methods of structural steel design. The latest specifications of the Canadian Standards Association[13] were followed. Finally the tensile and compressive forces induced by the moment at the connection were transmitted from the connecting shapes through welds into the anchor bars embedded longitudinally in the beam. These anchor bars were designed to resist both tension and bond, according to the ACI code[9] recommendations. Having completed the design of the elements and the dimensioning of the various connecting pieces of this first prototype, B-Cla, drawings were issued for fabrication. Figures 6 to 11 detail the various components and show the typical dimensions of

this first series of specimens. As it was mentioned earlier, the first experimental results indicated that further tests were required in order to improve the original design. The early development of cracks followed by premature failure of the right beam lead to the significant modifications noticed in the second model, prototype B-C1b. Test results obtained from this second test revealed that more representative figures should be obtained. Finally, with few minor design modifications, prototype B-C1c was fabricated and tested. Figures 12 and 13 illustrate the modified arrangements of prototypes B-C1b and B-C1c. The moment-rotation curve obtained for the third specimen shows that a satisfactory arrangement had been obtained and further studies on other prototypes were planned. Two additional prototypes using the same welded arrangement but designed to resist smaller loads were tested. Prototype B-C2 was proportioned to resist an ultimate bending moment of 100 k-ft. and a shear force of 25 kips. Prototype B-C3 had an ultimate moment transfer capacity of 50 k-ft. and could resist a shear force of 12.5 kips; Both prototypes are described in detail on Figures 14 to 19.

It is worth mentioning that the same column stub was used for the testing of the first three specimens, B-C1a, B-C1b and B-C1c. None of the connecting parts were seriously damaged throughout this series of test; it can therefore be said that the connection arrangement in the column adequately transferred the

ultimate design load. A column stub having the same dimensions and hardware arrangement was used for connection B-C2; in this case, however, no stiffener was provided for the seat angle. Prototype B-C3 used a column with the same connection arrangement but was of a smaller scale. In brief, none of the three column stubs underwent serious deterioration under the applied loads. From a practical standpoint, the hardware arrangement in the column was fully satisfactory.

The concrete used in all beams and columns was made with type III Portland Cement and 3/4 inch maximum size aggregate. The steel specifications were the same as for the column-base specimens. Prototype B-C1a was entirely fabricated in the structural laboratory, while the steel cages and the various hardware components for the remaining four were ordered from a local welding shop. All test specimens were cast in plywood forms and cured under a polyethylene sheet for a period of 6 to 7 days, after which they were removed for assembly.

b) Assembly of connections

The column stub was set in a vertical position and the beams were positioned on the erection seats. After the beams were properly aligned the erection bolts were tightened and the welding performed. The fastening operation being completed, the specimen could then be turned over in the testing position and hauled under the hydraulic press where the instrumentation was performed.

c) Instrumentation and test setup

i) Level Bars

Three identical level bars were used for measuring the deflections of the specimen under load. Each one consisted of a 6 inch vial level mounted on an aluminum channel 20 inches long. They were designed so that 1/1000 inch mechanical dial gages could be attached to one end, while the other end was the fixed point about which this 20 inch channel rotated. These level bars were fixed to the column stub and on the center line of the beam in the position shown on Figure 21. From the measured deflections, rotation of the beams relative to the column stub were computed to obtain moment-rotation curves.

ii) Dial Gages

Mechanical type dial gages were mounted on the center line of the beams with the plunger of the dials in contact with the column face (Dial Gages 4, 5, 6 and 7, Figure 21). The readings from these gages were also used to obtain the rotation of the beams relative to the column. Gage No. 8 was used to detect any lateral movement that may have occurred. Continuous record of the vertical deflection was obtained with DCDT's and a 320 Dual Channel Recorder coupled with a Harrison DC Power Supply (Hewlett-Packard Co., Serial No. 6204B).

d) Test procedure

A typical Assembly ready for testing is shown in Figure 38 (A). The specimen is directly located beneath the hydraulic Testing Machine with the beam supports placed at 45 inches from the face of the column stub. This arrangement induces shear and moment at the connection when load is applied to the column.

An initial load of 4 kips was applied and maintained on the specimen for about 15 seconds. It was then removed and all the gages were zeroed. The DCDT Recorder was reset to initial position and the first load increment was applied.

Loading of specimen B-C1a was done by increments of 2 kips up to a load of 30 kips. Beyond that value, 4 kips increments were applied. Failure was recorded at a load of 70.7 kips. Prototypes B-C1b and B-C1c were loaded with 4 kips increments up to failure. A maximum load of 100 kips was attained for B-C1b while specimen B-C1c failed a value of 120 kips. For the two smaller scale prototypes, B-C2 and B-C3, load increments of 2 kips were applied throughout. The recorded failure loads were respectively of 52.2 kips and 25 kips. In all cases the same reading procedure was followed: After the application of each load, the level bars were levelled and the values of the mechanical gages were recorded. Visual inspection of the various components of the connection was promptly carried out and cracks, if any, were marked.

Characteristic moment-rotation curves and collapse mode of each specimen are described in detail in the following chapters.

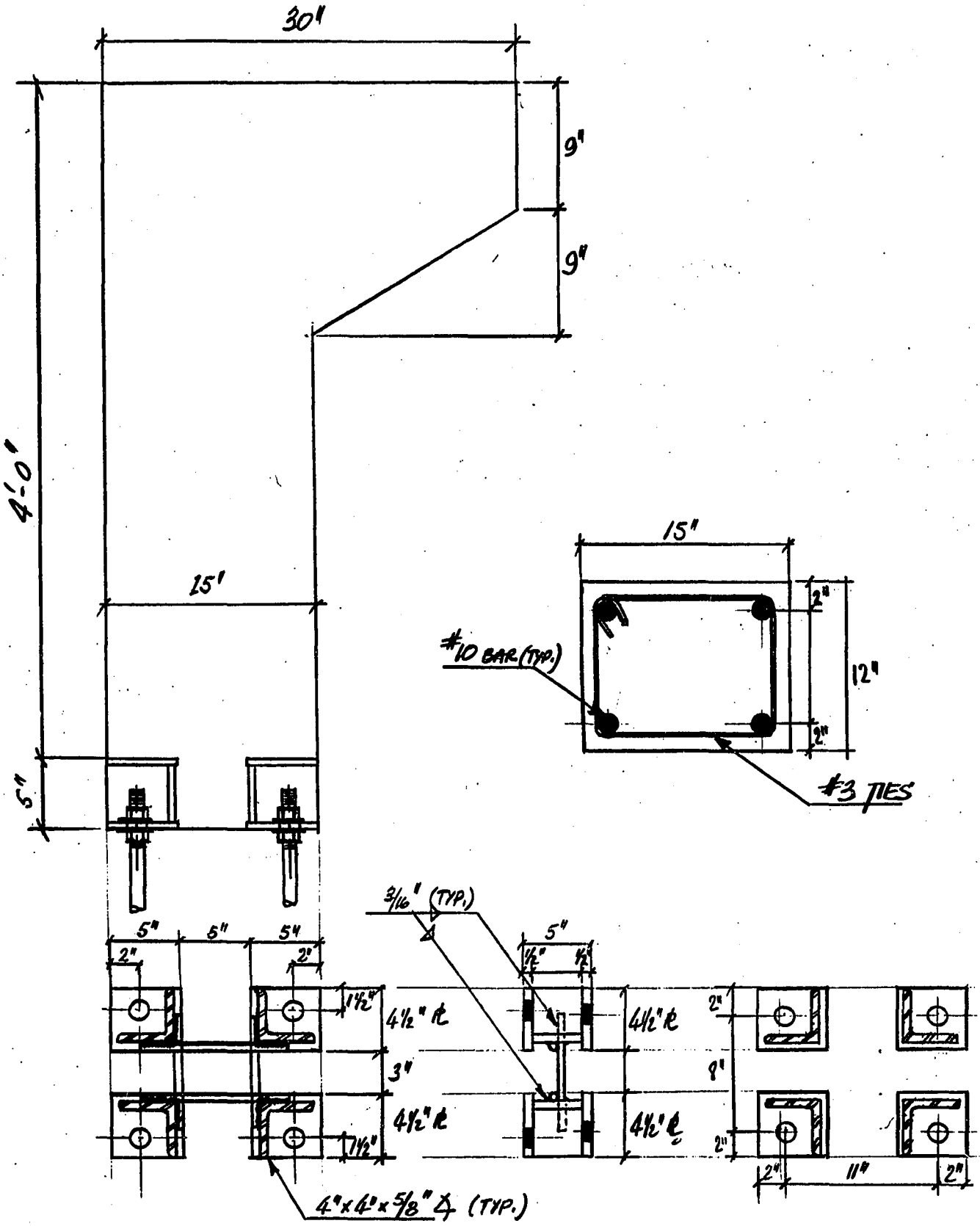

FIGURE 1. Column - base connection, Type I

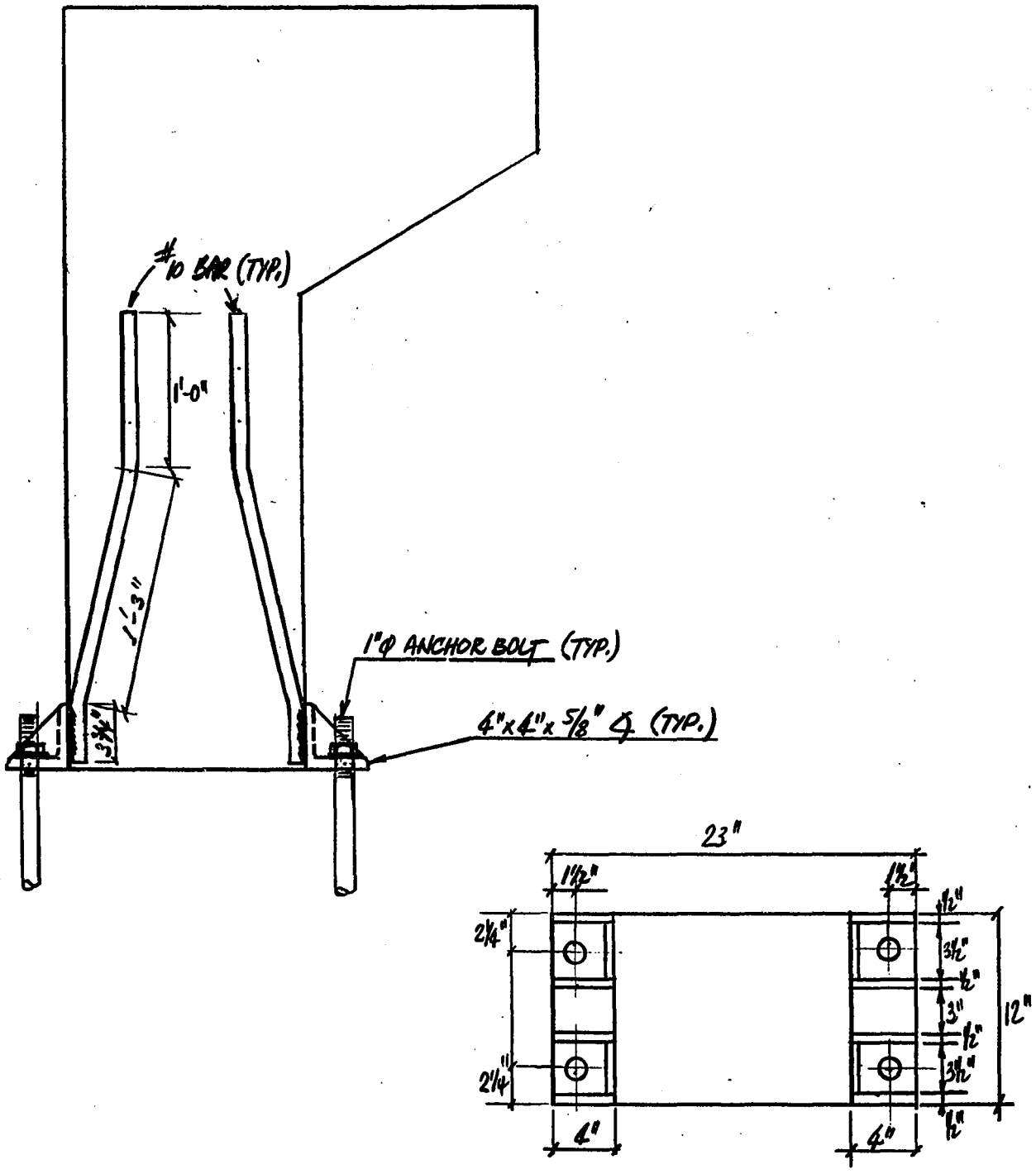

FIGURE 2. Column-base connection, Type II

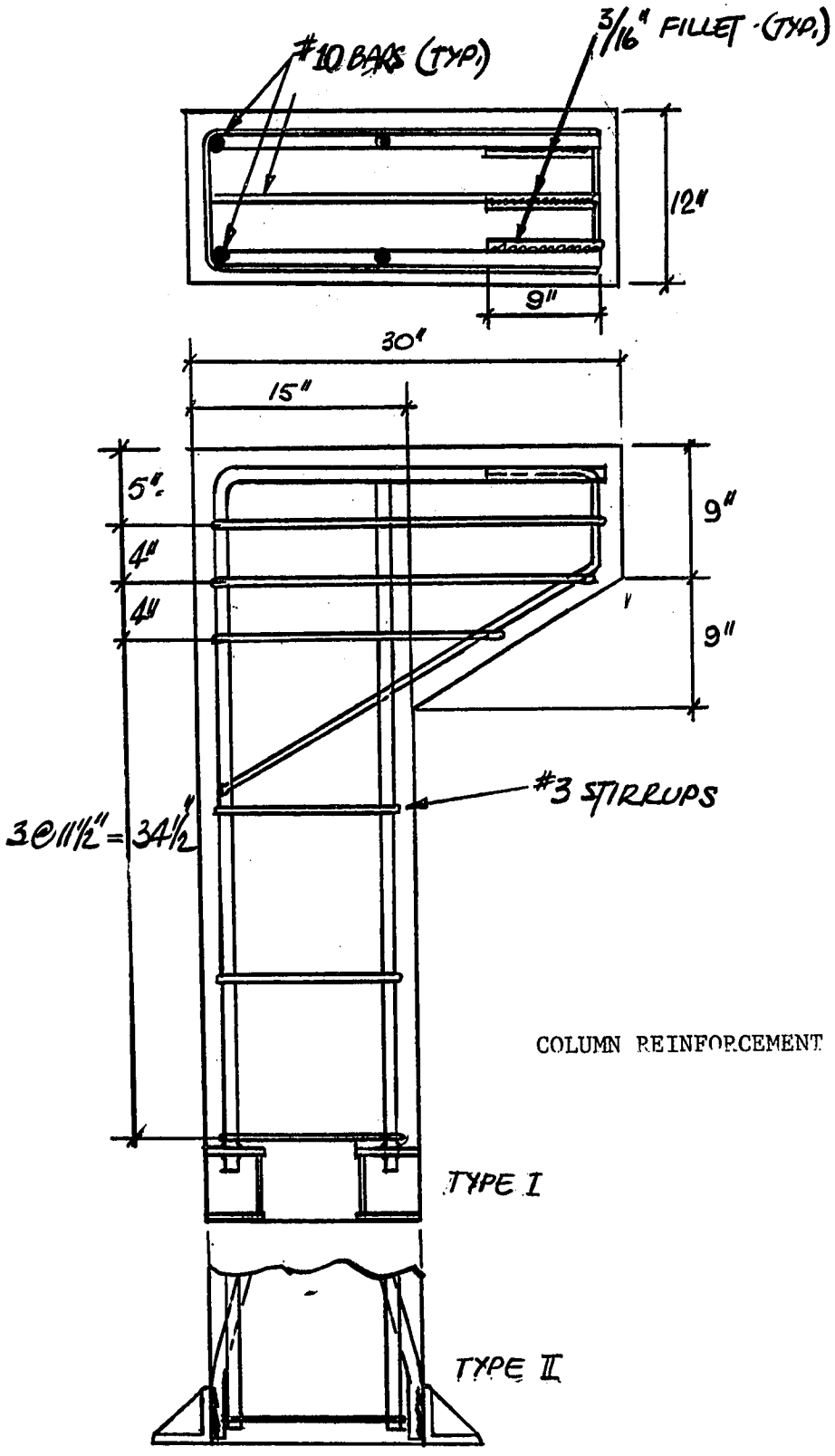

FIGURE 3. -- COLUMN-TO-BASE CONNECTION

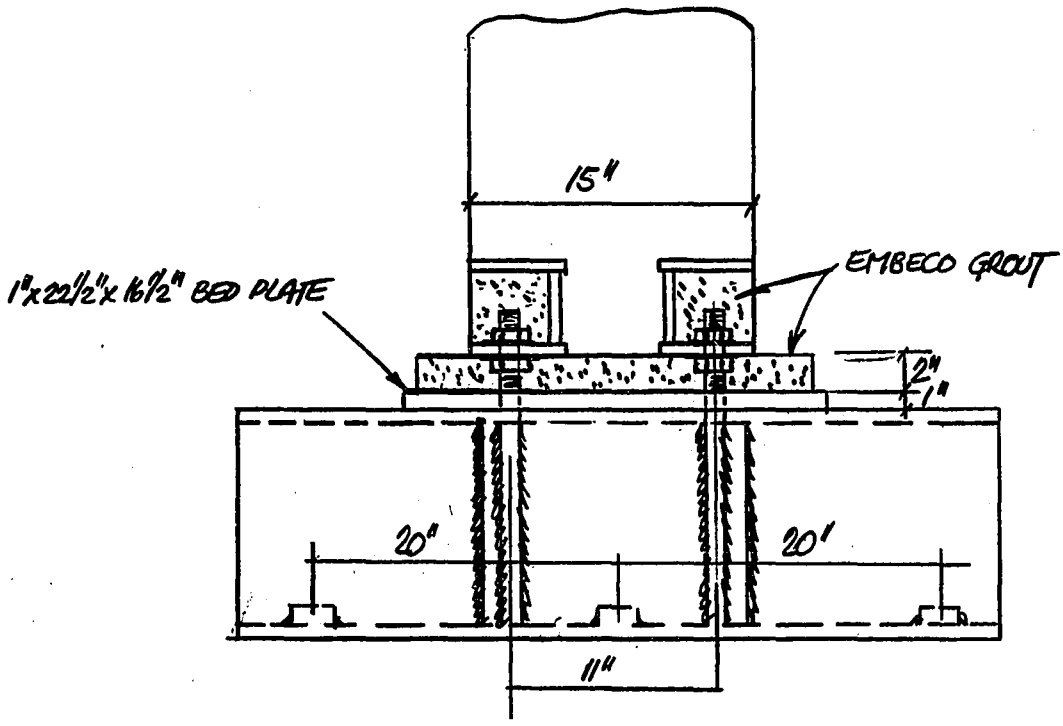

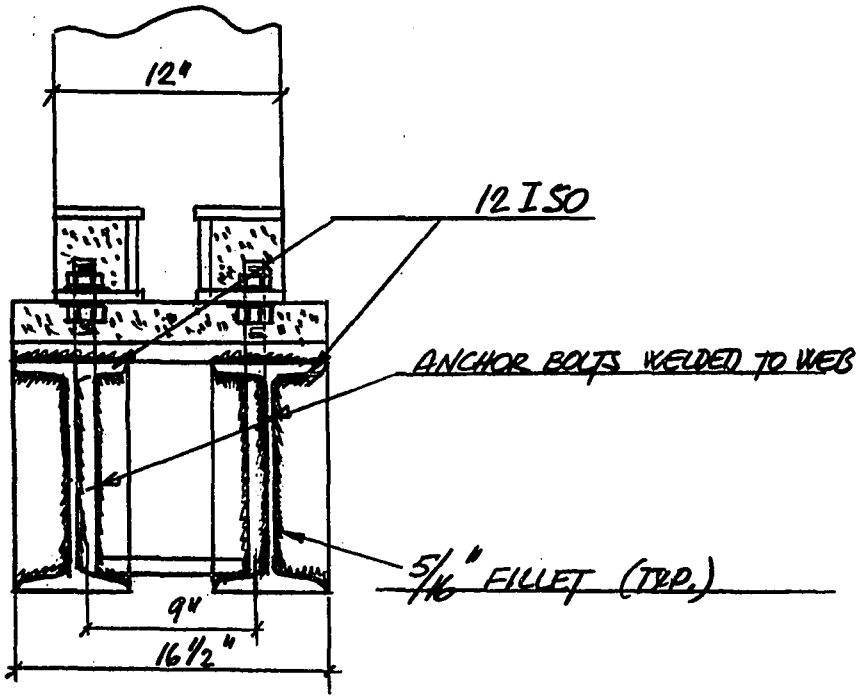

FIGURE 4. - Support arrangment - Type I

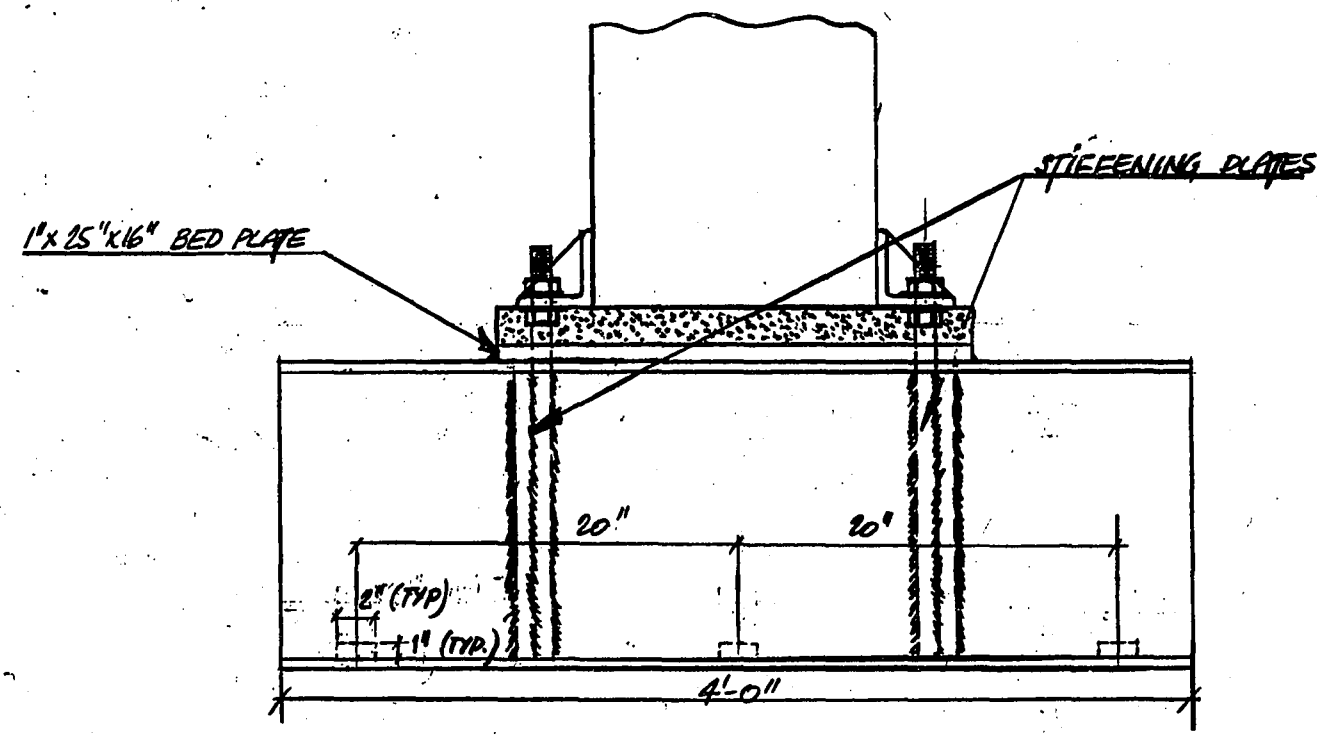

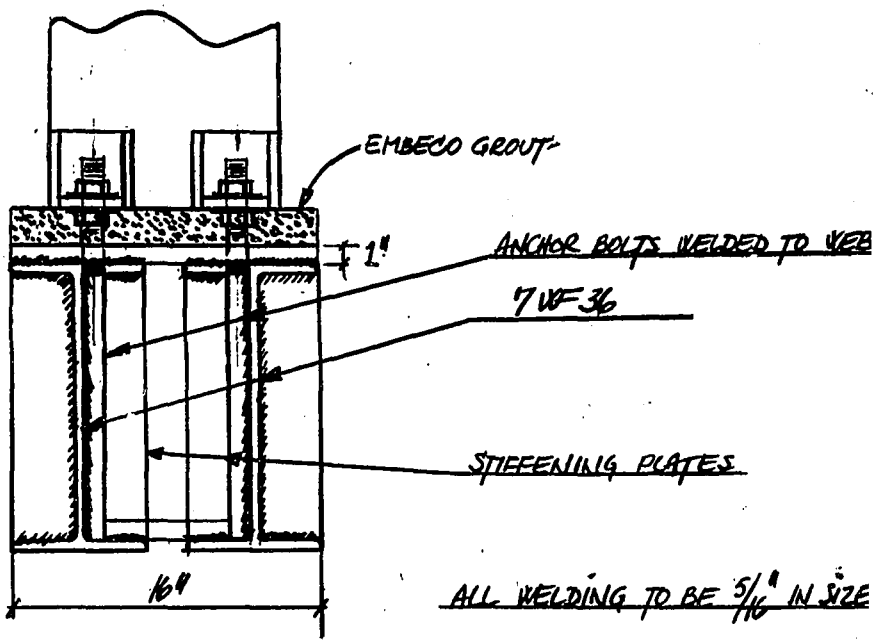

FIGURE 5. - Support arrangment - Type II

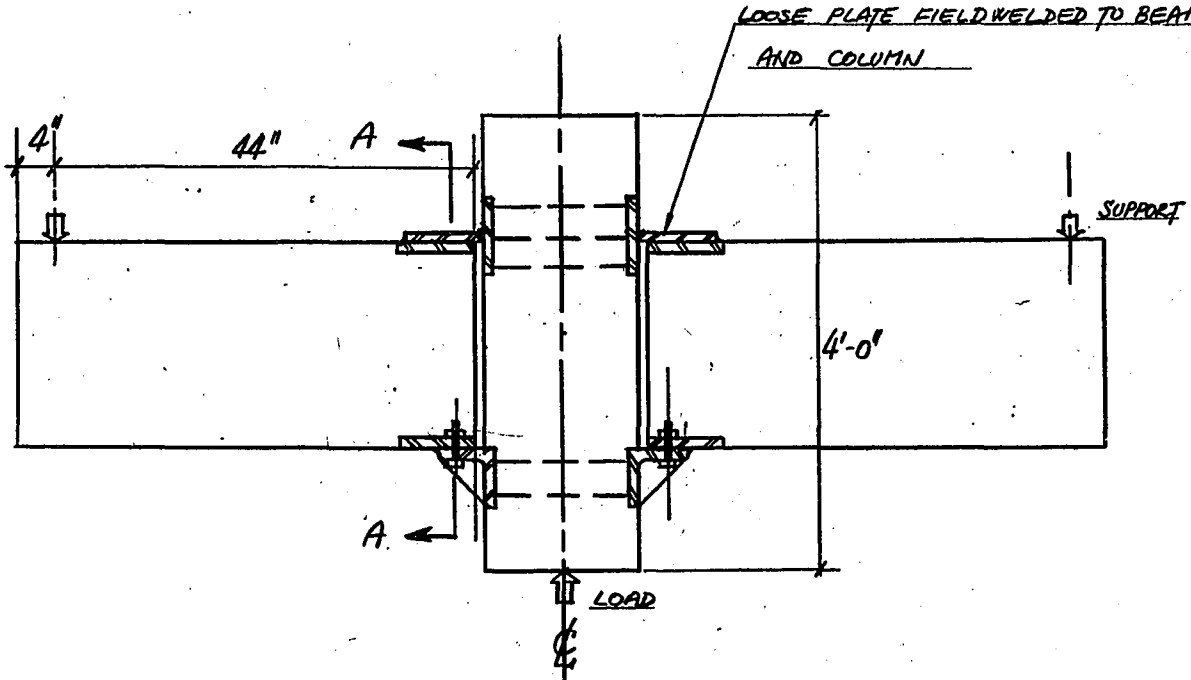

EXTERNAL ARRANGEMENT OF BEAM-COLUMN CONNECTION

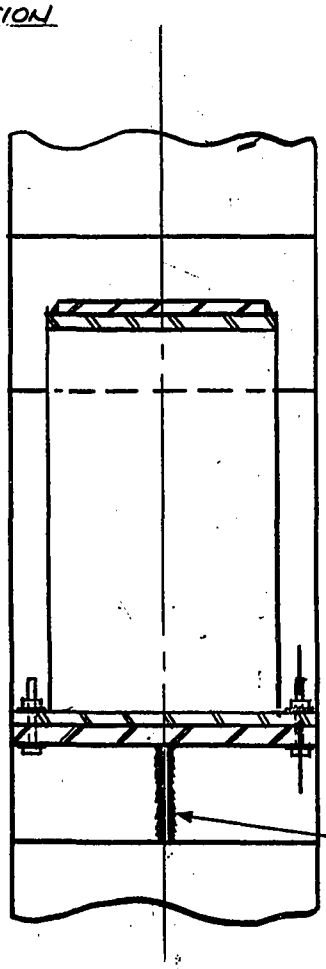

SECTION A-A

ALL DIMENSIONS ARE VARIABL

FIGURE 6

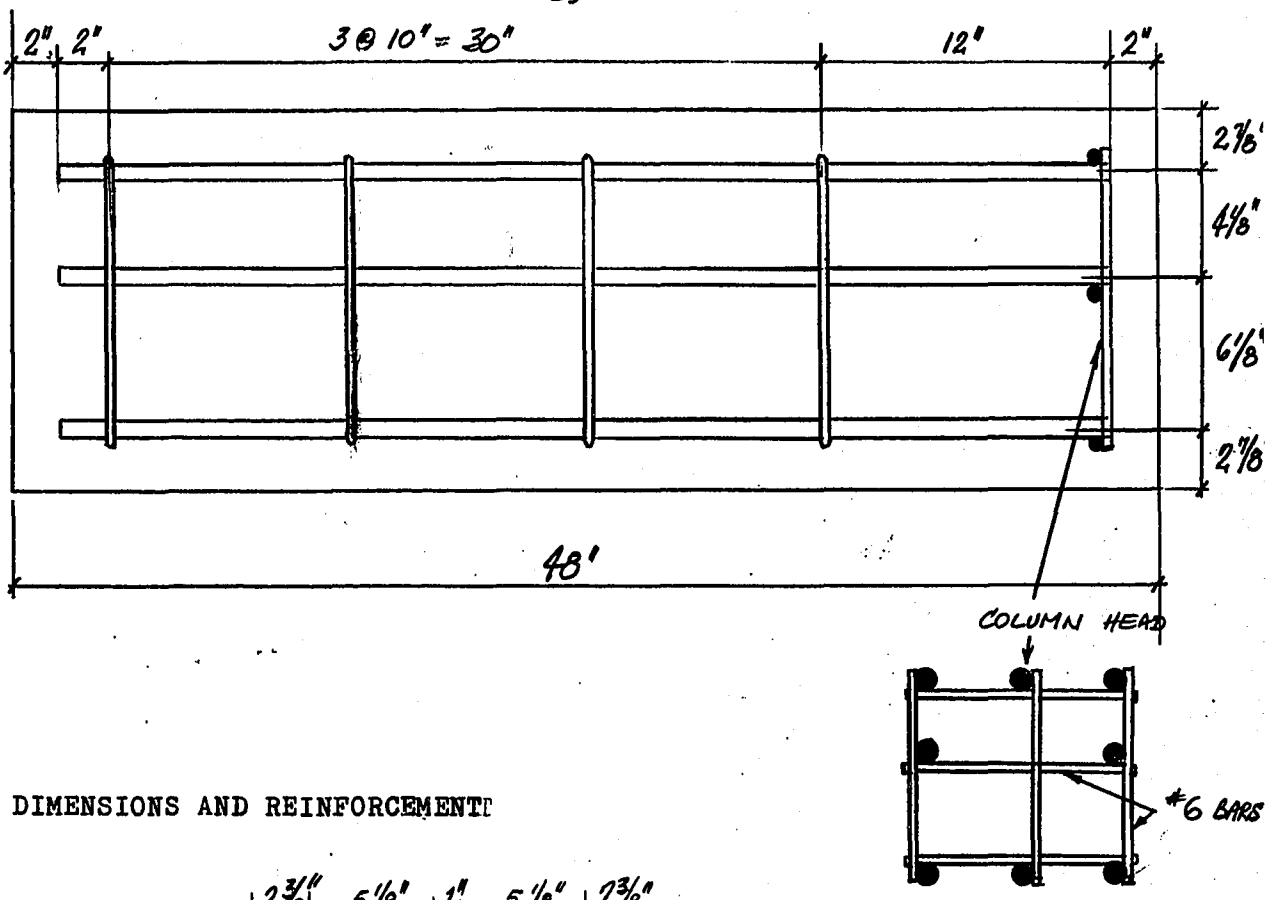

DIMENSIONS AND REINFORCEMENT

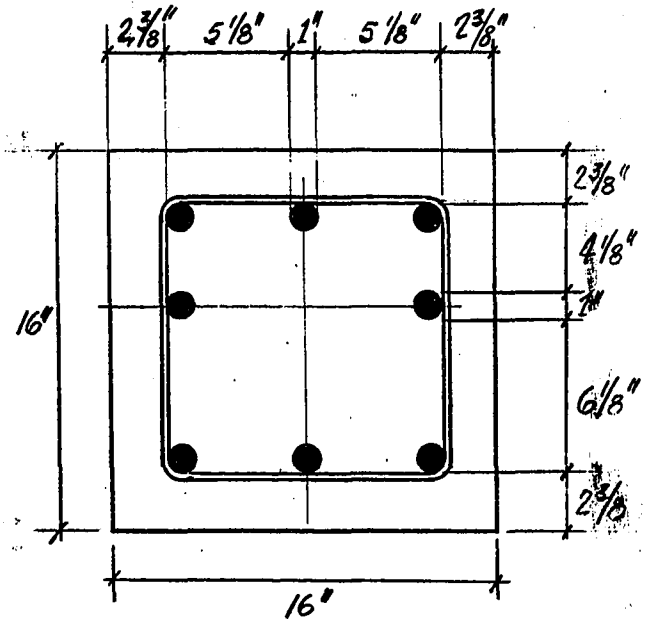

FIGURE 7. - PROTOTYPES B-C1a, B-C1b, B-C1c, B-C2 COLUMN

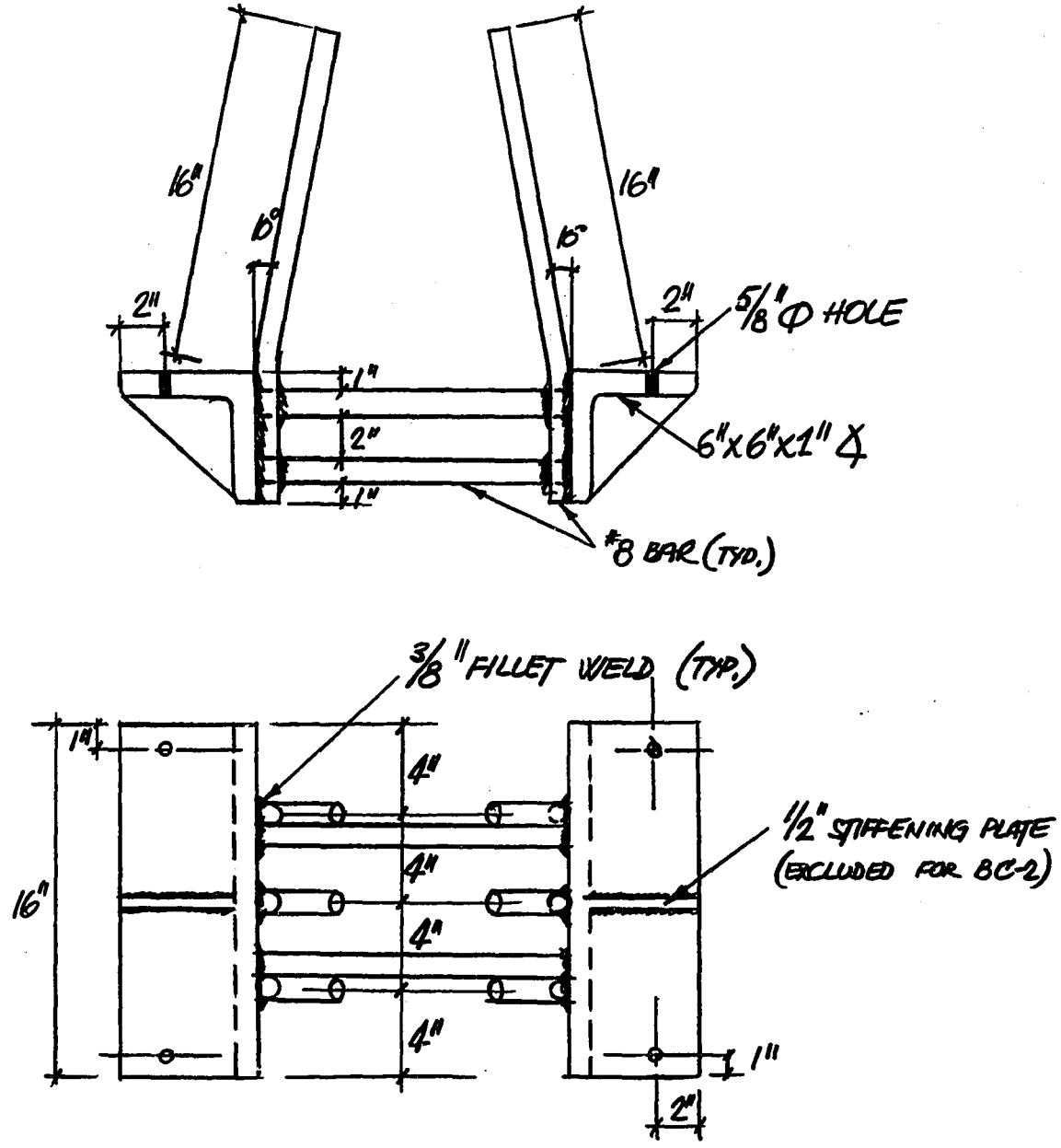

FIGURE 8. - PROTOTYPES B-C1a, B-C1b, B-C1c, B-C2. COLUMN SEAT ANGLES

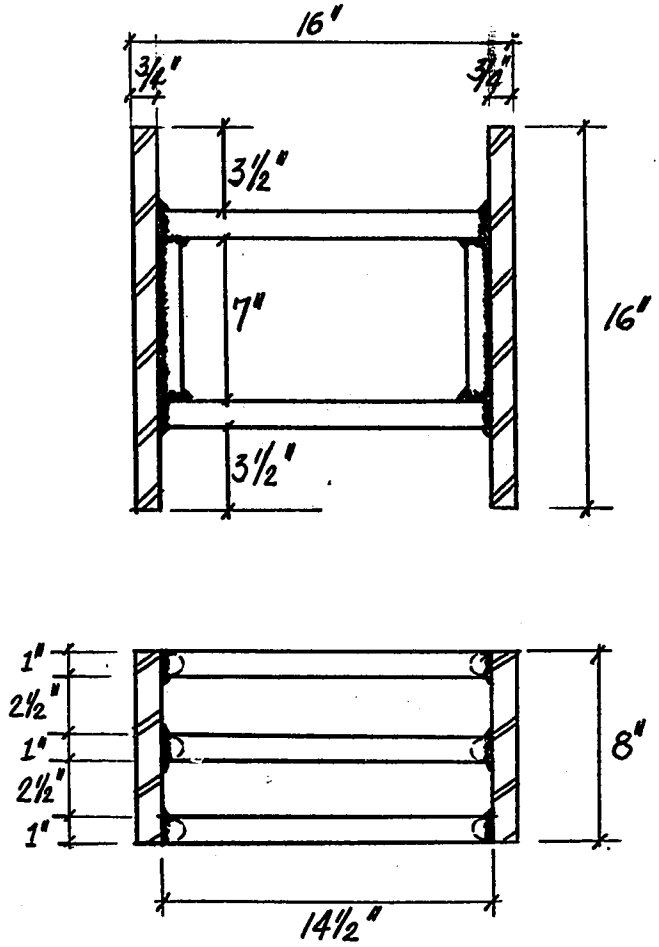

FIGURE 9. - PROTOTYPES B-C1a, B-C1b, B-C1c, B-C2 - COLUMN TOP ANCHOR PLATES

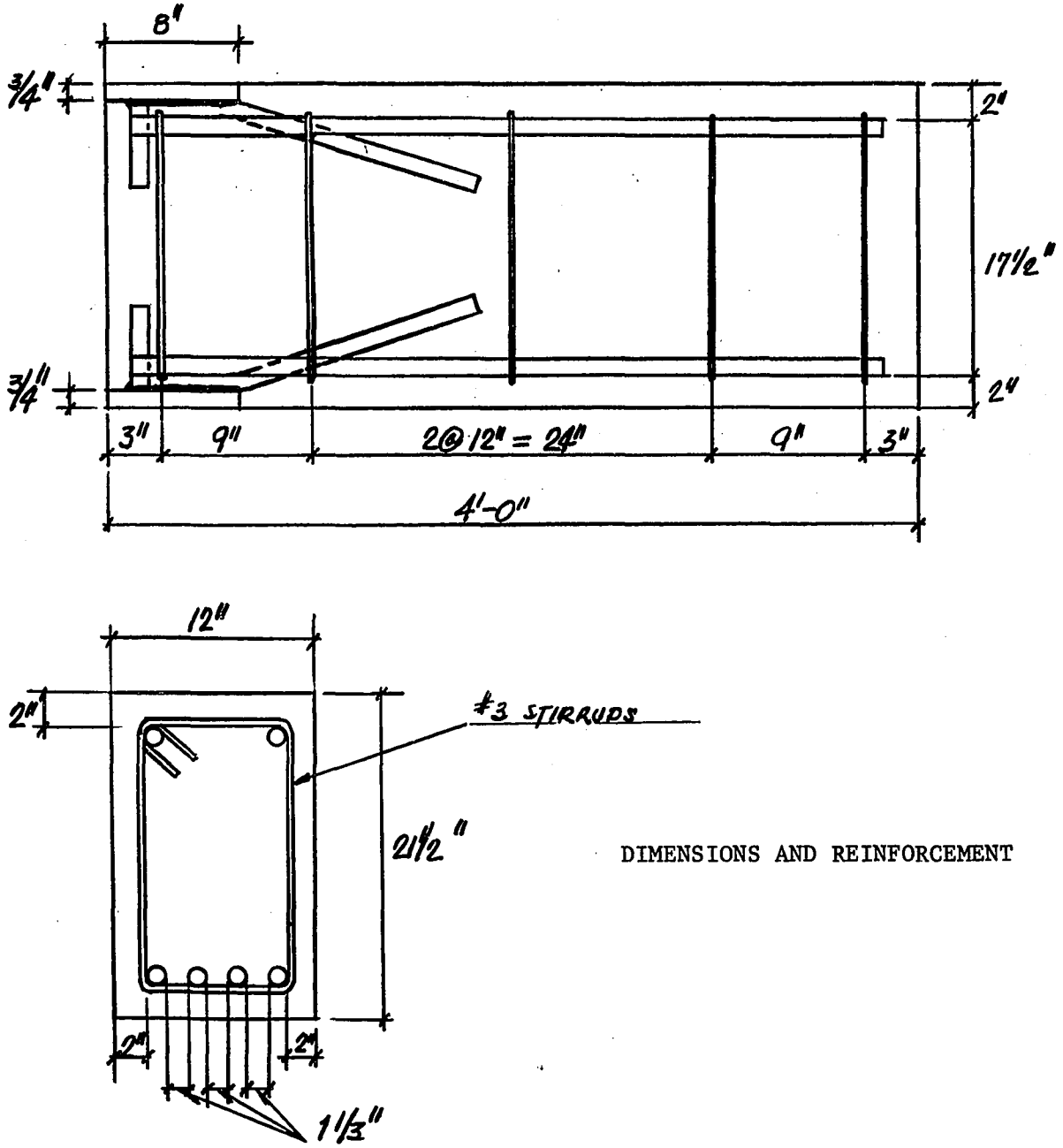

DIMENSIONS AND REINFORCEMENT

FIGURE 10. - PROTOTYPE B-C1a - BEAM.

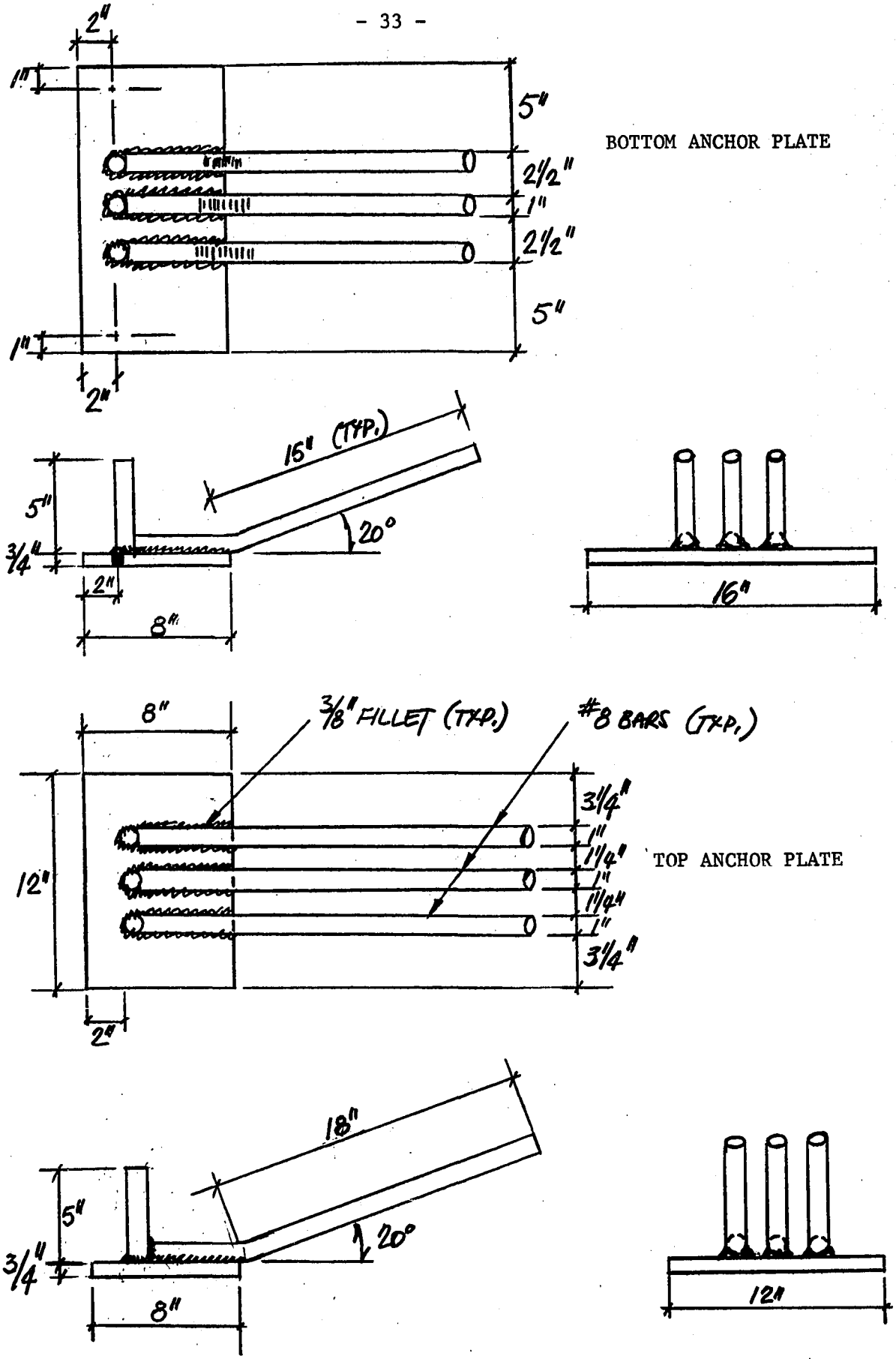

FIGURE 11. - PROTOTYPE B-C1a - BEAMS ANCHORING DEVICE.

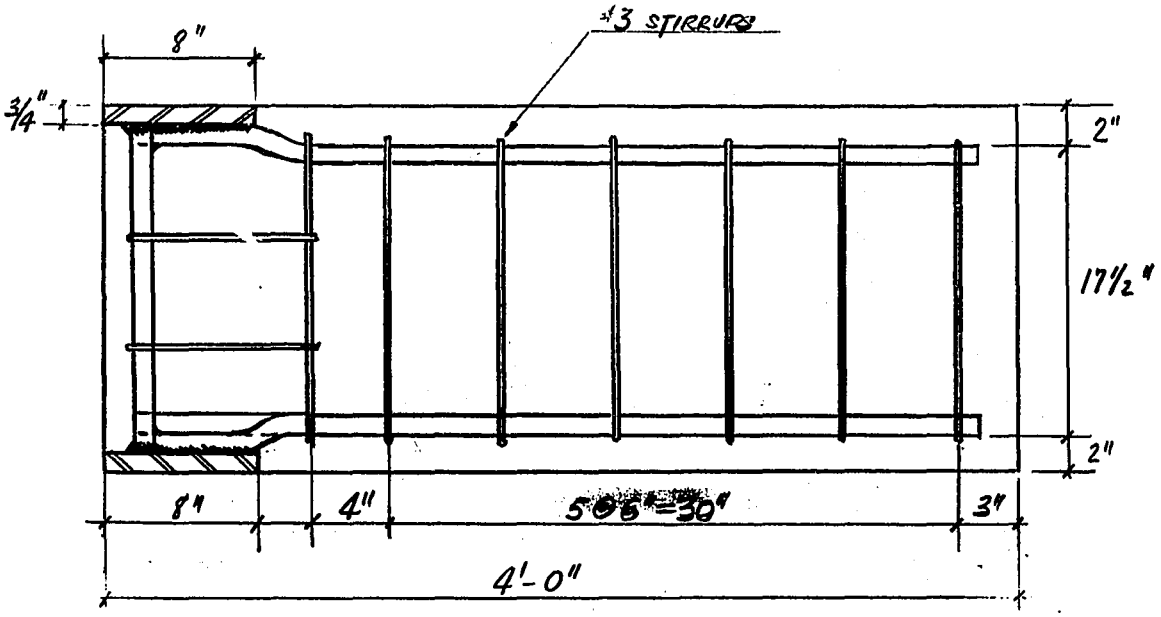

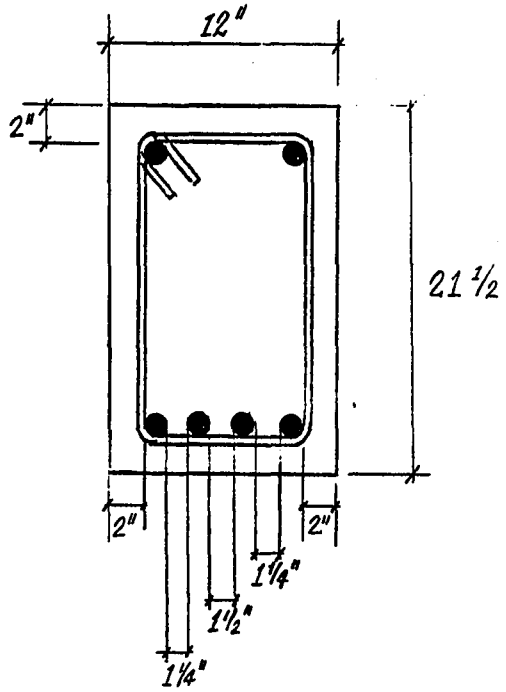

DIMENSIONS AND REINFORCEMENT

FIGURE 12. - PROTOTYPES B-C1b AND B-c1c - BEAM.

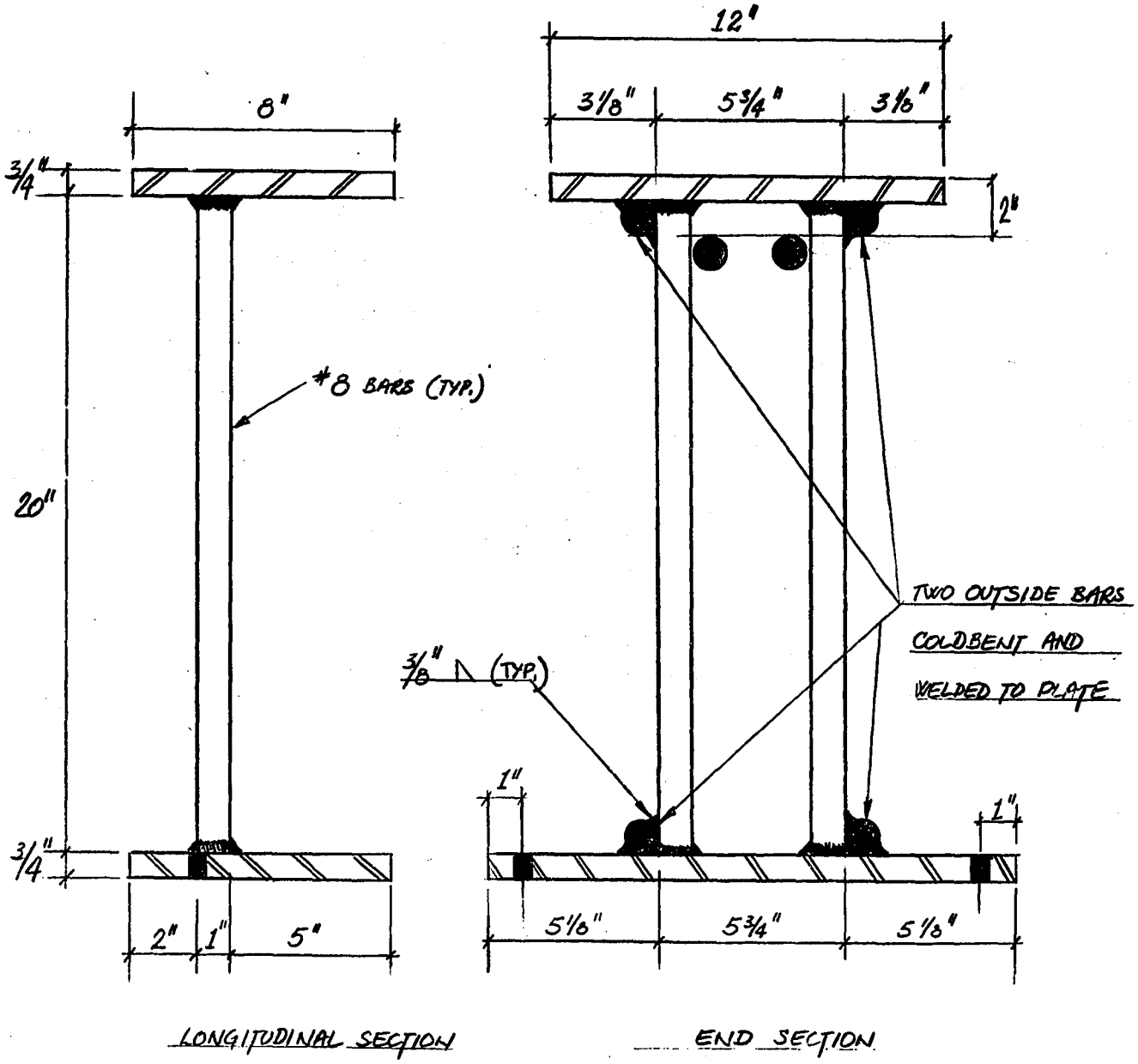

FIGURE 13. - PROTOTYPES B-C1b and B-C1c

BEAM ANCHORING DEVICE.

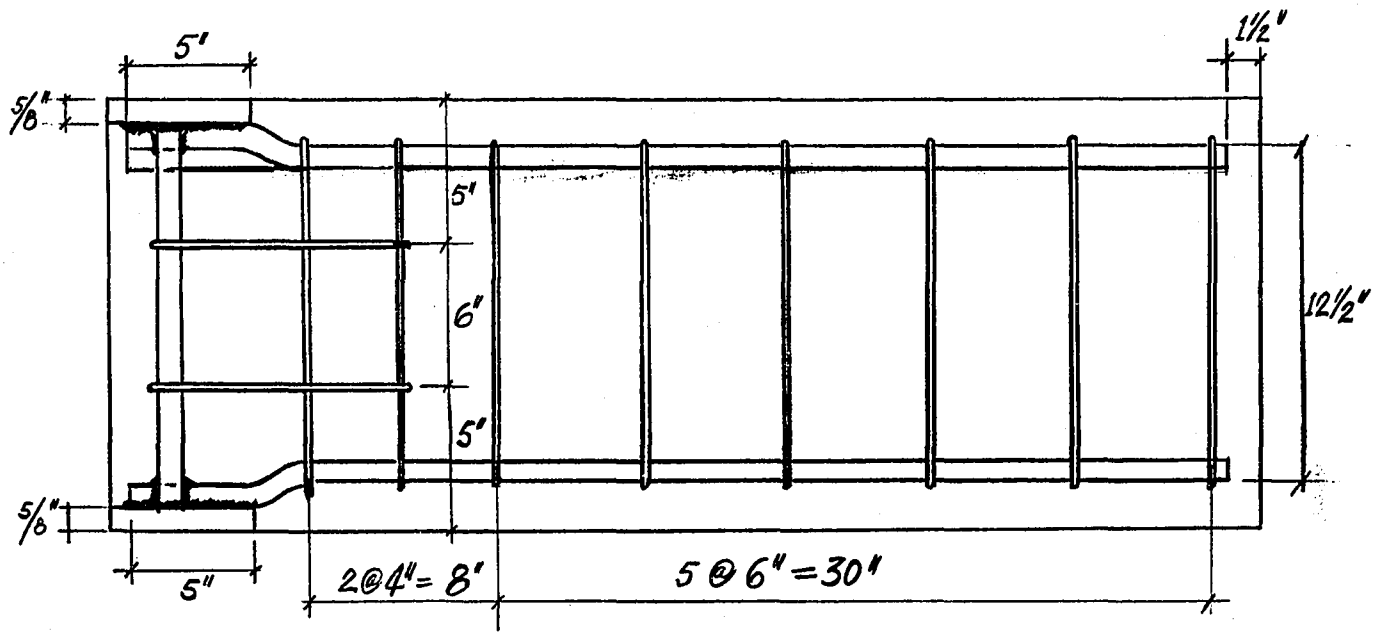

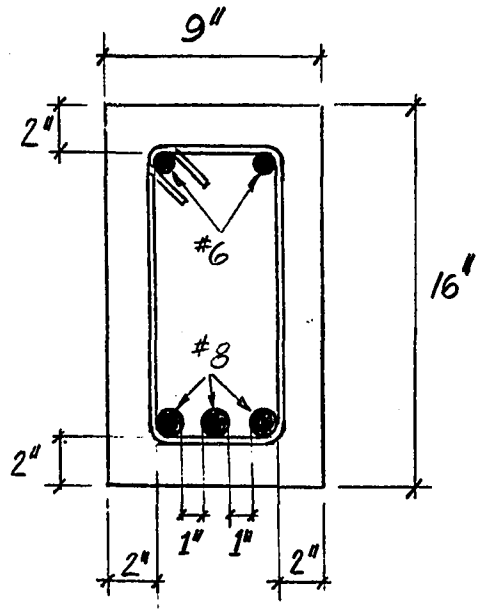

DIMENSIONS AND REINFORCEMENT

FIGURE 14. - PROTOTYPE B-C2 - BEAM.

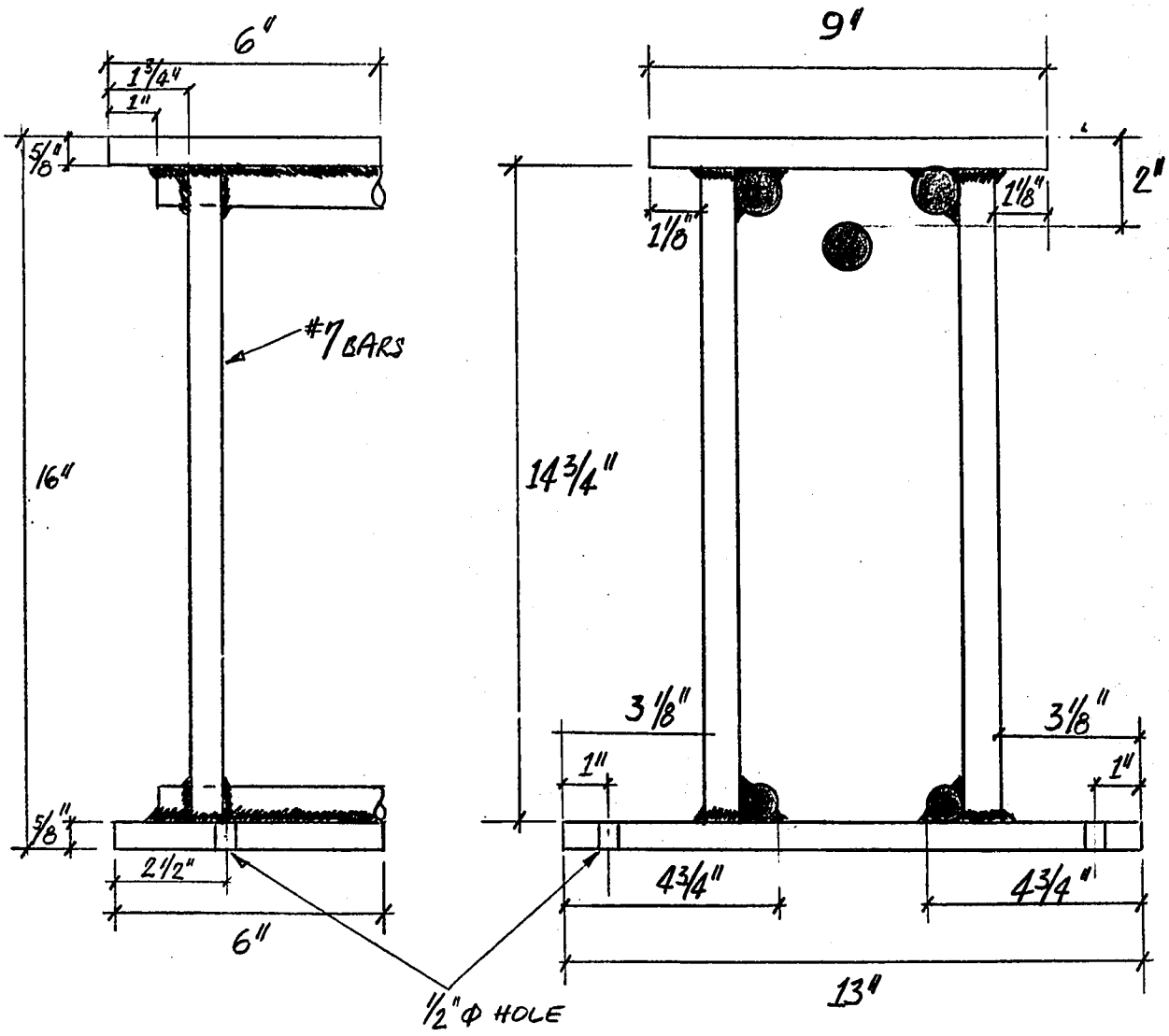

FIGURE 15. - PROTOTYPE B-C2 - BEAM ANCHORING DEVICE.

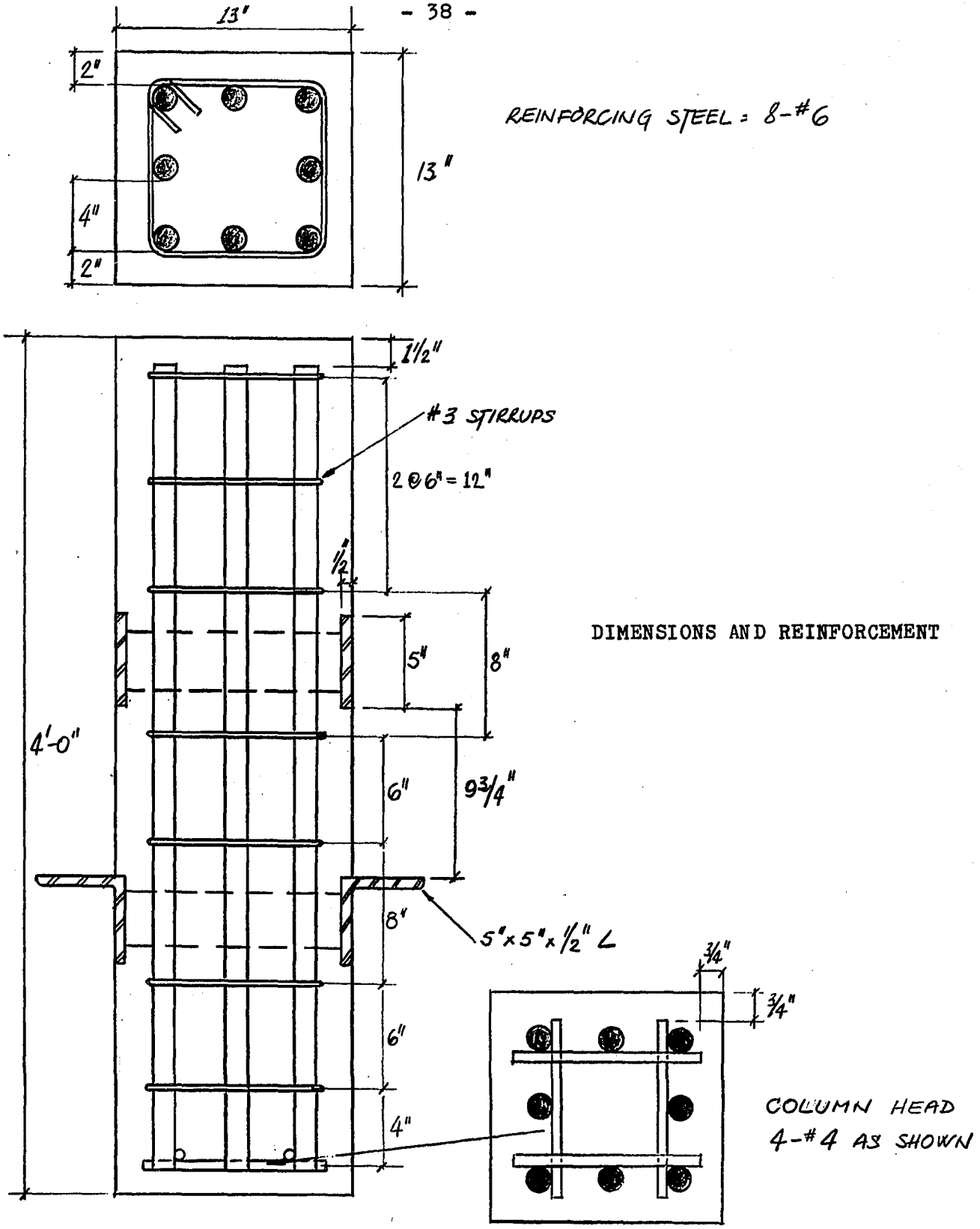

FIGURE 16. - PROTOTYPE B-C3 - COLUMN.

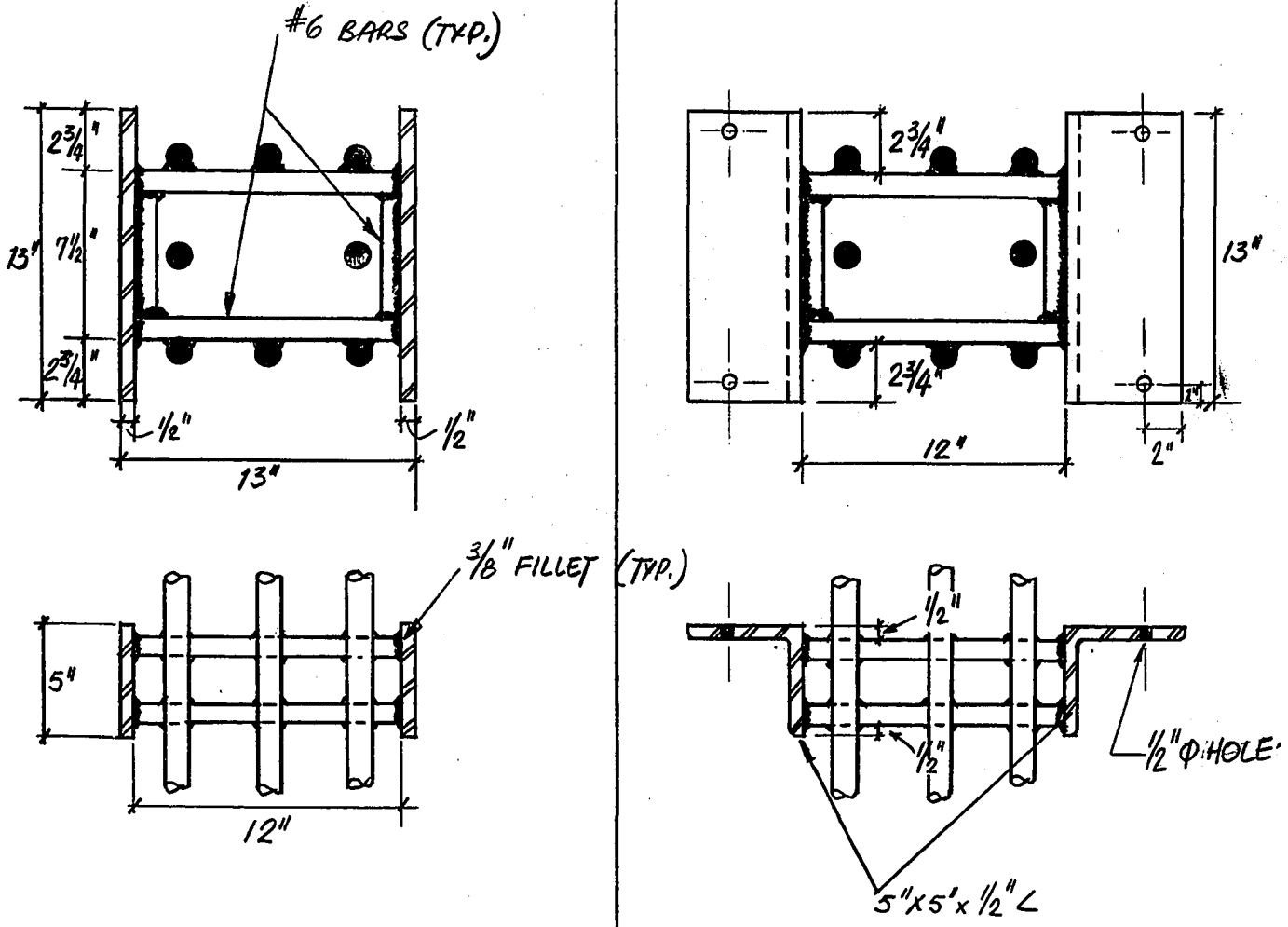

FIGURE 17. - PROTOTYPE B-C3 - COLUMN

TOP ANCHOR PLATES AND SEAT ANGLES

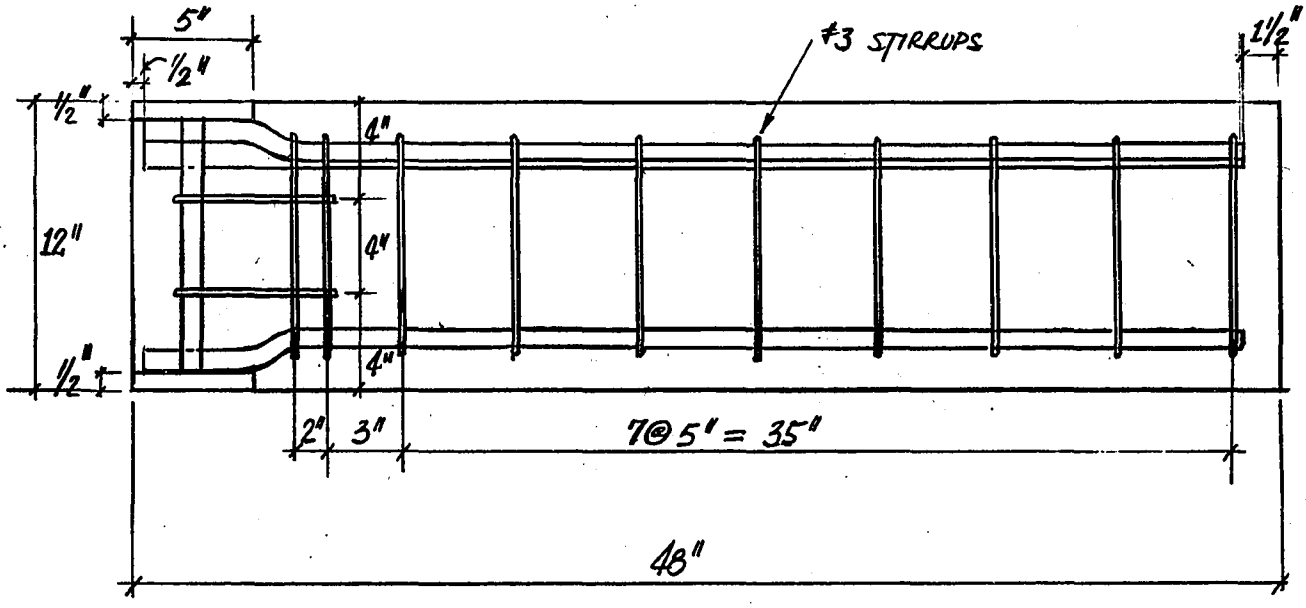

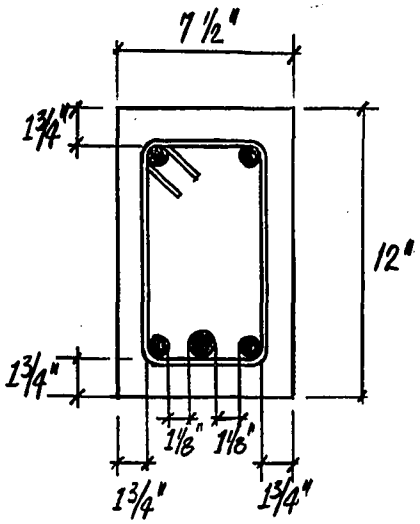

DIMENSIONS AND REINFORCEMENT

FIGURE 18. - PROTOTYPE B-C3 - BEAM.

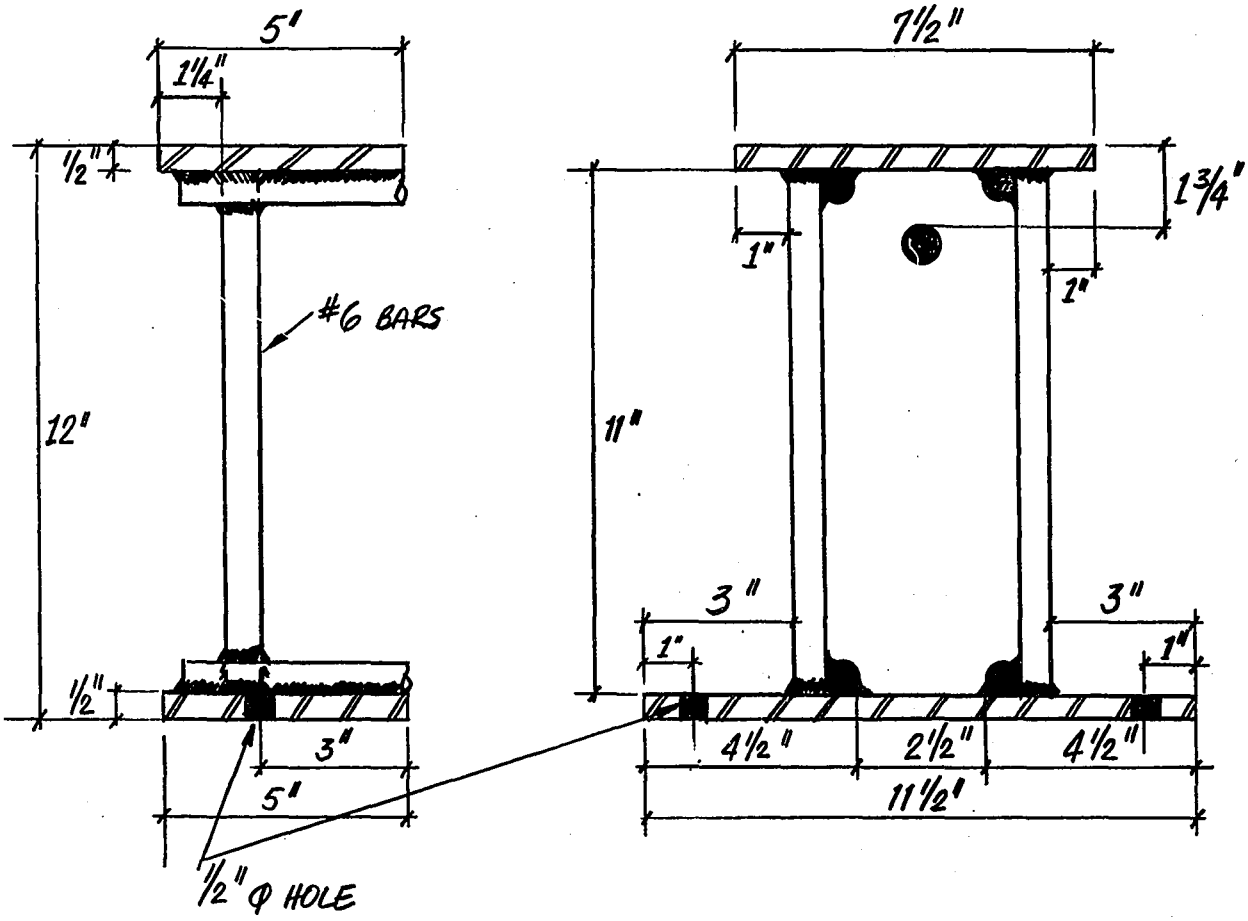

FIGURE 19. - PROTOTYPE B-C3 - BEAMS ANCHORING DEVICE

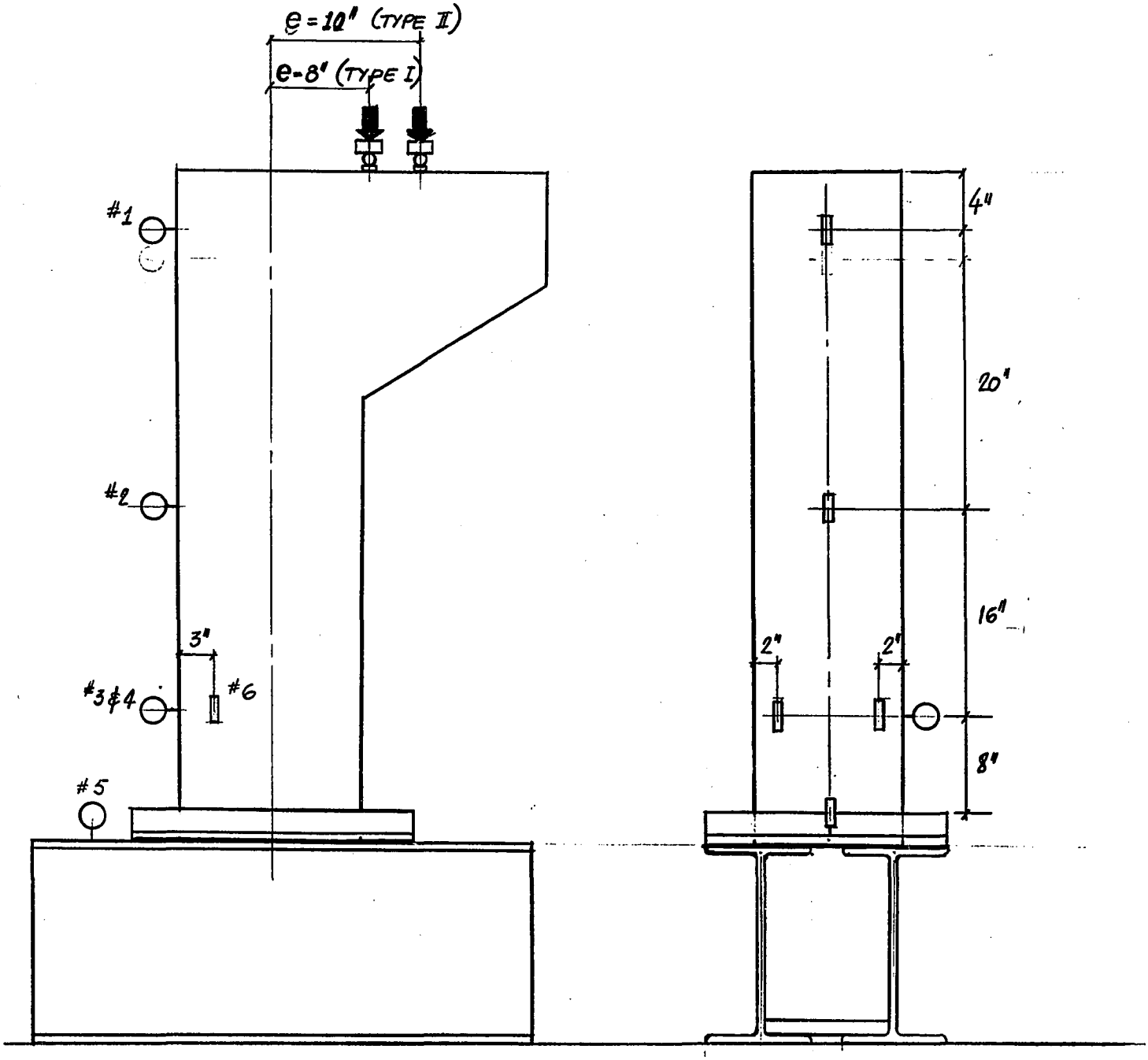

○- IDENTIFICATION AND LOCATION OF 1/1000 DIAL GAGES

FIGURE 20. - COLUMN-BASE CONNECTION

LOCATION OF DIAL GAGES AND TEST SETUP.

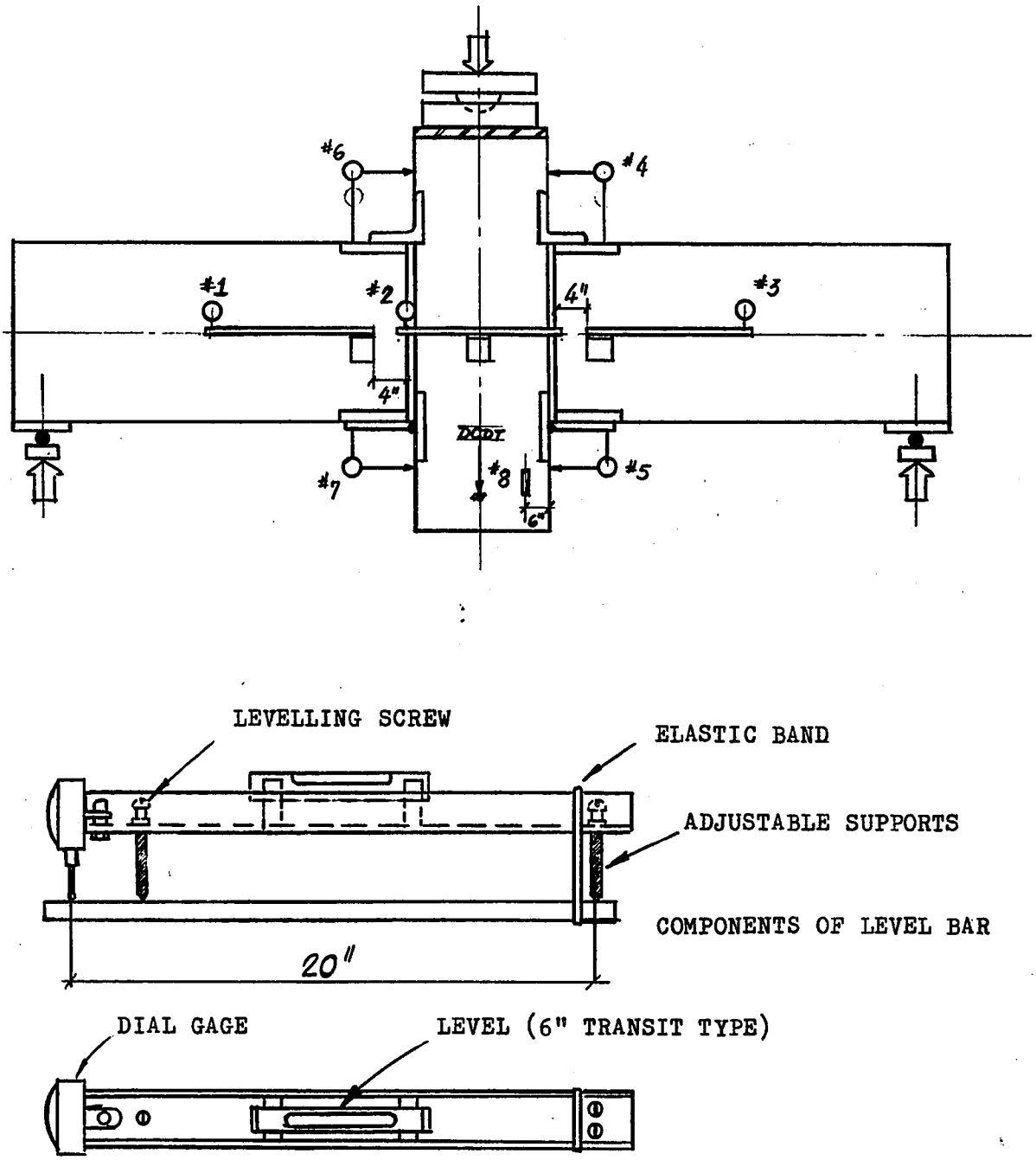

FIGURE 21. - BEAM-TO-COLUMN CONNECTION.

○- IDENTIFICATION AND LOCATION OF DIAL GAGES

CHAPTER V - TEST RESULTS

5.1 Column-to-Base Connection

The deflections recorded by dial gages No. 2, 3 and 4 were used to calculate the rotation of the connections. In both cases it is observed that the rotation computed from gage No. 2 and from gage No. 3 and 4 are almost identical. For type I, the average of the three sets of readings was taken. In the case of Type II, only the deflections obtained from gage No. 2 were used, dials No. 3 and 4 having given inconsistent readings. Figures 22 and 23 present the moment-rotation curves of the two specimens; both graphs are superposed, in Figure 24. For all practical purposes, the two connections offer the same rigidity characteristics.

In the case of Type I, the callipers readings were used to evaluate the gradual deformations of the steel pockets, as moment increased. Dividing each gradual increment by the initial opening gives a strain which characterizes the connection deformation. Figure 25 gives these results in a graph showing the moment at the connection versus the measured strain. It can be noticed that, as expected, the compression side was the most severely damaged. Tables of the experimental results and calculation examples are given in Appendix A.

5.2 Beam-to-Column Connection

The calculations converting the experimental deflections

into final rotations relative to horizontal were performed on the IBM 7044 computer. The computer program and the results are presented in Appendix A.

Two M-Q curves for each test assembly have been plotted; one is for the left hand beam (Q_L) and the other is for the right hand beam (Q_R). It can be noted from the tabulation that both Q_L and Q_R resulted from the average of two sets of Q readings. One set is obtained from the level bar readings given by gage Nos. 1 and 2 (for Q_L) and by gage Nos. 2 and 3 (for Q_R). The other set is obtained from gage Nos. 6 and 7 (for Q_L) and from gage Nos. 4 and 5 (for Q_R). The purpose of having these two independent methods of measuring was twofold. First, a double check is obtained and second, the average of these two sets of readings yields more representative rotation values.

From the experimental data provided by the DCDT Recorder, Load-Deflection curves for each specimen are obtained. With this device, vertical deflections were continuously recorded, until collapse occurred. Detailed observations on the experimental work and an analysis of the obtained results follow.

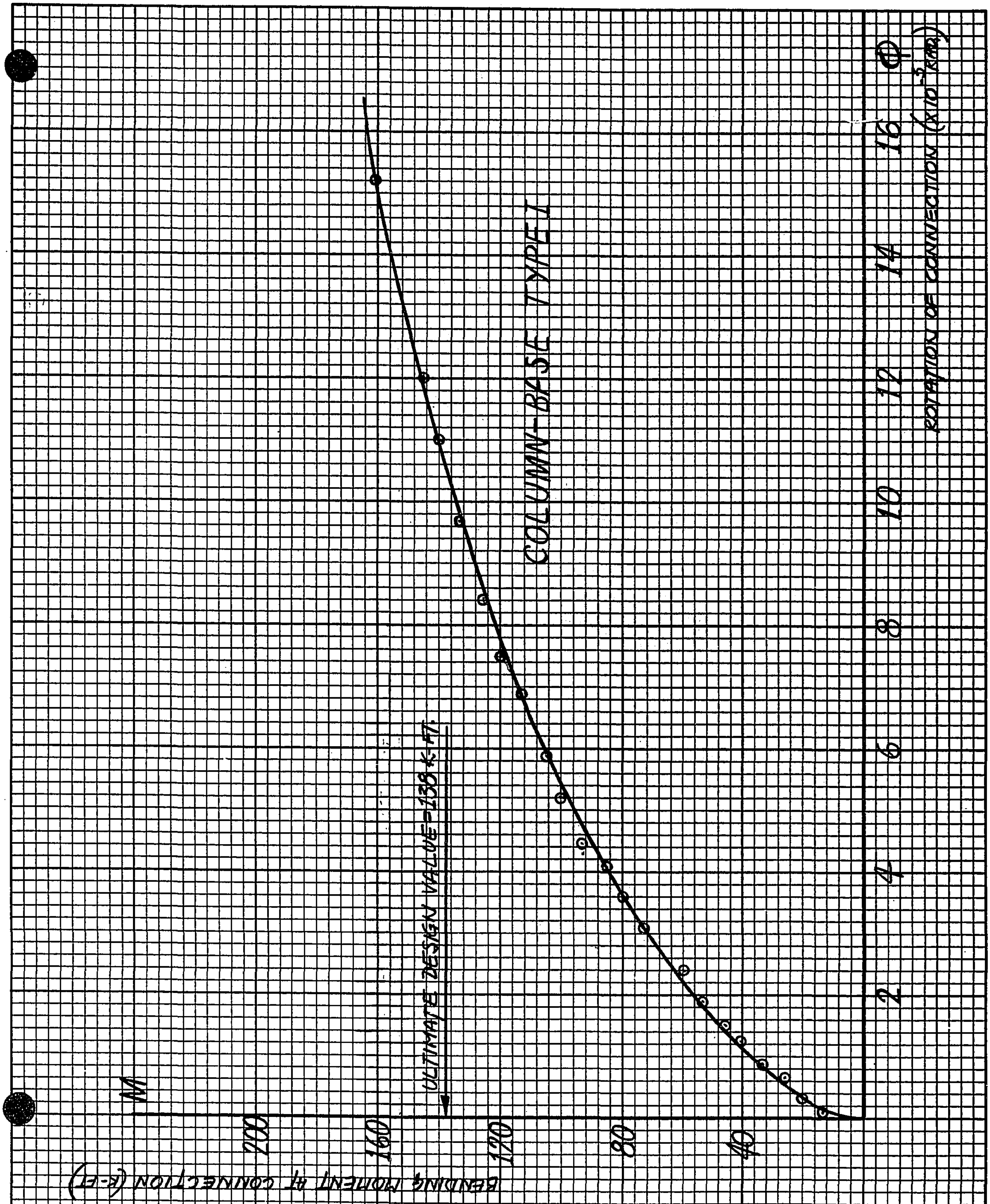
COLUMN-BASE TYPE I
ULTIMATE DESIGN VALUE=130 K-FT.
M
200
160
120
80
40
2
4
6
8
10
12
14
16
φ
ROTATION OF CONNECTION (X10^{-3} RAD.)
BENDING MOMENT AT CONNECTION (K-FT)

FIGURE 22

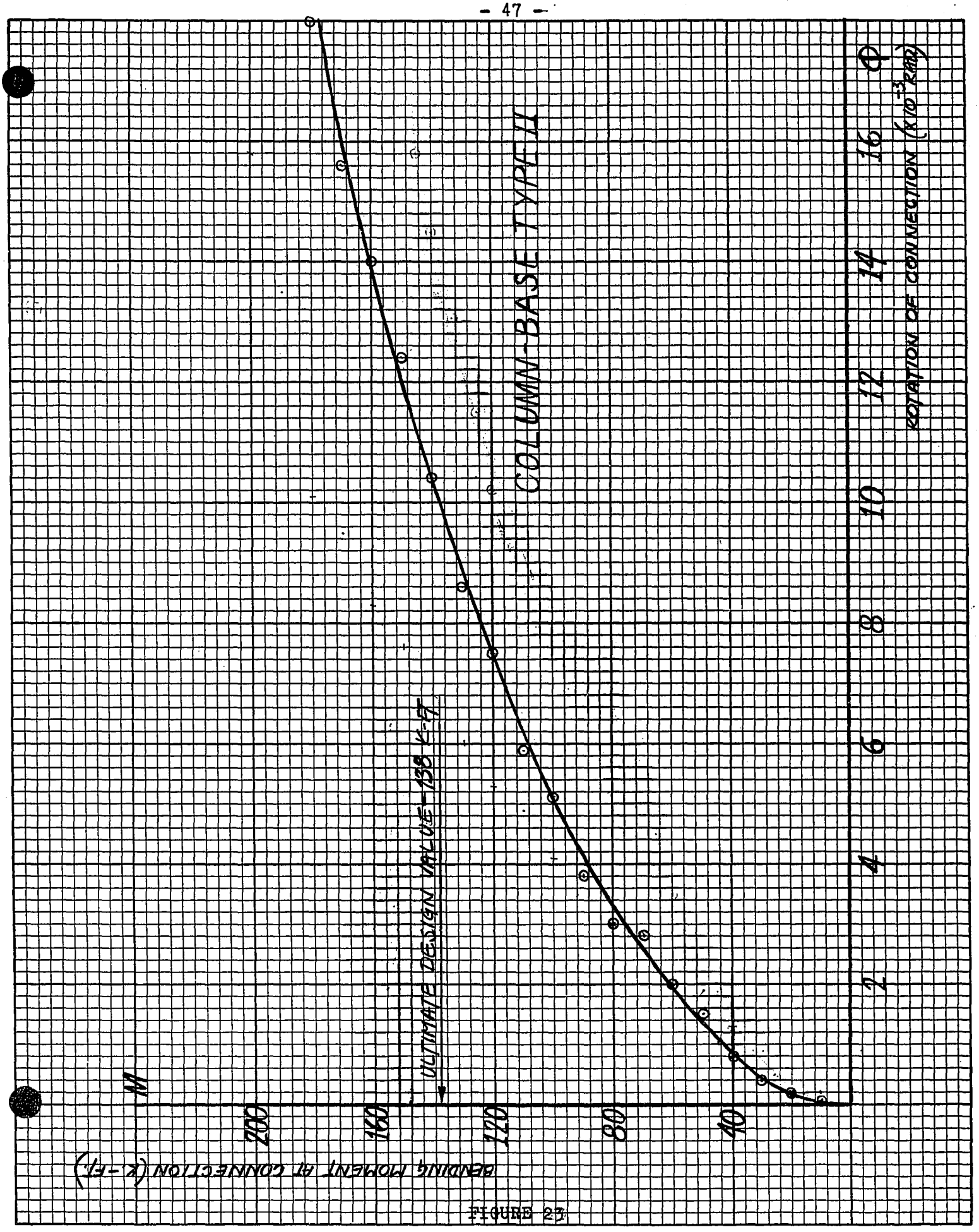
T-FLANGE COLUMN-BASE-TYPE
ROTATION OF CONNECTION ($K\times10^{-3}$ RAD)
0
2
4
6
8
10
12
14
16
40
80
120
160
200
240
BENDING MOMENT AT CONNECTION ($K\cdot ft$)
ULTIMATE DESIGN MOMENT = 138 $K\cdot ft$

FIGURE 23

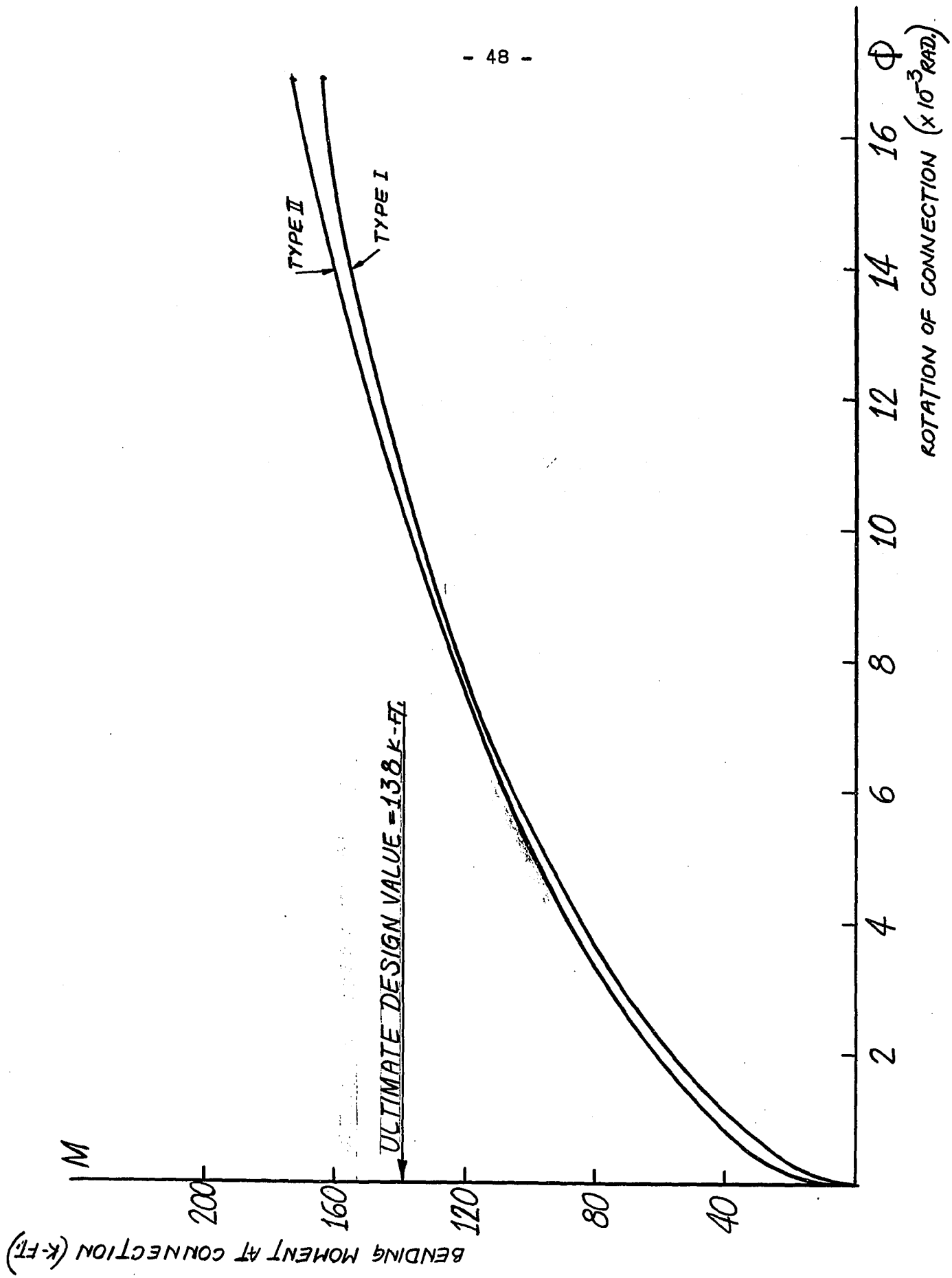
BENDING MOMENT AT CONNECTION (K-FT.)
M
200
160
120
80
40
ULTIMATE DESIGN VALUE = 138 K-FT.
TYPE II
TYPE I
2
4
6
8
10
12
14
16
Φ
ROTATION OF CONNECTION (x 10⁻³ RAD.)

FIGURE 24

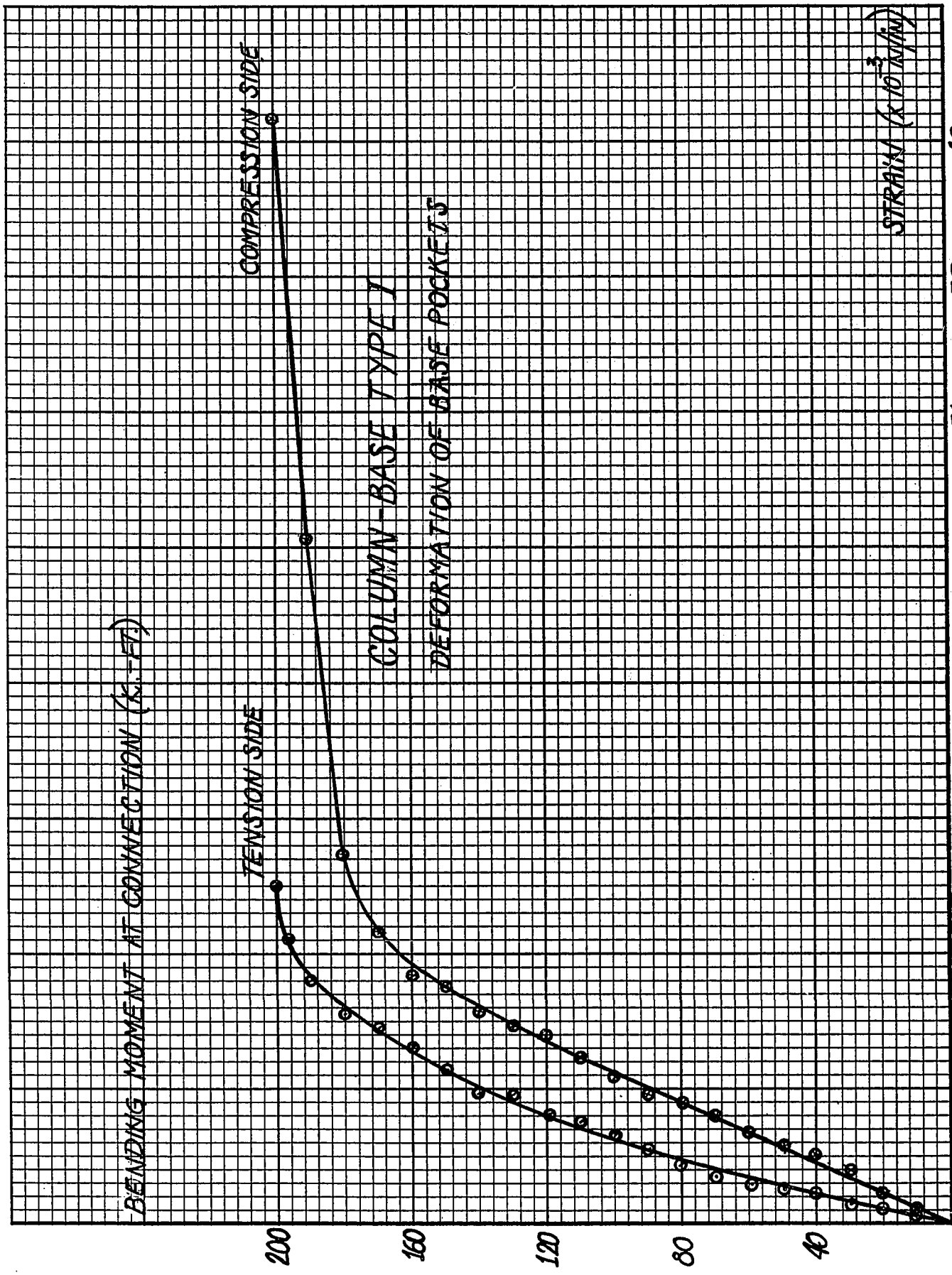
COLUMN-BASE TYPE I
DEFORMATION OF BASE POCKETS
COMPRESSION SIDE
TENSION SIDE
BENDING MOMENT AT CONNECTION (K.-FT.)
STRAIN (X10⁻³ IN/IN)
200
160
120
80
40
5
10
15
20
25
30
35
40

FIGURE 25

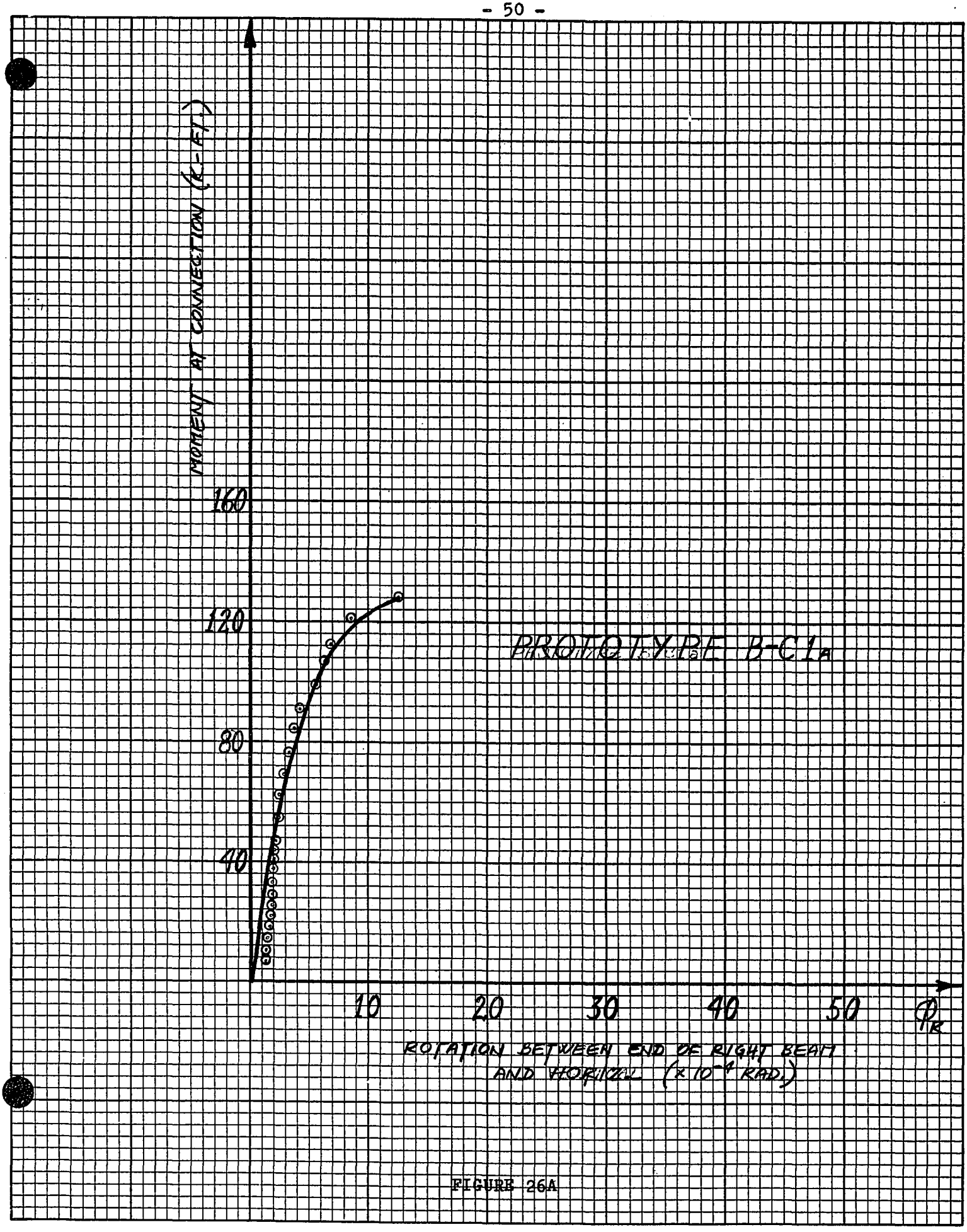
MOMENT AT CONNECTION (K-FT.)
160
120
80
40
PROTOTYPE B-C1A
10
20
30
40
50
ϕ_R
ROTATION BETWEEN END OF RIGHT BEAM AND HORIZ. (x 10⁻⁴ RAD.)

FIGURE 26A

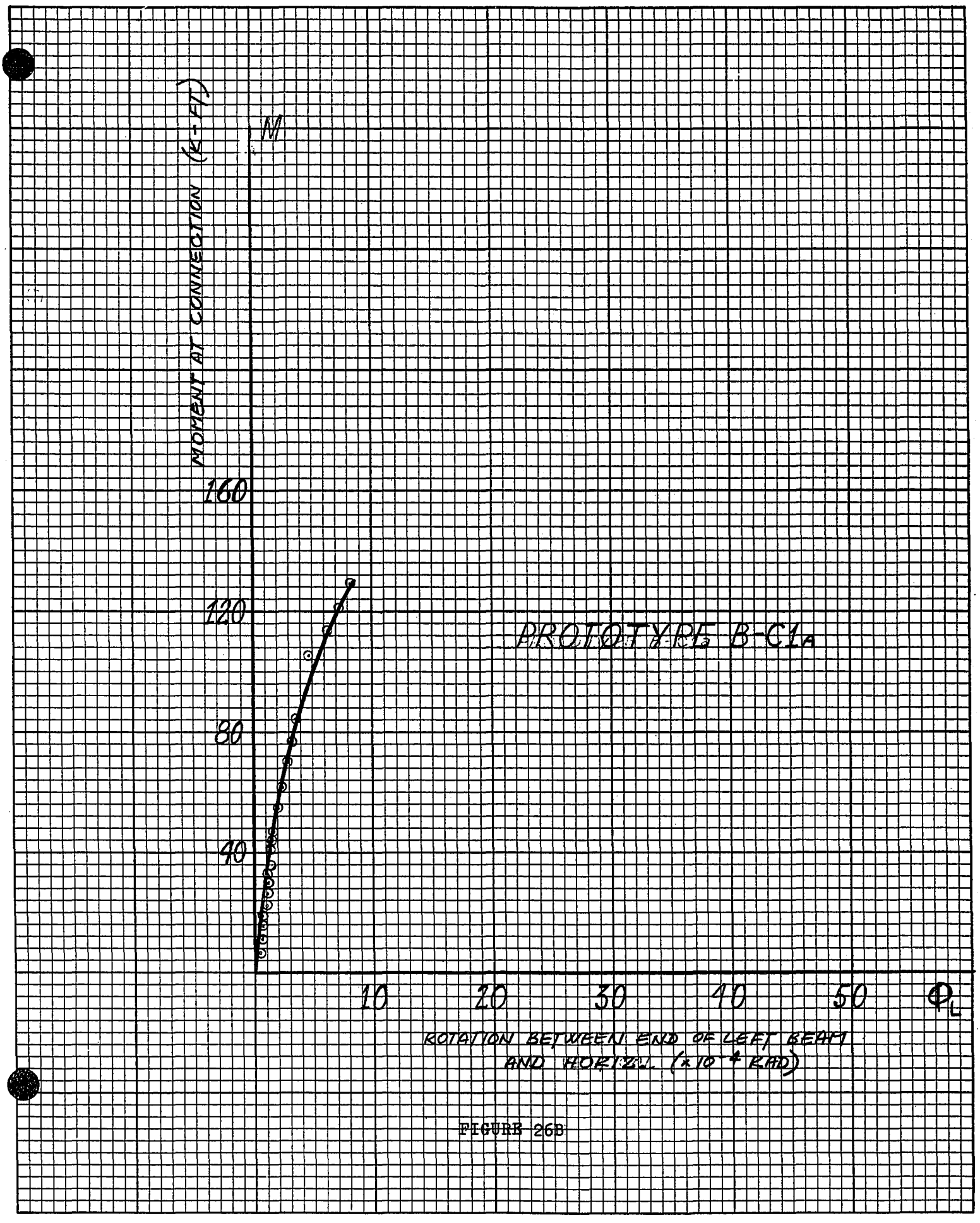
MOMENT AT CONNECTION (K-FT)
M
160
120
80
40
PROTOTYPE B-C1A
10
20
30
40
50
Φ_L
ROTATION BETWEEN END OF LEFT BEAM AND HORIZ. (×10⁻⁴ RAD)

FIGURE 26B

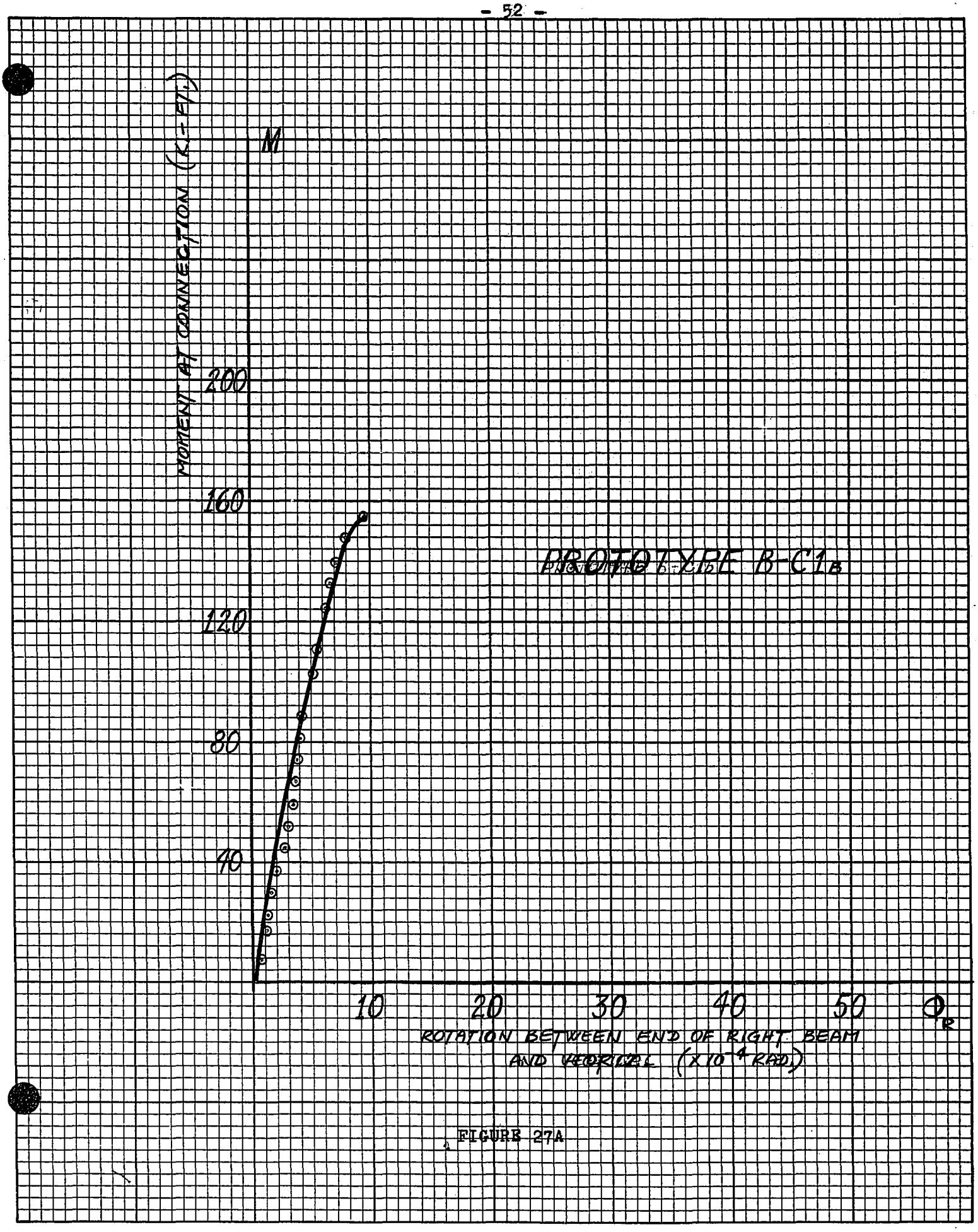
MOMENT AT CONNECTION (K-FT)
M
200
160
120
80
40
PROTOTYPE B-C1B
10
20
30
40
50
Φ_R
ROTATION BETWEEN END OF RIGHT BEAM AND VERTICAL ($\times 10^{-4}$ RAD)

FIGURE 27A

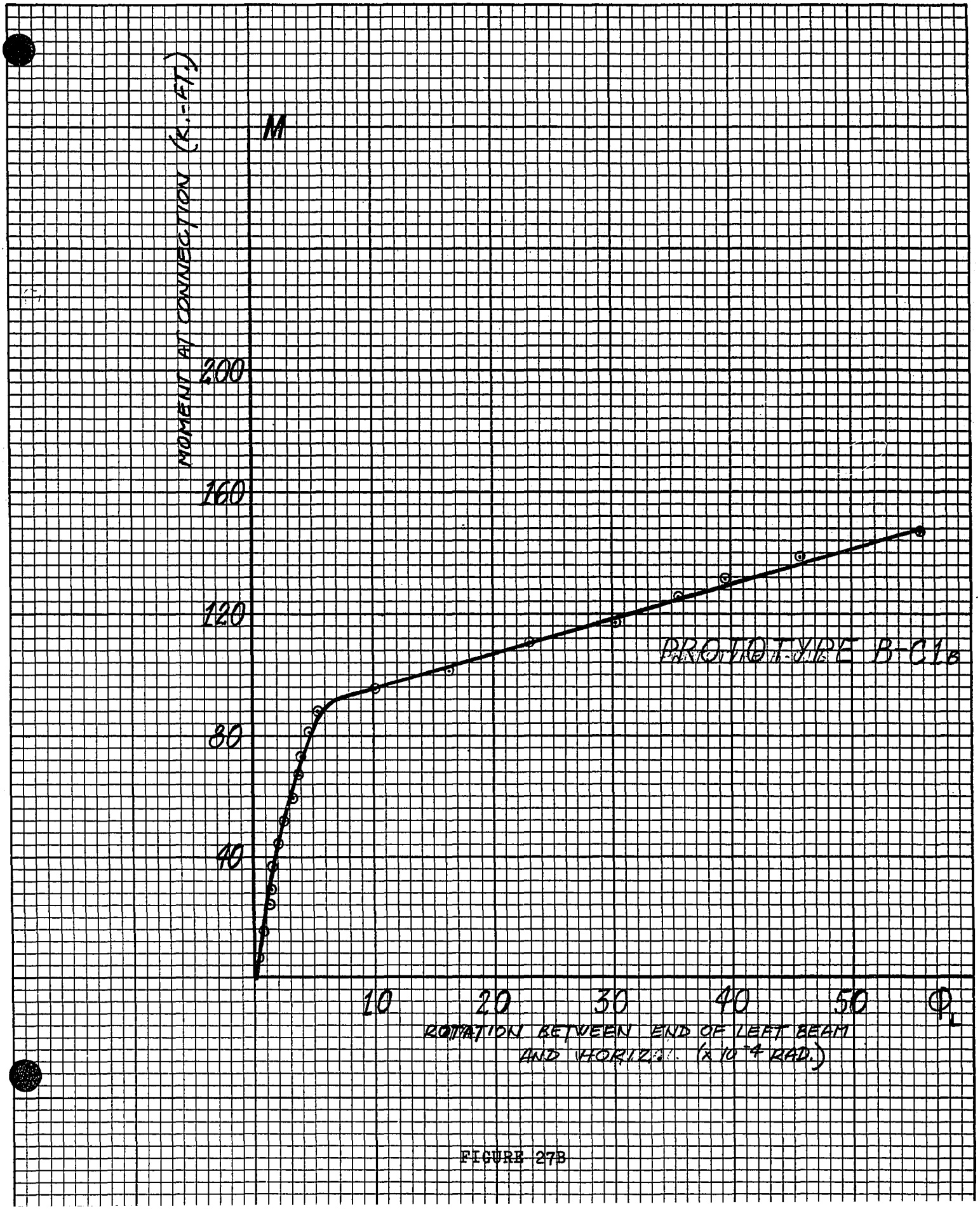
MOMENT AT CONNECTION (K.-FT.)
M
200
160
120
80
40
PROTOTYPE B-C1B
10
20
30
40
50
θ_L
ROTATION BETWEEN END OF LEFT BEAM AND HORIZ. (x 10⁻⁴ RAD.)

FIGURE 27B

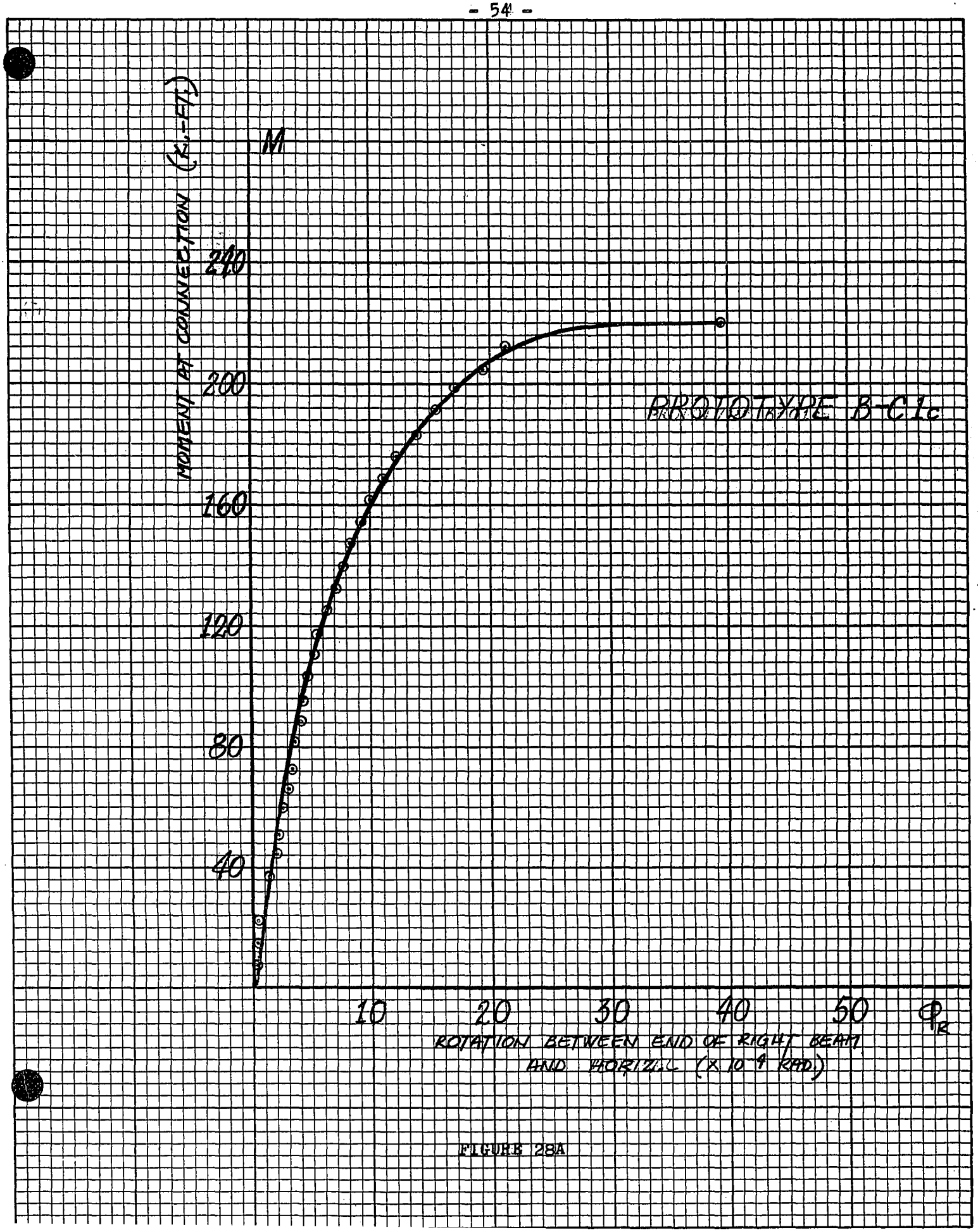
M
MOMENT AT CONNECTION (K-FT)
240
200
160
120
80
40
PROTOTYPE B-C1c
10
20
30
40
50
φ_R
ROTATION BETWEEN END OF RIGHT BEAM AND HORIZ. (X 10⁻⁴ RAD)

FIGURE 28A

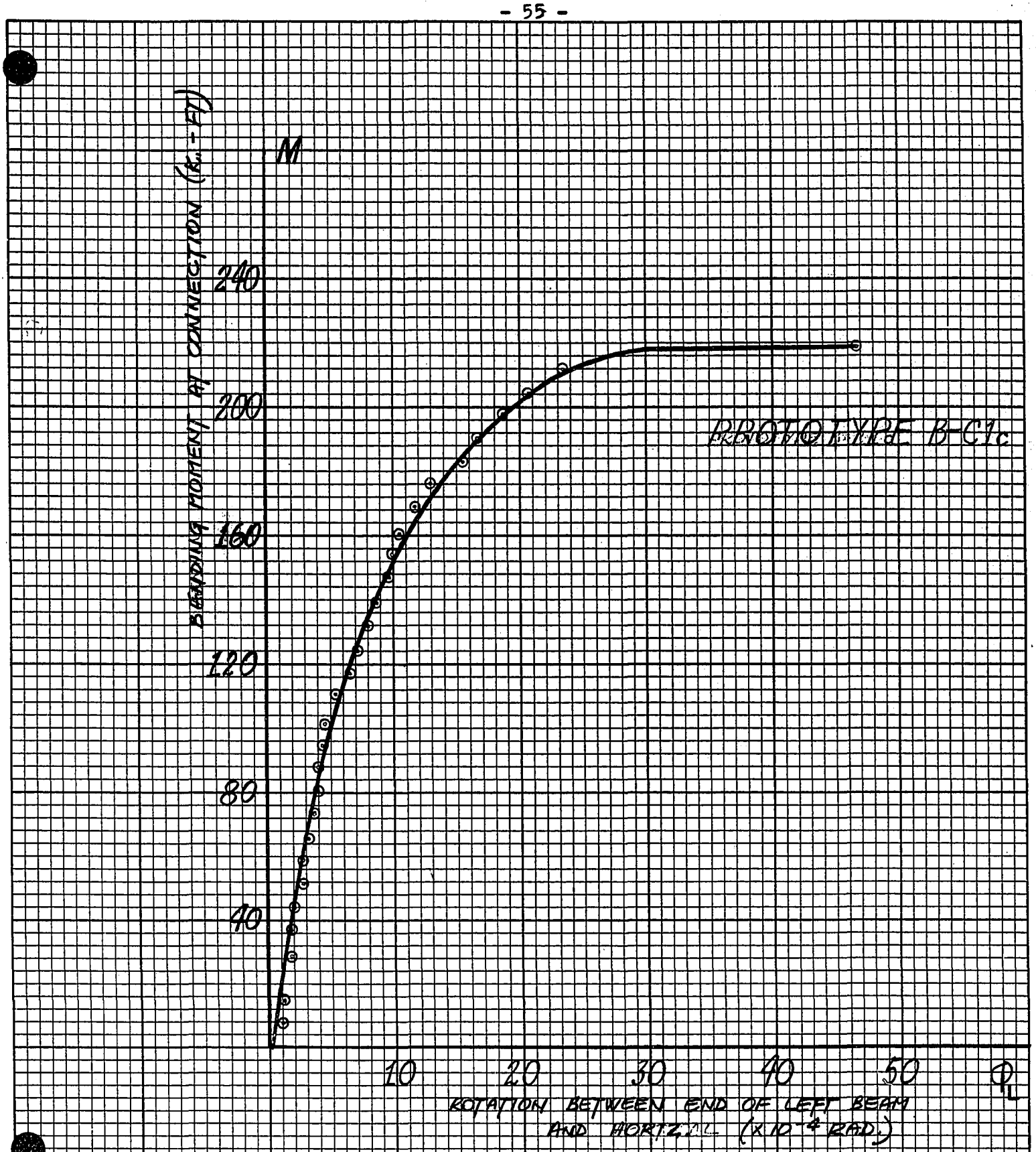
M
BENDING MOMENT AT CONNECTION (K.-FT)
240
200
160
120
80
40
PROTOTYPE B-C1c
10
20
30
40
50
θ_L
ROTATION BETWEEN END OF LEFT BEAM AND HORIZONTAL (X 10⁻⁴ RAD.)

FIGURE 28B

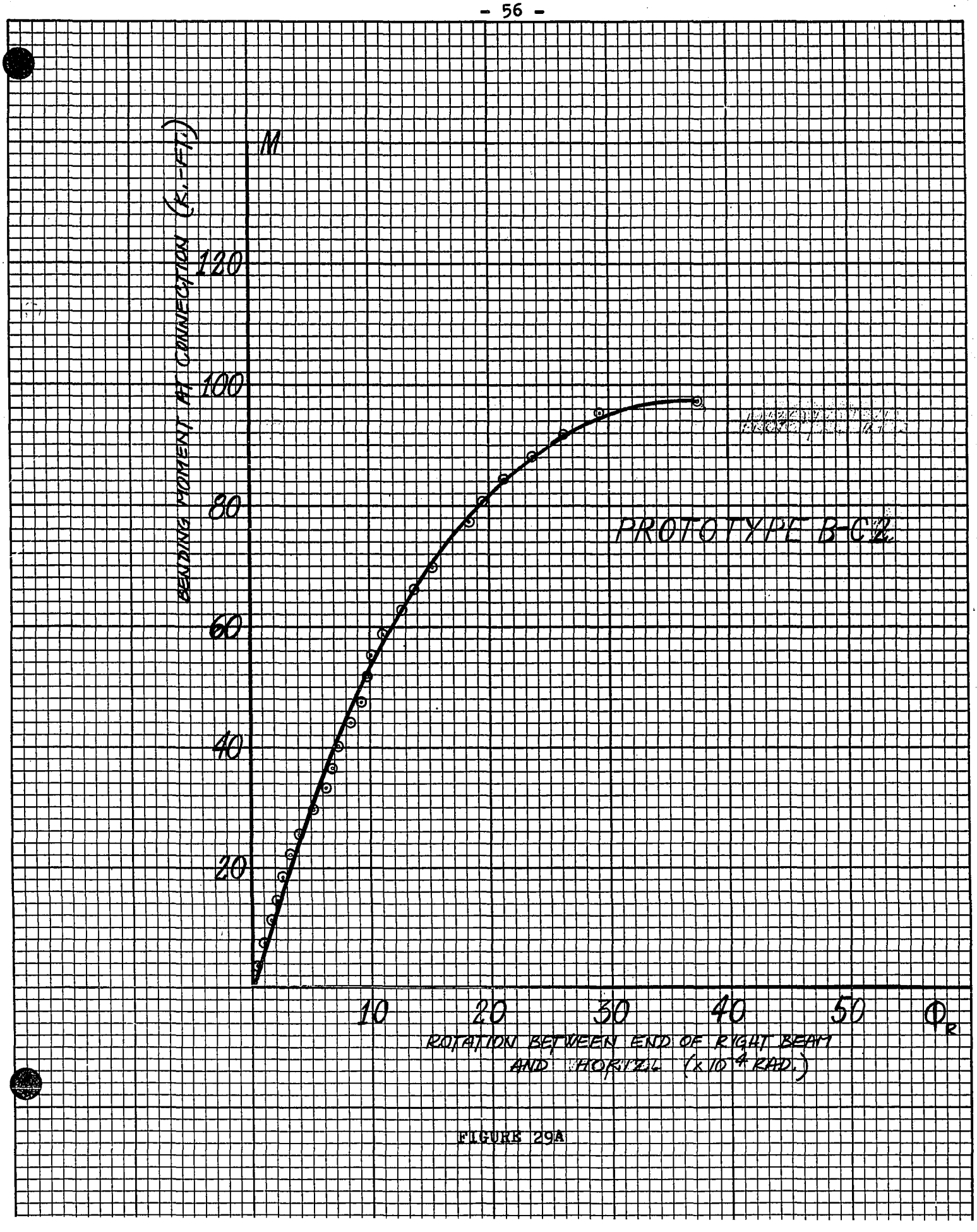
M
BENDING MOMENT AT CONNECTION (K.-FT.)
120
100
80
60
40
20
PROTOTYPE B-C2
10
20
30
40
50
Θ_R
ROTATION BETWEEN END OF RIGHT BEAM AND HORIZ. (x10^{-4} RAD.)

FIGURE 29A

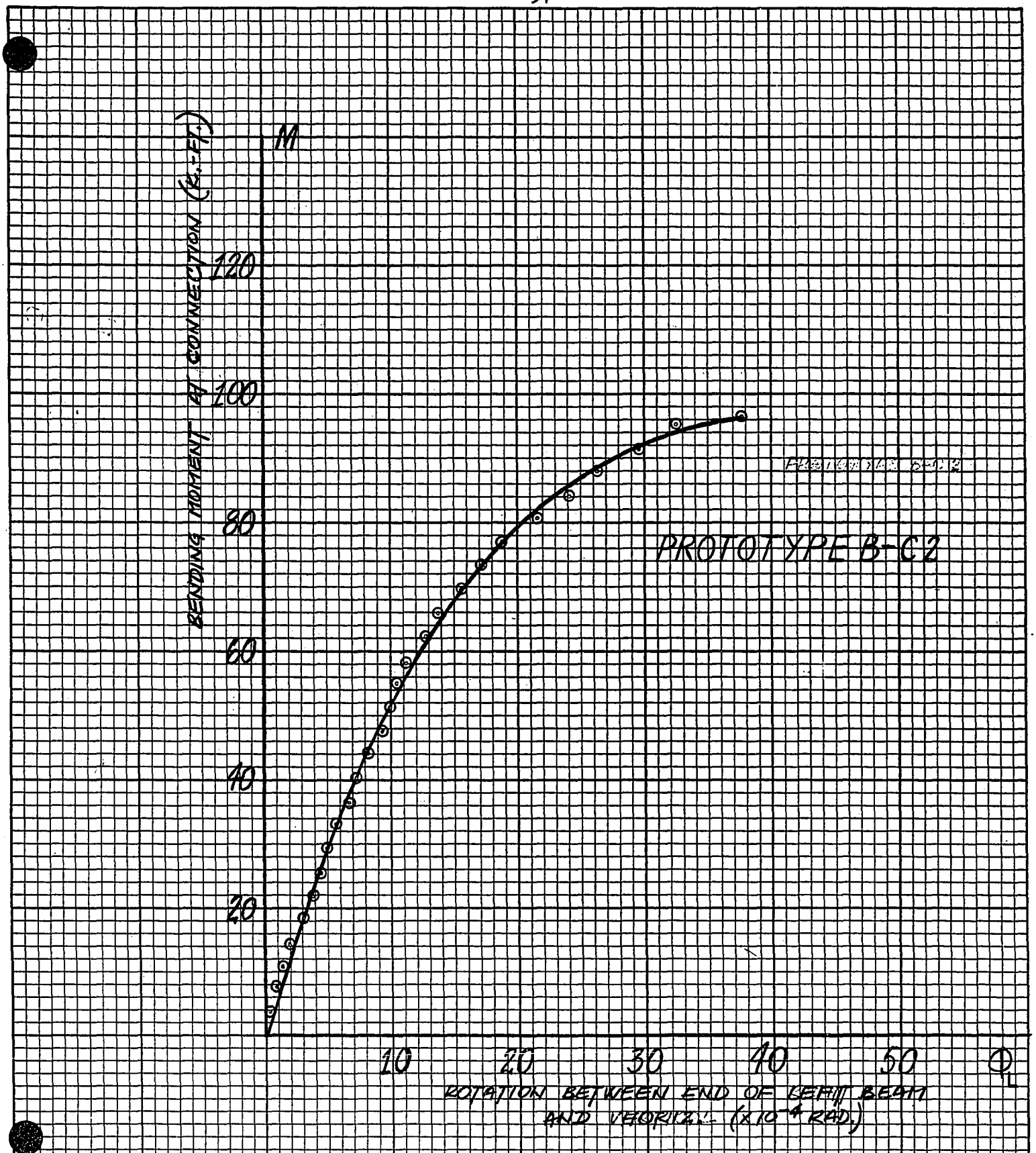
M
BENDING MOMENT AT CONNECTION (K.-FT.)
120
100
80
60
40
20
PROTOTYPE B-C2
10
20
30
40
50
Φ_L
ROTATION BETWEEN END OF CERT. BEAM AND VERTICAL (X 10^{-4} RAD.)

FIGURE 29B

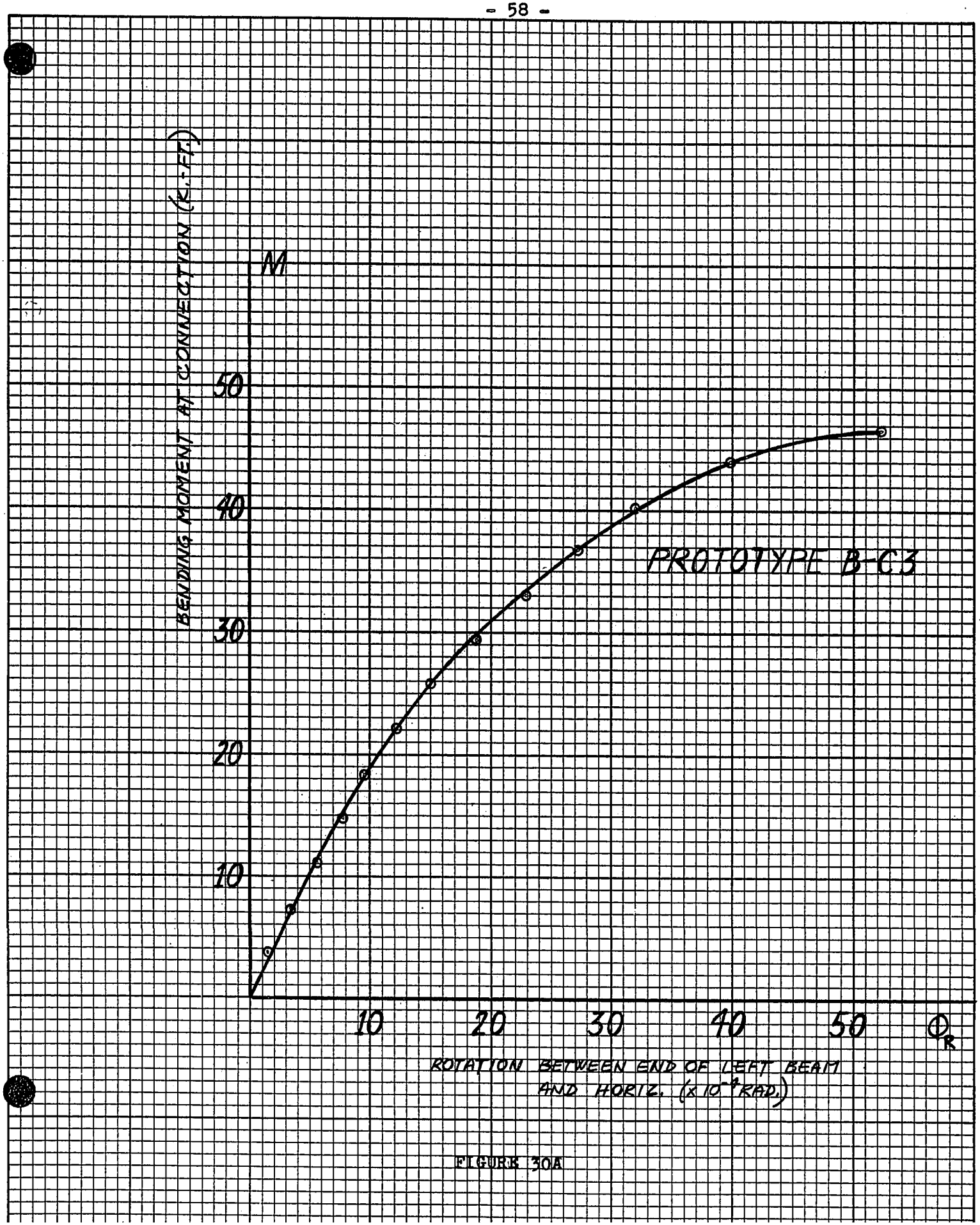
BENDING MOMENT AT CONNECTION (K.-FT.)
M
50
40
30
20
10
PROTOTYPE B-C3
10
20
30
40
50
Φ_R
ROTATION BETWEEN END OF LEFT BEAM AND HORIZ. ($\times 10^{-4}$ RAD.)

FIGURE 30A

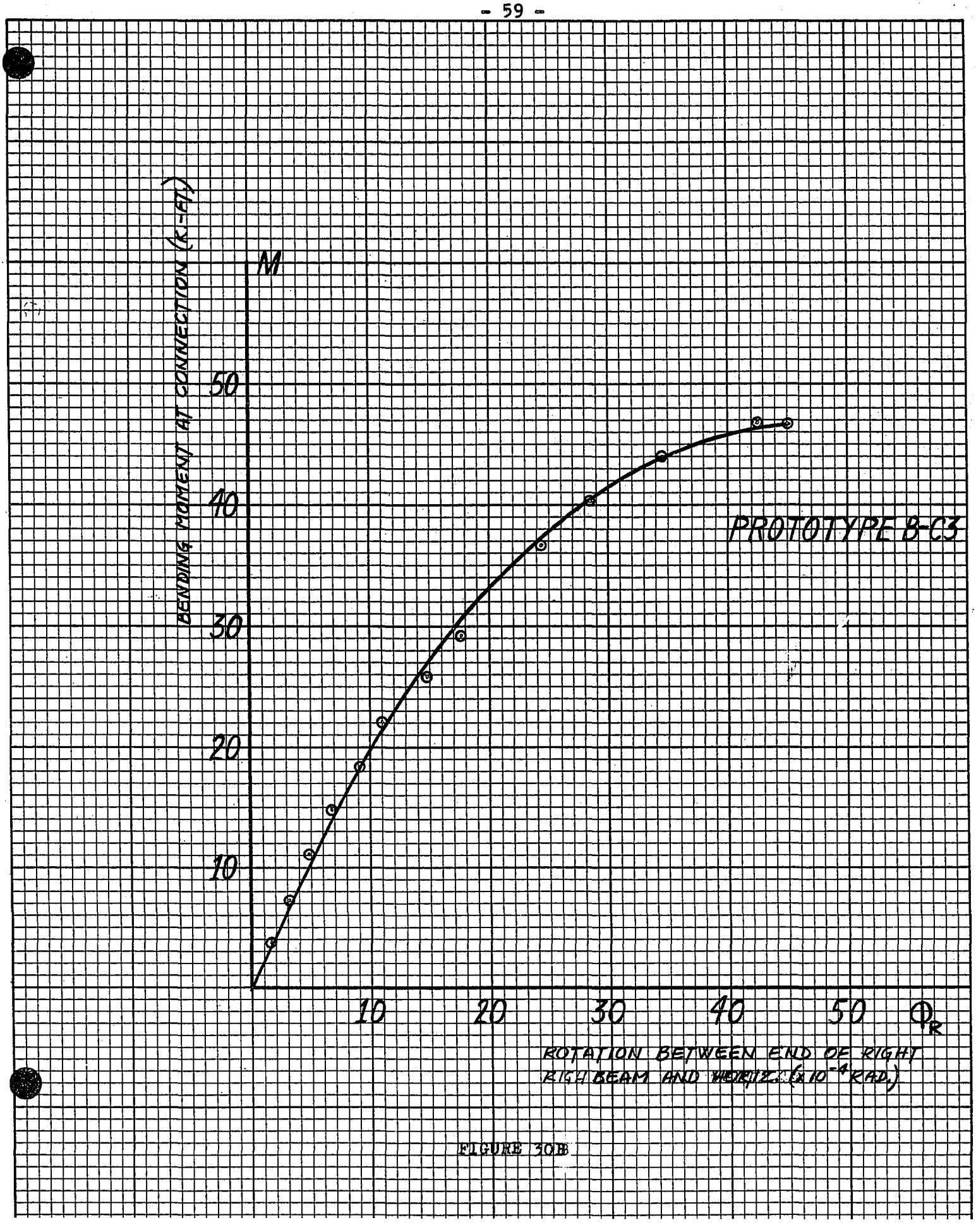
BENDING MOMENT AT CONNECTION (K-FT.)
M
50
40
30
20
10
PROTOTYPE B-C3
10
20
30
40
50
Φ_R
ROTATION BETWEEN END OF RIGHT RIGH BEAM AND HORIZ. ($\times 10^{-4}$ RAD.)

FIGURE 30B

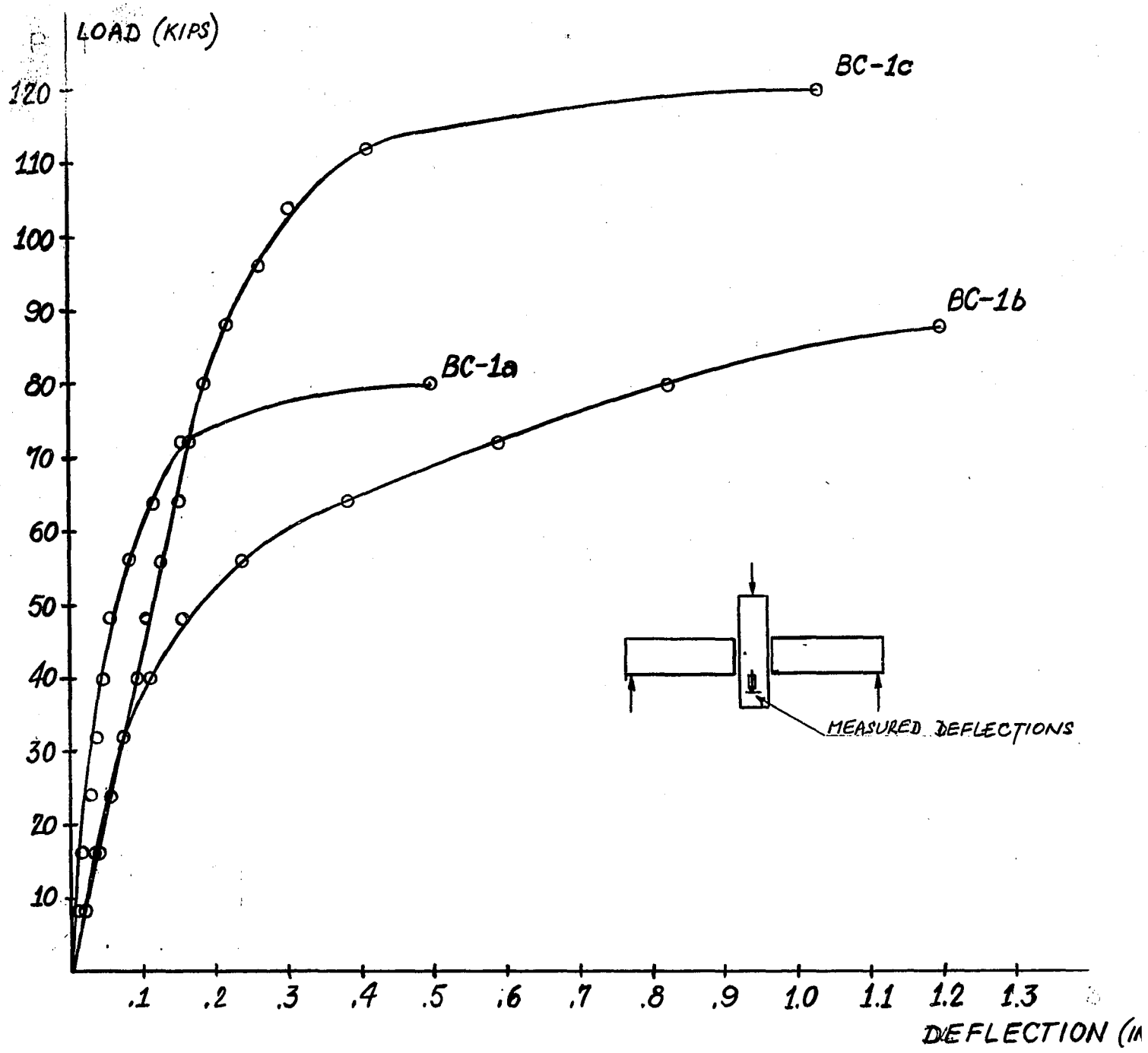

FIGURE 31. - LOAD-DEFLECTION CURVES

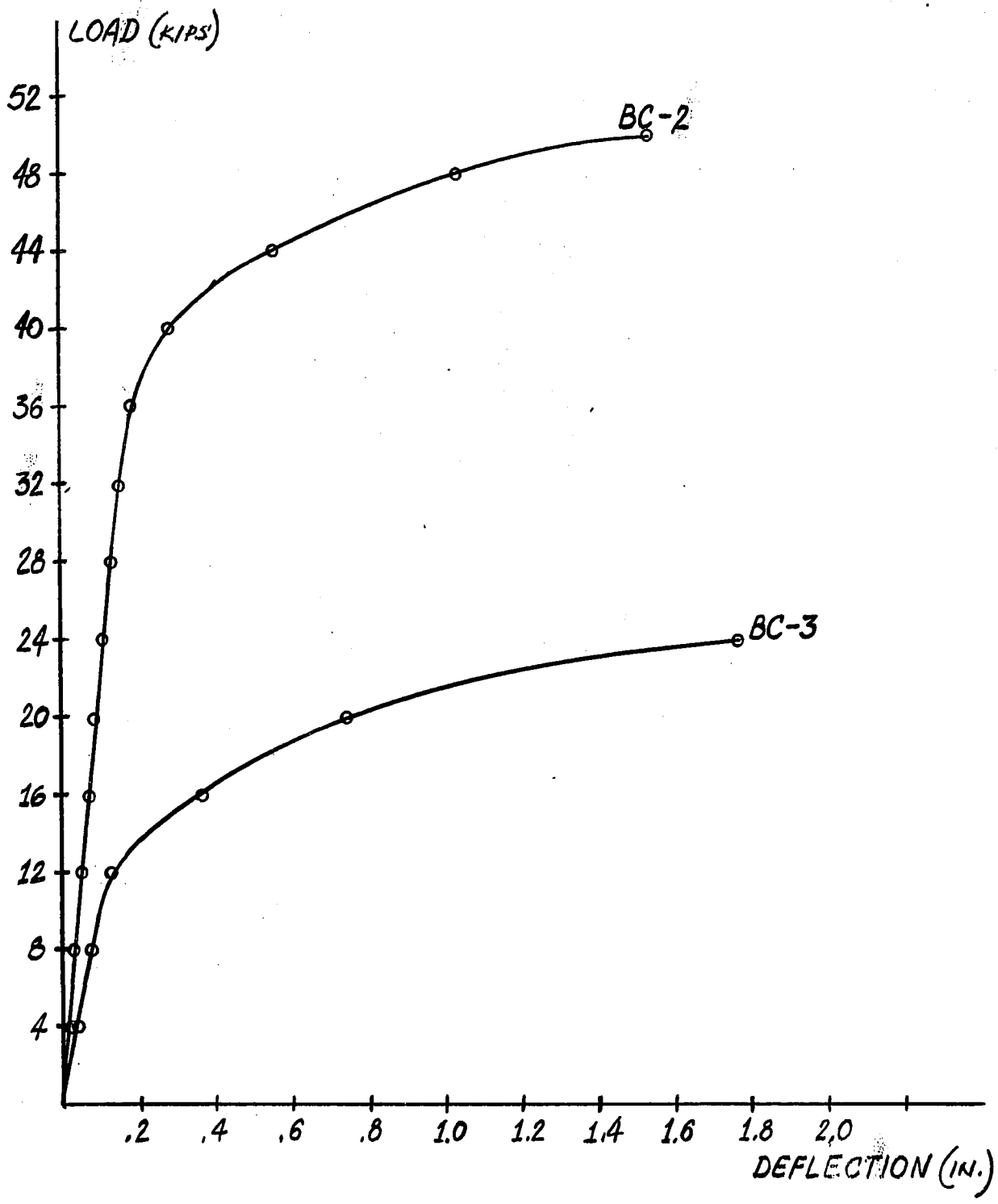

FIGURE 32. - LOAD-DEFLECTION CURVES

CHAPTER VI - ANALYSIS OF TEST RESULTS

6.1 Column-to-Base Connections

a) Moment-rotation behavior

The rotation of this type of connection is influenced by one major variable : the hardware characteristics at the base. Its effect on the M - θ curve is rather evident; a system made of a stiff hardware arrangement will sustain low deformations and will correspondingly yield small rotations. The present experimental program analyses the stiffness characteristics of two different base arrangements and presents the results through overall moment-rotation curves.

Both specimens are tested to failure with a nominal constant moment to axial force ratio of .85. Figure 24 shows the superposed M-θ graphs for the two test specimens. It is noticed that both curves depart from linearity at the origin and display significant ductility, as the load is increased. Except at initial loading, where Type II is shown to be slightly more rigid, the two specimens have almost the same rigidity characteristics, up to ultimate.

Moment-rotation curves for some other column-to-base arrangements are reported in an earlier study.[3] It is found that the curves are made up of two phases. The first one, nearly linear, characterizes the elastic response of the connection; the second one, clearly non-linear starts to develop at the onset of yielding of the reinforcing steel. In the present study, although yielding of the steel is apparent, after

the development and opening of cracks on the tension face, it is not possible to detect these two distinct phases. It is believed that the measuring apparatus was not sensitive enough to record the transition from the linear to the non-linear stage.

For Type I, the deformations of the steel pockets at the base were recorded throughout the testing. Figure 25 shows graphs of moment versus deformation of the pockets on both the tension and compression sides. It is interesting to note that the hardware on the compression side sustained considerable deformations as compared to the tension side, due to the fact that cracks have developed extensively on the tensile face and thus relieved the stresses in the steel hardware.

b) Mode of failure

The crack pattern and the mode of failure were identical for both specimens. Cracks first appeared on the tension side of the column at a moment approximately equal to 30% of the ultimate. They gradually developed toward the compressive zone, as the load was further increased. In the case of Type I, concrete between the pockets and the grout within the pockets on the compression side started to crush at a moment of 140 kips.-ft. (70% of ultimate). The horizontal deflections of the column and the deformations of the pockets were recorded up to a bending moment of 165 kips.-ft. For Type II, the region directly above the brackets on the compression side cracked and scaled off at a moment of 190 kips.-ft. (97% ultimate). Record of

the horizontal deflections of the column was carried until a bending moment of 200 kips.-ft. had been attained.

The two specimens failed by shear at the face of the corbel. At that stage, both connections had undergone significant rotations, as seen on the M-ϕ curves. The bases were damaged to the extent that for all practical purposes, they were considered as inoperative. Figures 34 and 35 show the two prototypes after failure.

FIGURE 33. - COLUMN-TO-BASE CONNECTION. TEST SET UP.

FIGURE 33. - COLUMN-TO-BASE CONNECTION. TEST SET UP.

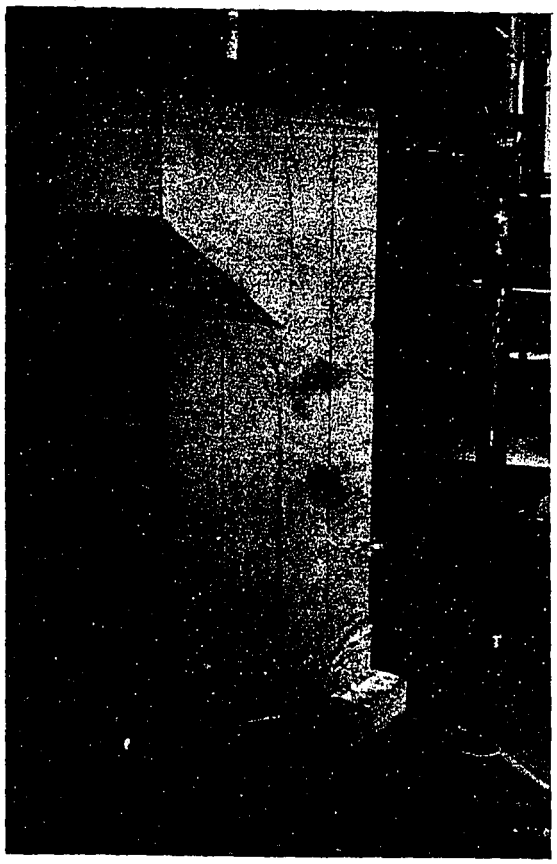

A

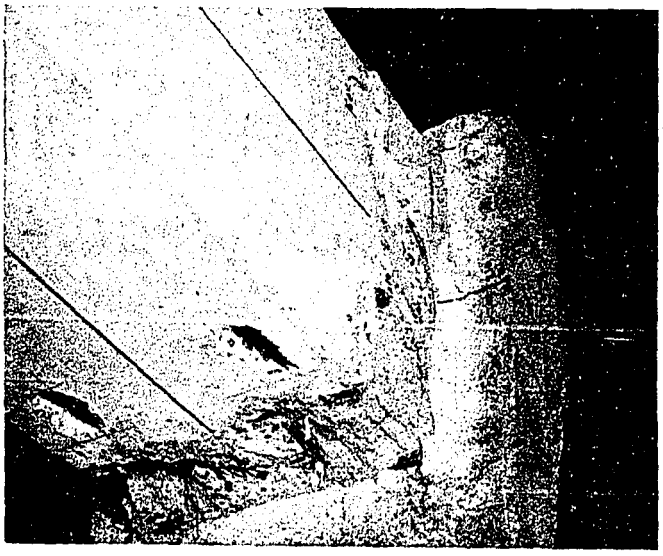

B

FIGURE 34. - COLUMN-BASE TYPE I AFTER FAILURE.

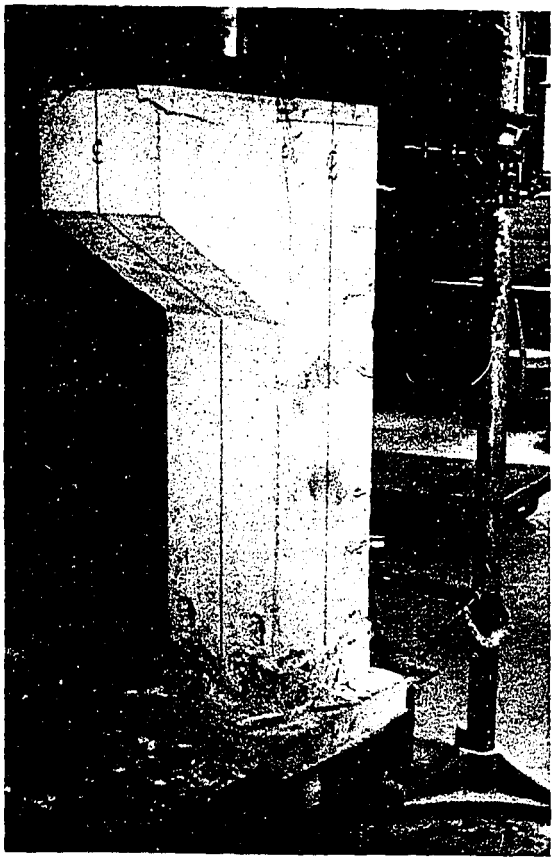

A

B

FIGURE 34. - COLUMN-BASE TYPE I AFTER FAILURE.

A

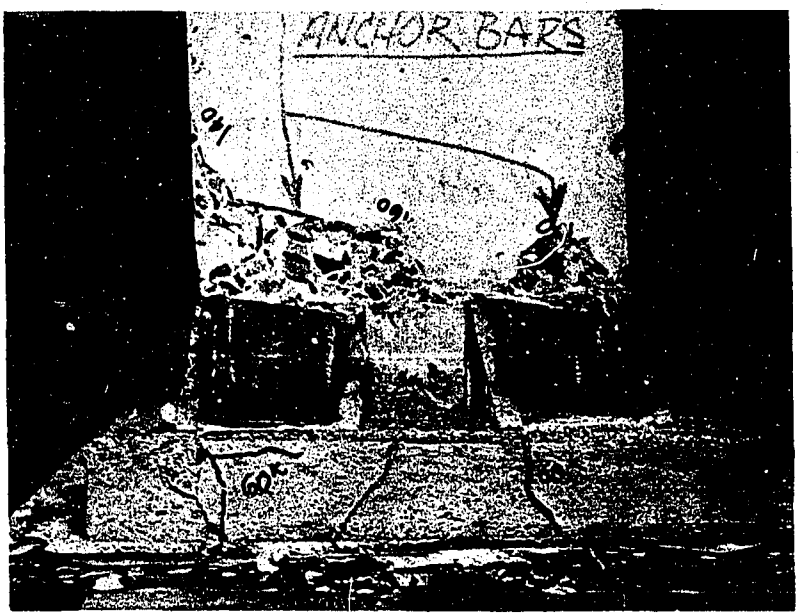

B

FIGURE 35. - COLUMN-BASE TYPE II AFTER FAILURE.

A

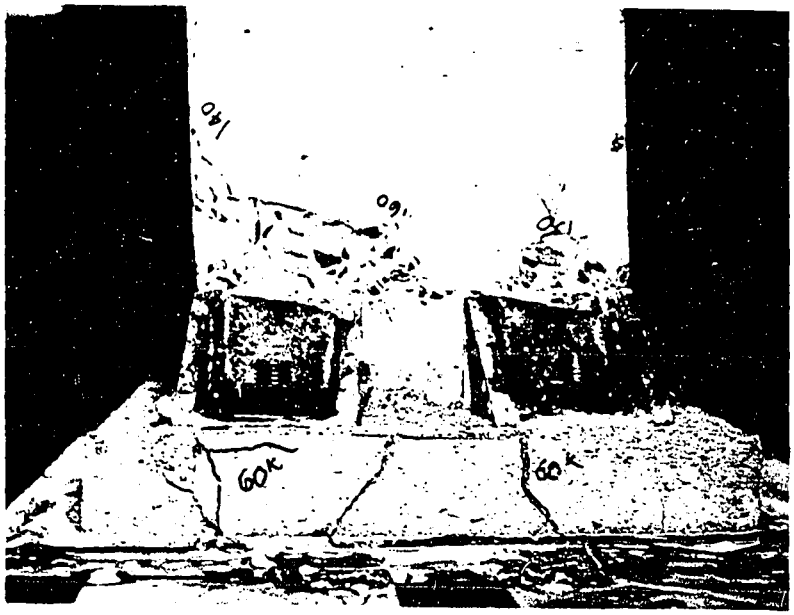

B

FIGURE 35. - COLUMN-BASE TYPE II AFTER FAILURE.

c) Connection fixity

Information of great interest to the designer is the extent of moment transfer developed through the connection. In order to evaluate the fixity characteristics of the system, the following method was used: With the actual cross section of 12" x 15" and a practical length of 20'-0", the M- ϕ characteristics of the column are calculated assuming that the ends are pinned. This theoretical M- ϕ curve is then superposed on the corresponding M-ϕ curve obtained experimentally. The fixity of the connection is estimated as the ratio of the yield moment of the column to the moment developed in the connection, at the same value of ϕ. This ratio, expressed in percentage, gives an indication of the connection rigidity. As shown in Figure 36, fixity ratios of 67% and 70% are obtained for connections Type I and Type II respectively. From these two values it is apparent that the two connections provide the same amount of fixity. For this reason, the selection criterion would be one of base arrangement and as such would be determined by considerations of costs and aesthetics. Calculations of the theoretical rotations are presented in Appendix B.

d) Applicability to design

In the light of the experimental data obtained for these two column-to-base connections, either system would resist an ultimate moment of 180 kips-ft. occurring at the base of a column, in any precast concrete frame. The designer using the connection of his

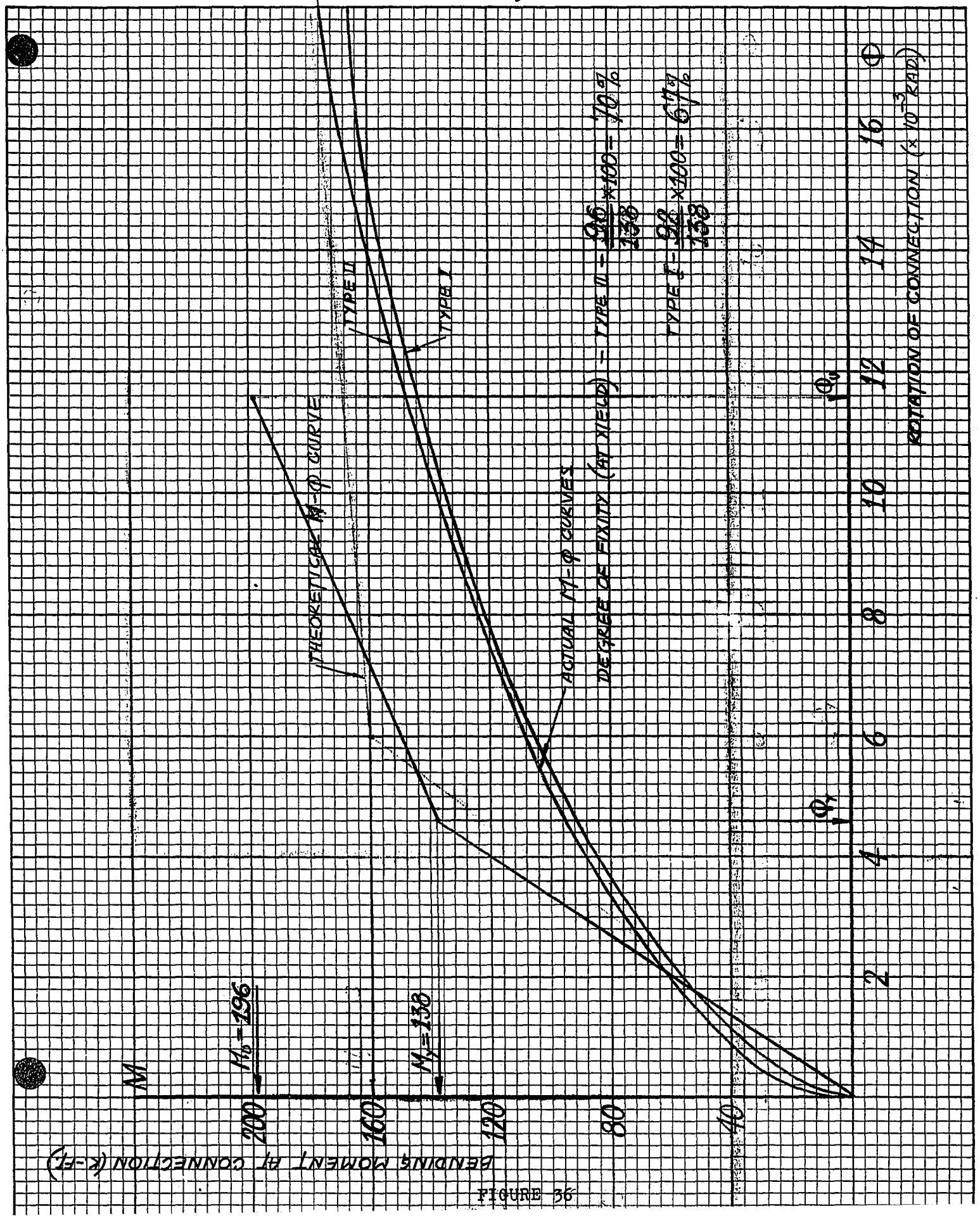
BENDING MOMENT AT CONNECTION (K-FT)
200
160
120
80
40
M_b=196
M_x=138
THEORETICAL M-Φ CURVE
TYPE II
TYPE I
ACTUAL M-Φ CURVES
DEGREE OF FIXITY (AT YIELD) = TYPE II = 196/138 ×100 = 70 %
TYPE I = 96/138 ×100 = 61 %
Φ_y
Φ_x
2
4
6
8
10
12
14
16
ROTATION OF CONNECTION (× 10^{-3} RAD)

FIGURE 36

choice would be convinced of its reliability, having in hand the experimental proof that the selected connection has the capability of transferring this calculated ultimate moment with significant ductility.

6.2 Beam-to-Column Connections

a) Moment-rotation behavior

In the problem of joining beams and columns, the first aim is to obtain an arrangement capable of transferring moments, while satisfying the previously mentioned design requirements. The development of a suitable system is illustrated in Figure 37, where the superposition of the M-θ curves obtained for the first series of prototypes is given. The graphs clearly show the gradual improvement of the connection, from B-C1a to B-C1c. While the three prototypes display the same initial response to load, system B-C1c is seen to offer the best characteristics of initial linearity and subsequent ductility, with higher ultimate capacity.

As mentioned earlier, both specimens B-C2 and B-C3 have the same connection arrangements but are designed to transfer smaller moments. The M-θ curves obtained for these two connections show that they have a noticeably lower stiffness than the first series of tests (B-C1a, B-C1b and B-C1c). This observation is explained in Graph A.

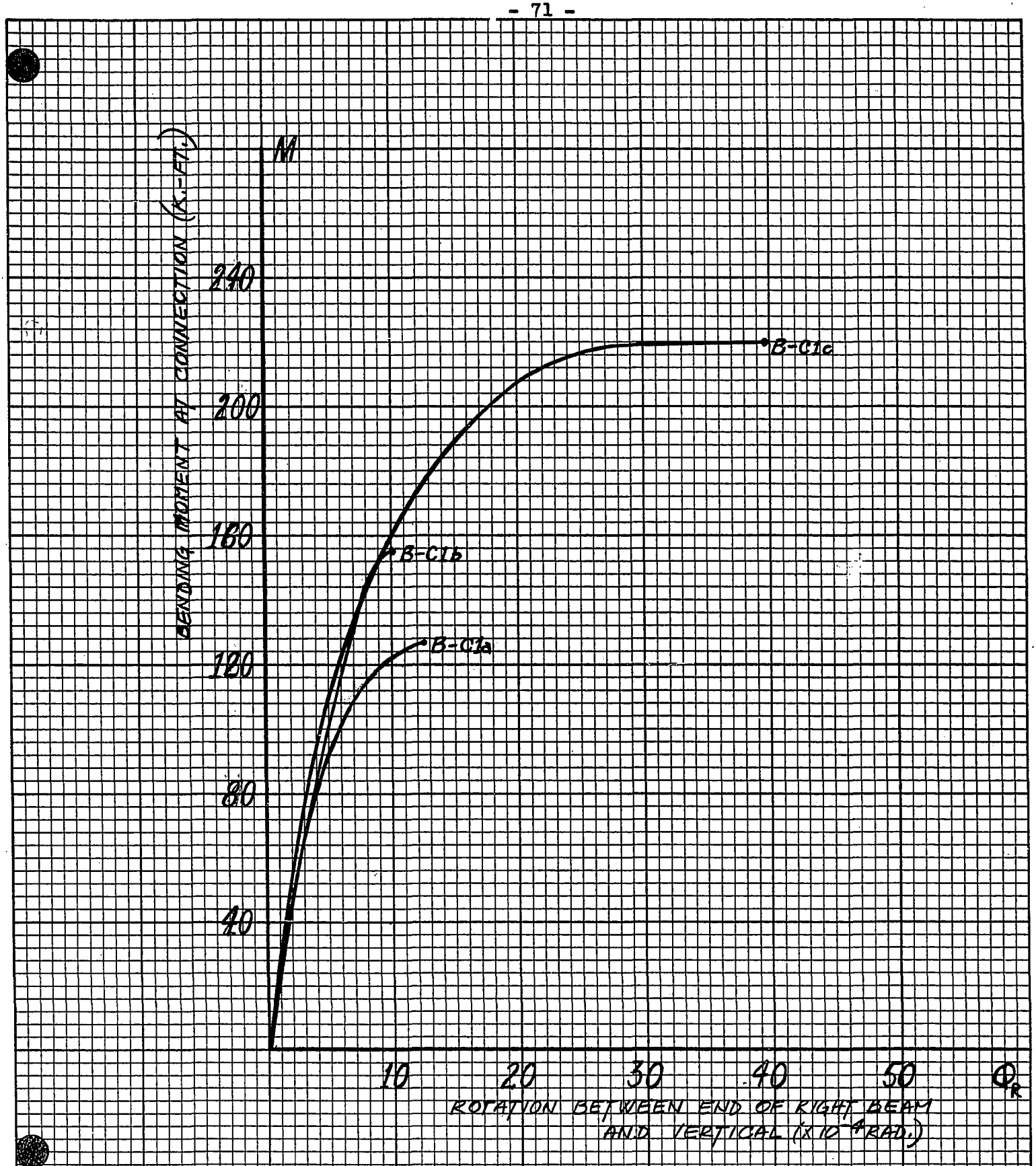
M
BENDING MOMENT AT CONNECTION (K.-FT.)
240
200
160
120
80
40
B-C1c
B-C1b
B-C1a
10
20
30
40
50
Φ_R
ROTATION BETWEEN END OF RIGHT BEAM AND VERTICAL (X 10^{-4} RAD.)

FIGURE 37

M_{yl}, I_{tl} = PROTOTYPE BC-1c

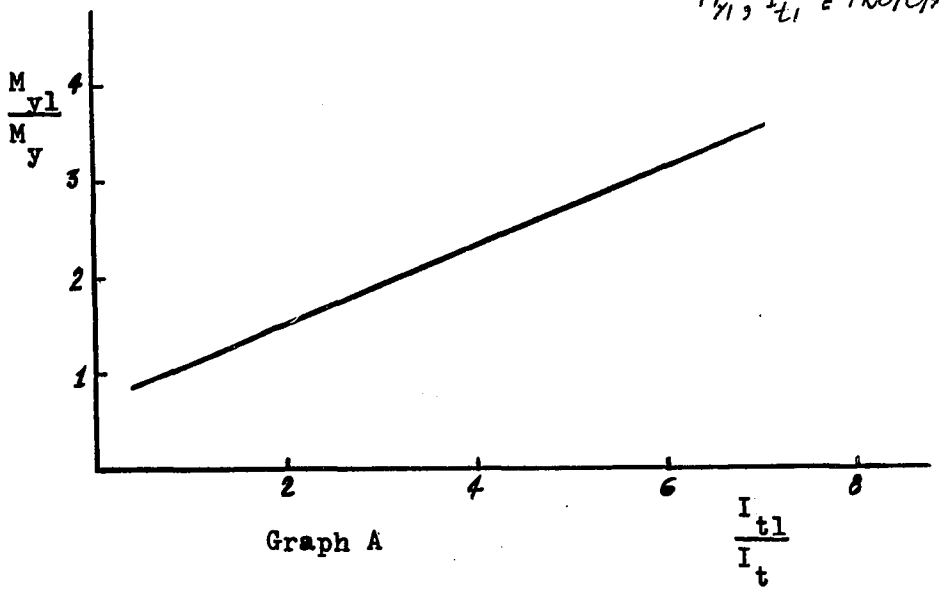

Graph A

Relative ratios of yield moments versus relative ratios of moments of inertia are plotted. As expected, the curve is a straight line having a positive slope; as the five specimens were tested with the same shear to moment ratio of 0.25, sections having the lowest stiffness $EI_{t/L}$ will rotate the most.

Inspection of the moment-rotation curves yields the following observations, as to the behavior of the connections under load:

1 - From the origin to a moment of approximately 50% of the failure value, the curve is seen to be approximately linear.

2 - Under increasing load, the steel components deform, therefore contributing to the rotation, in addition to the cracks developing in the beams. The upper portion of the curve, from 50% of the ultimate moment onwards shows that the specimen has significant ductility.

When cracks propagated beyond the center line of the beams and failure became imminent, all the mechanical dial gages were removed.

Only the DCDT Recorder was maintained on the specimen until failure was reached.

b) Failure mechanisms

The first specimen, B-C1a, failed at a moment approximately equal to 70% of the ultimate design value (189 kips.ft.). Flexural cracks in the beams started to develop at a moment of 85 kips.ft. and gradually propagated toward the compression zone. A moment of 130 kips.ft. had just been developed through the connection when failure occurred. As shown on Figure 38(b), the mode is typical with a crack extending diagonally across the corner of the right beam, from the tip of the tension anchor plate to a vertical distance equal to half the depth of the section. This premature failure is explained by the inadequacy of the link between the longitudinal reinforcement and the plate anchor bars.

The M- ϕ curve obtained for specimen B-C1c demonstrates that the modified design is satisfactory, since the ultimate moment capacity is exceeded and that there exists sufficient ductility. Two vertical bars extending throughout the depth of the section and welded to the top and bottom plates eliminated the development of any diagonal crack such as occurred in B-C1a. The result of this modification is that the connection can develop a higher moment. In fact, failure occurred at a load of 120 kips, developing a moment at the connection equal to 116% of the ultimate design value. The two

longitudinal bars welded to the plate on the tension side failed in a brittle manner, as illustrated in Figure 39(B). At that time, severe damage in the connecting region was noticed; a crack propagated along the vertical bars and suddenly widened when the weld between the vertical bars and the tension plate slipped. Figure 39(A) shows the condition of the connection at failure.

Prototype B-C2 failed at a moment equal to the ultimate design value. The crack pattern was identical as that of B-C1c. In this case the two longitudinal bent up bars snapped in a brittle manner as in B-C1c. Figure 40 shows the deteriorated connection after collapse.

Failure of prototype B-C3 occurred when the butt weld, fixing the loose plate to the column, broke in tension. A moment of 46 kips-ft. (92% of ultimate) had just been reached when the weld broke. No serious deterioration was observed in the other parts of the connection. It is evident that the connection would have carried higher moments if the weld would have been properly applied. Figure 41 shows the specimen after failure.

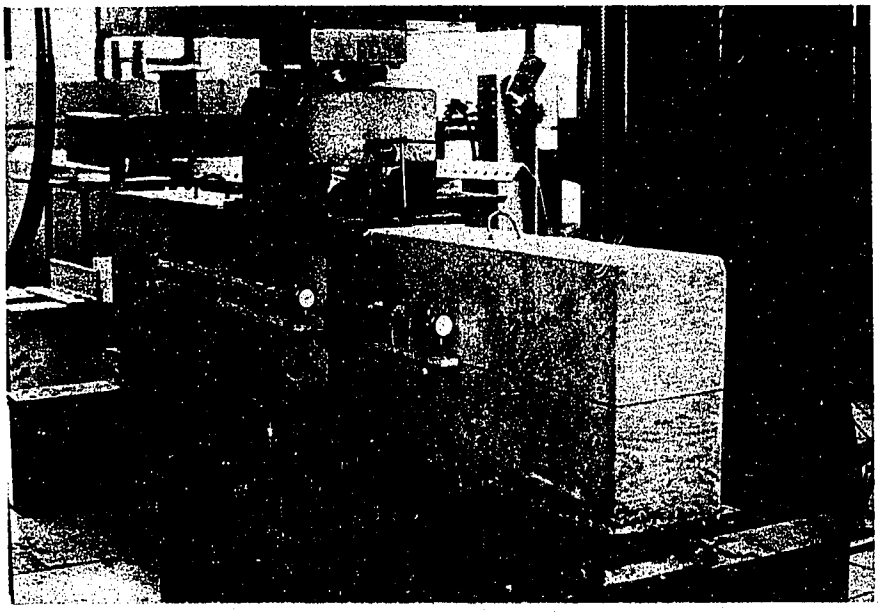

A

BEAM-TO-COLUMN CONNECTION. TEST SET UP

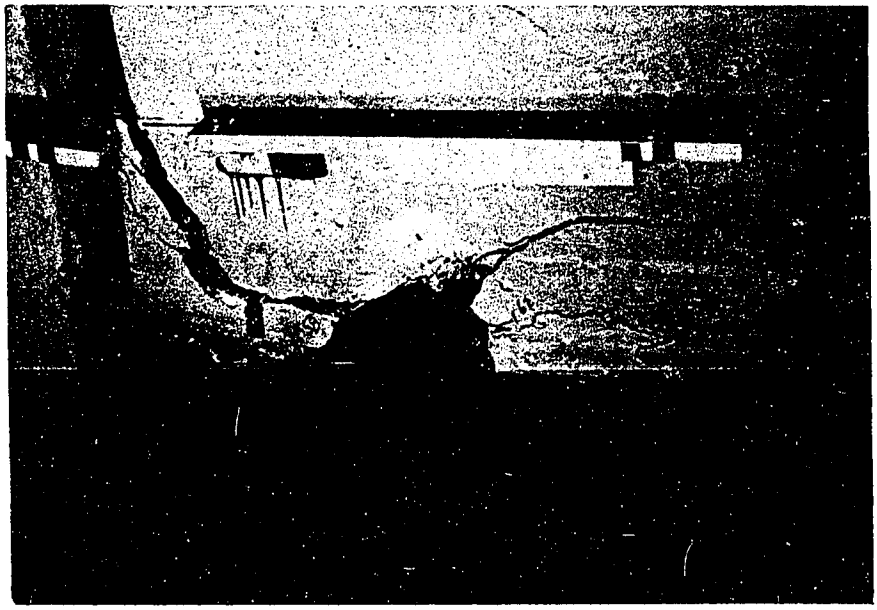

B

FIGURE 38. - PROTOTYPE B-C1a AFTER FAILURE.

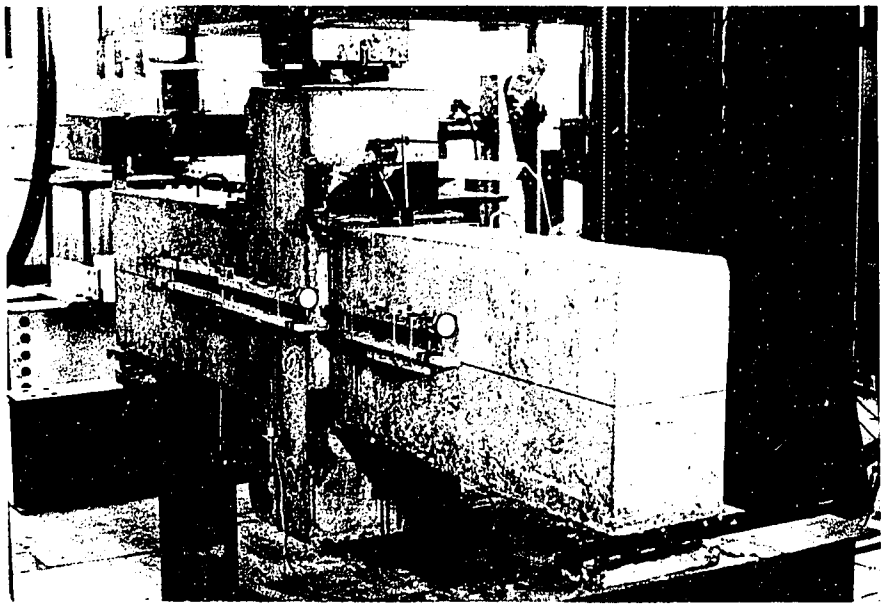

A

BEAM-TO-COLUMN CONNECTION. TEST SET UP

B

FIGURE 38. - PROTOTYPE B-C1a AFTER FAILURE.

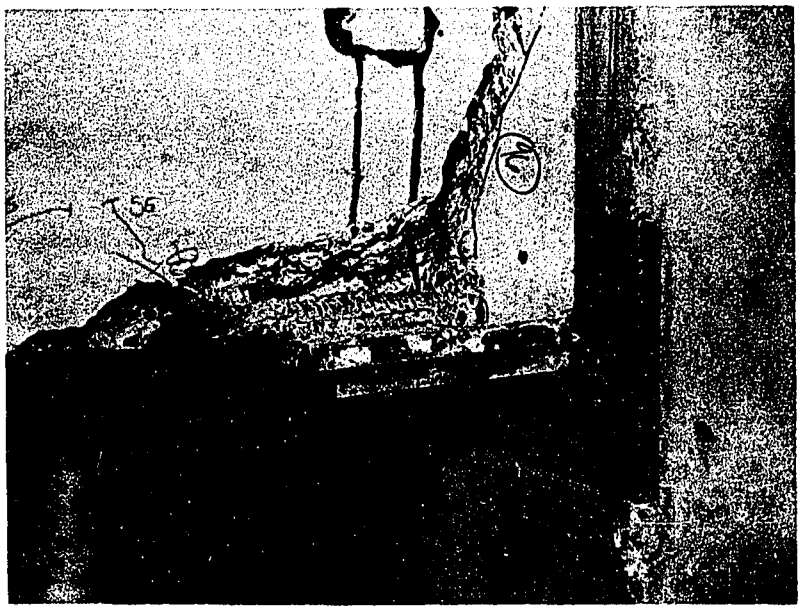

A

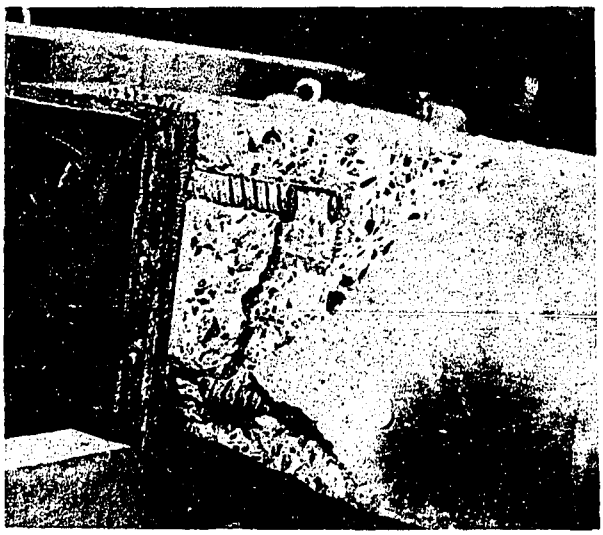

B

FIGURE 39. - PROTOTYPE B-C1c AFTER FAILURE.

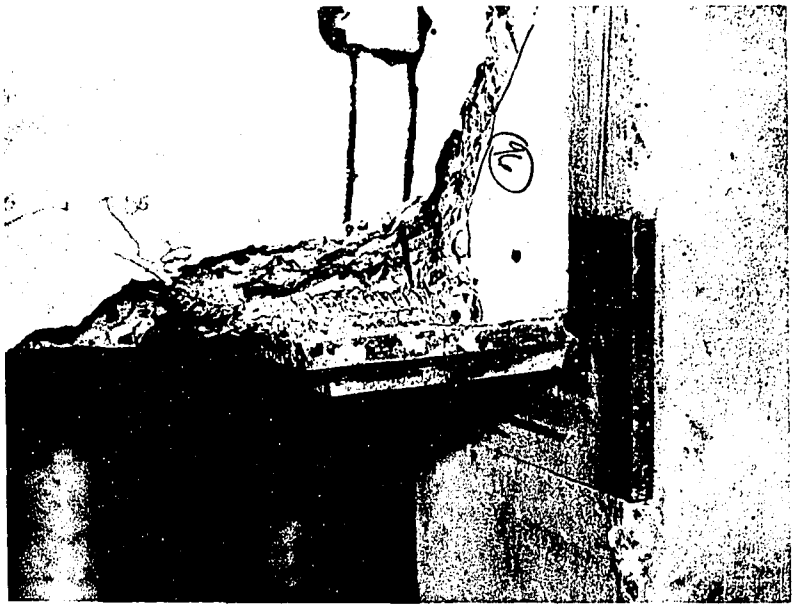

A

B

FIGURE 39. - PROTOTYPE B-C1c AFTER FAILURE.

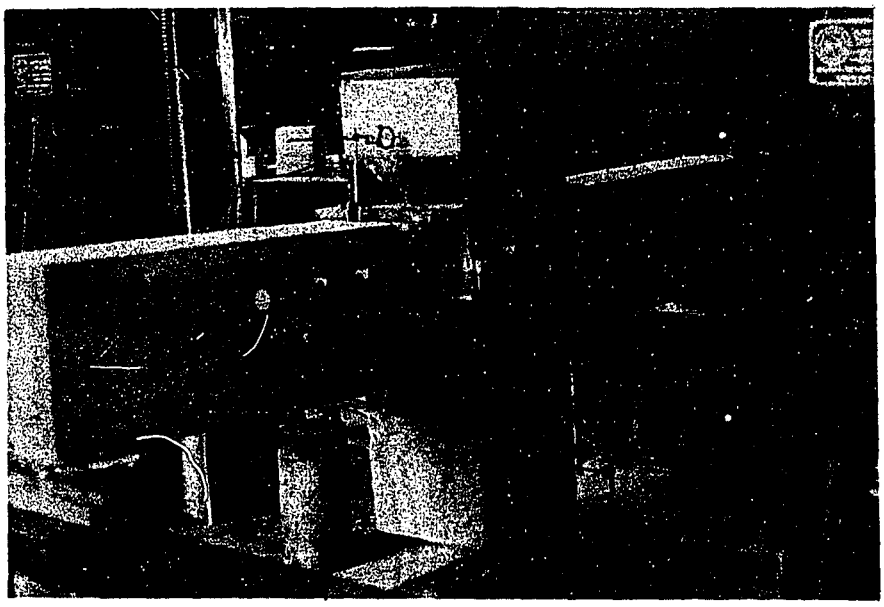

A

B

FIGURE 40. - PROTOTYPE BC-2 AFTER FAILURE.

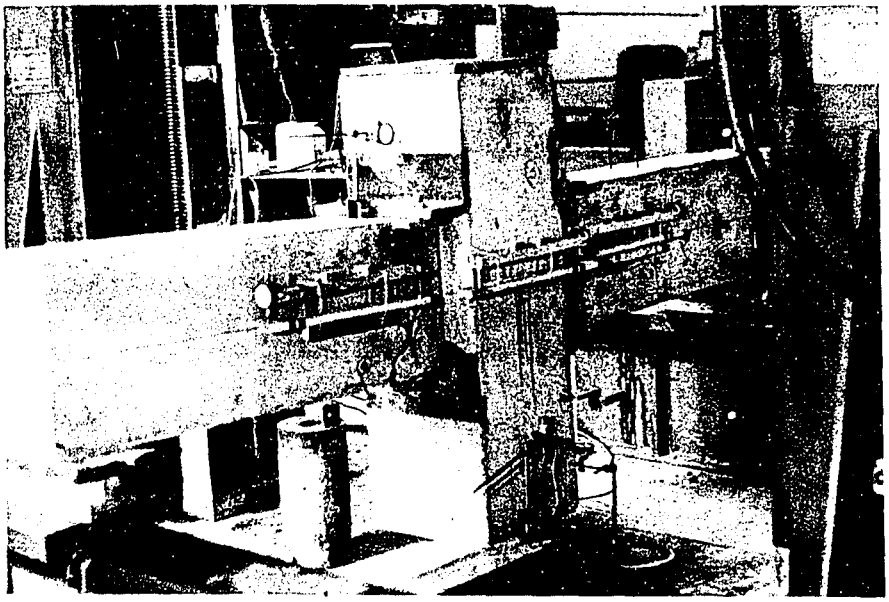

A

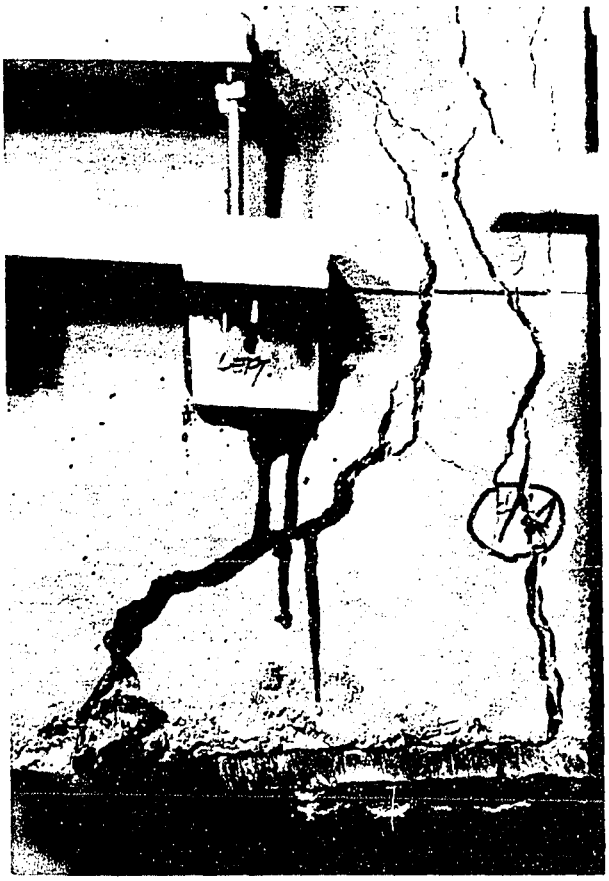

B

FIGURE 40. - PROTOTYPE BC-2 AFTER FAILURE.

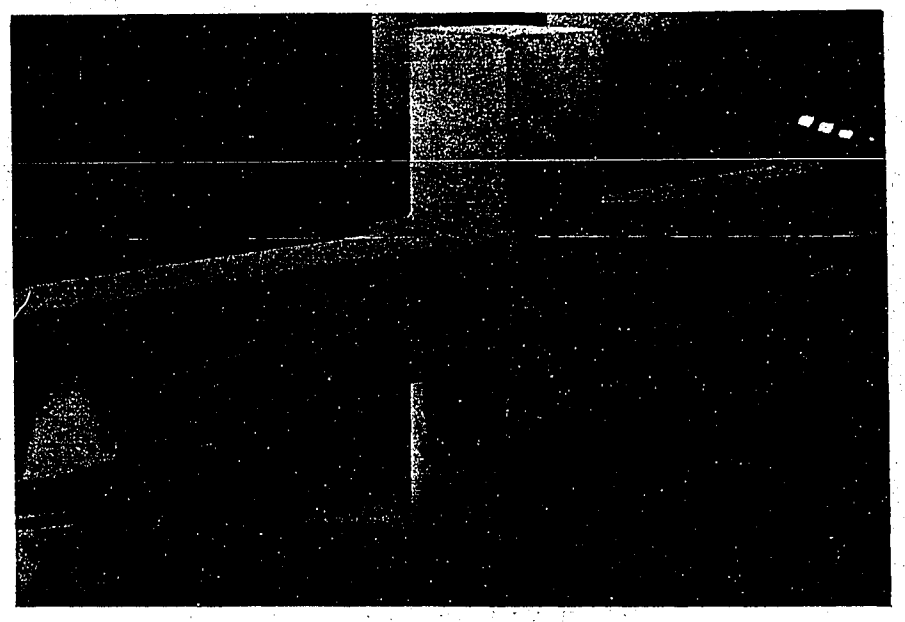

A

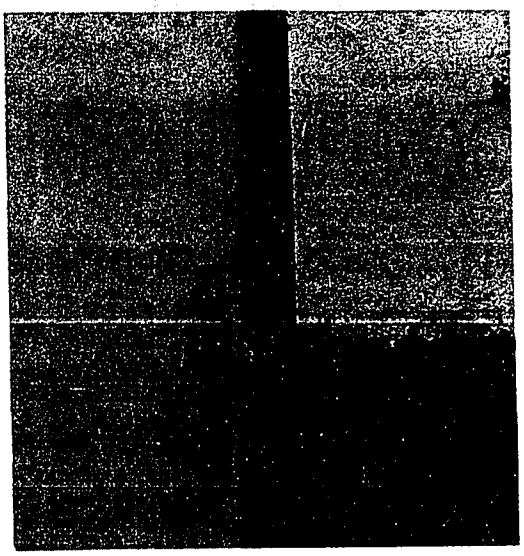

B

FIGURE 41. - PROTOTYPE BC-3 AFTER FAILURE.

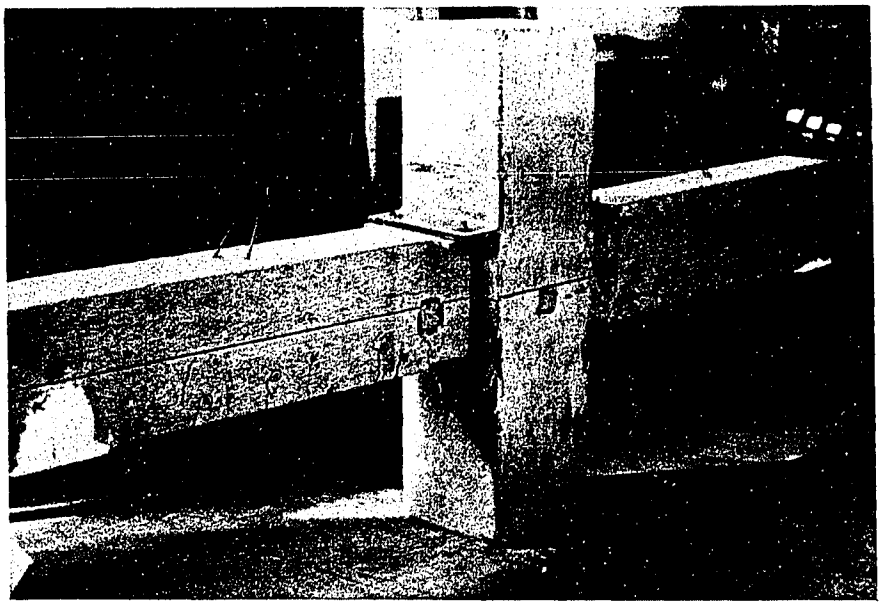

A

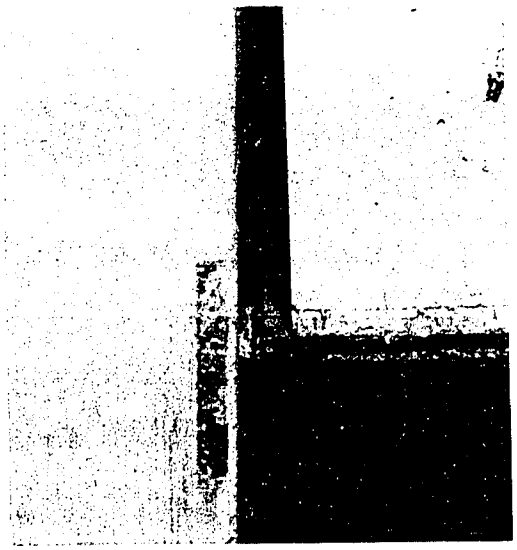

B

FIGURE 41. - PROTOTYPE BC-3 AFTER FAILURE.

An estimate of the connection fixity is now presented in a manner similar to that used in the case of the column-base connections.

c) Connection fixity

The moment transfer capability of the connection prototypes is obtained simply. The theoretical moment-rotation characteristics of a simply supported beam with the same dimensions and reinforcement are compared to the corresponding experimental data. This comparison shows that the introduction of the connection into this beam reduces its stiffness. The reduction is illustrated by the superposition of the M-φ curves obtained in the two cases, as shown in Figure B.

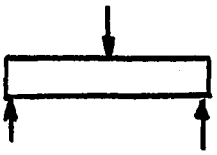

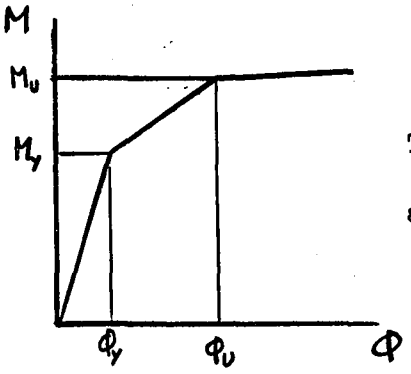

Theoretical M-φ curve.

a - Simply supported beam

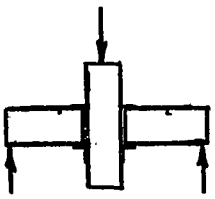

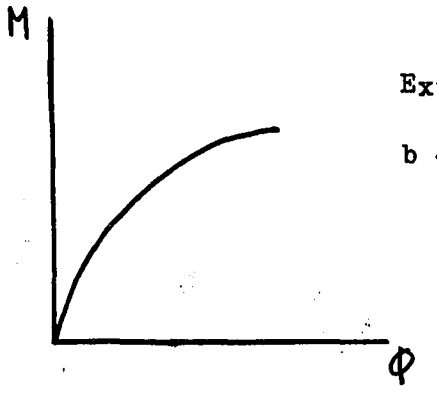

Experimental M-φ curve.

b - Same simply supported beam with connection introduced at mid-span.

c-Superposing the two curves.

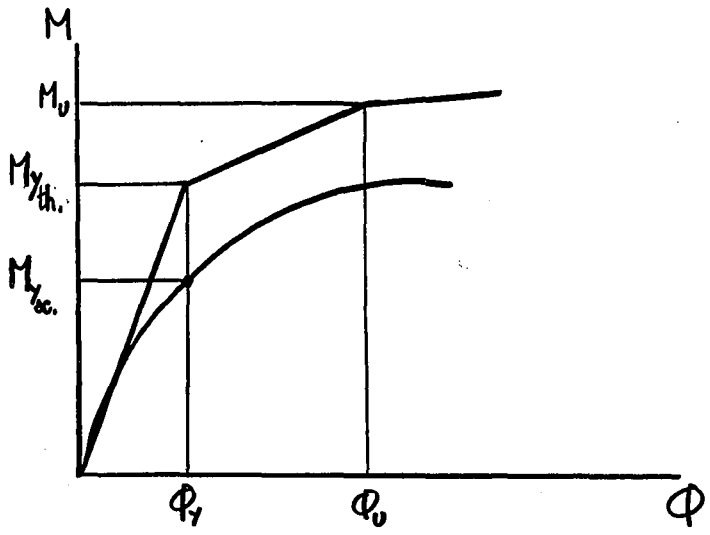

$\frac{My_{th.}}{My_{ac.}}$ = degree of fixity of the connection (%)

FIGURE B

To maintain similarity between the two systems the calculated quantities must correspond to those measured during testing. For instance the computed rotations have to be the ones actually occurring at a section situated 40 inches from the support, as measured in the laboratory. The values of the moments at yield and at ultimate are calculated using Mattock's method [16]; the corresponding rotations at yield or just prior to are obtained by the conjugate beam method [17]. The rotations at ultimate are estimated by Mattock's[16] formula for the ultimate curvature which is then transformed to a rotation taking place in the length of the beam (40 inches). The calculations are presented in Appendix B.

In the following Figures (42, 43, 44) M-Φ curves for the right and the left beams of each connection are superposed on the corresponding theoretical M-Φ curve. As for the column-to-base connections, an estimate of the connection fixity for each system is given. Connection B-C1c has a

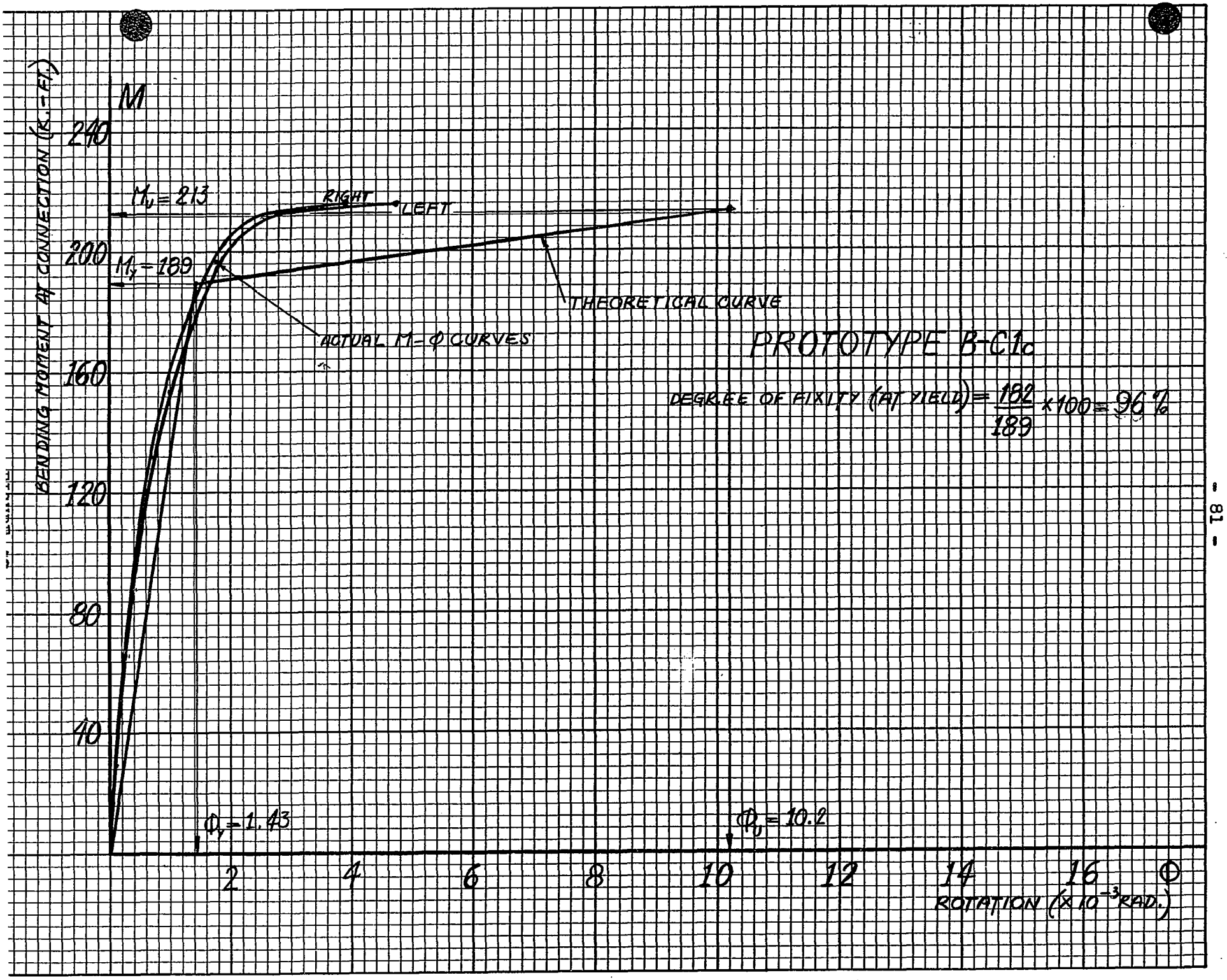
M
BENDING MOMENT AT CONNECTION (K.-FT.)
240
200
160
120
80
40
$M_u = 213$
$M_y = 189$
RIGHT
LEFT
THEORETICAL CURVE
ACTUAL M-Φ CURVES
PROTOTYPE B-C1c
DEGREE OF FIXITY (AT YIELD) = $\frac{182}{189} \times 100 = 96\%$
$\Phi_y = 1.43$
$\Phi_u = 10.2$
2
4
6
8
10
12
14
16
Φ
ROTATION ($\times 10^{-3}$ RAD.)

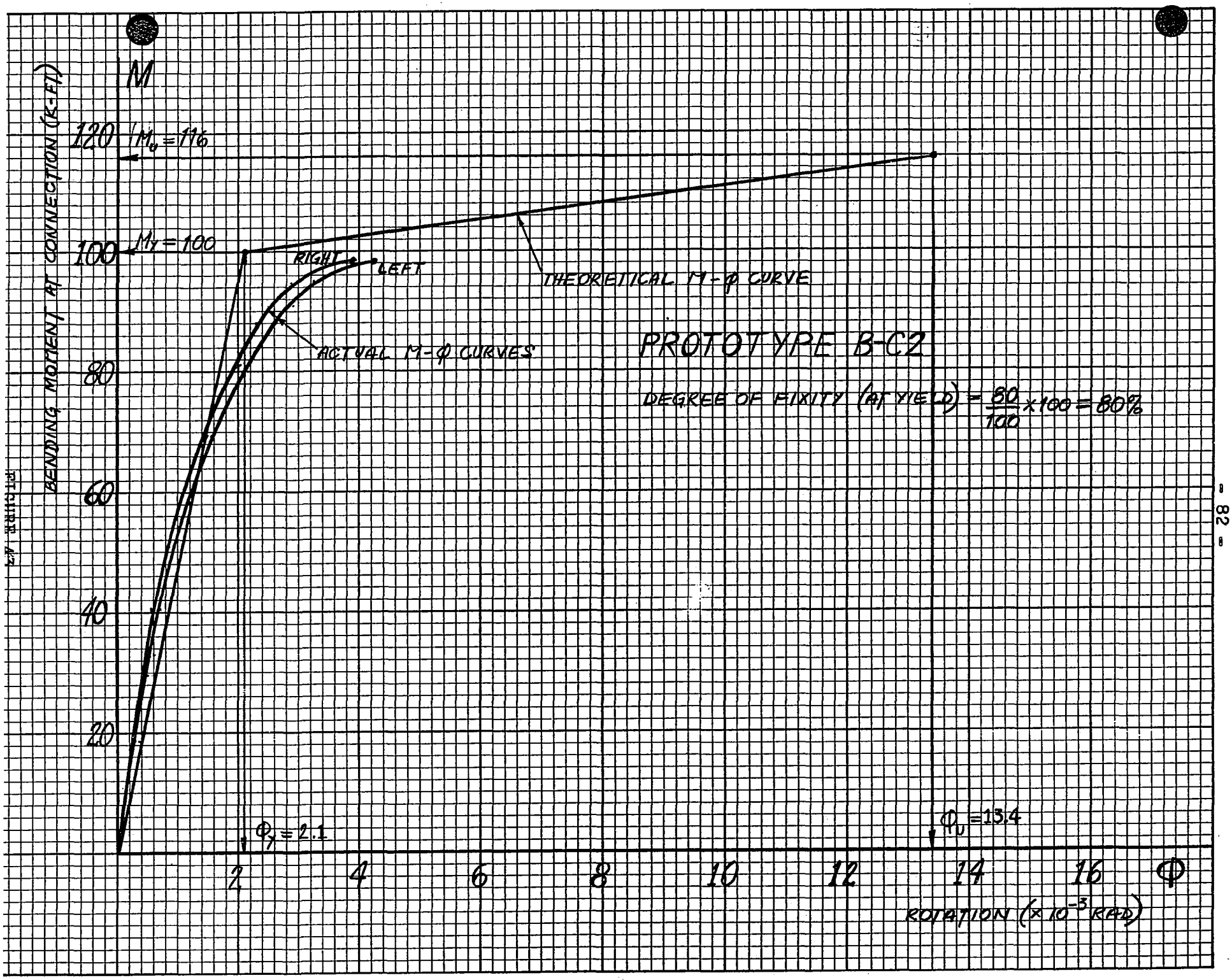
M
BENDING MOMENT AT CONNECTION (K-FT)
120
100
80
60
40
20
$M_u = 116$
$M_Y = 100$
RIGHT
LEFT
THEORETICAL M-φ CURVE
ACTUAL M-φ CURVES
PROTOTYPE B-C2
DEGREE OF FIXITY (AT YIELD) = $\frac{80}{100} \times 100 = 80\%$
$\phi_Y = 2.1$
$\phi_U = 13.4$
2
4
6
8
10
12
14
16
φ
ROTATION ($\times 10^{-3}$ RAD)

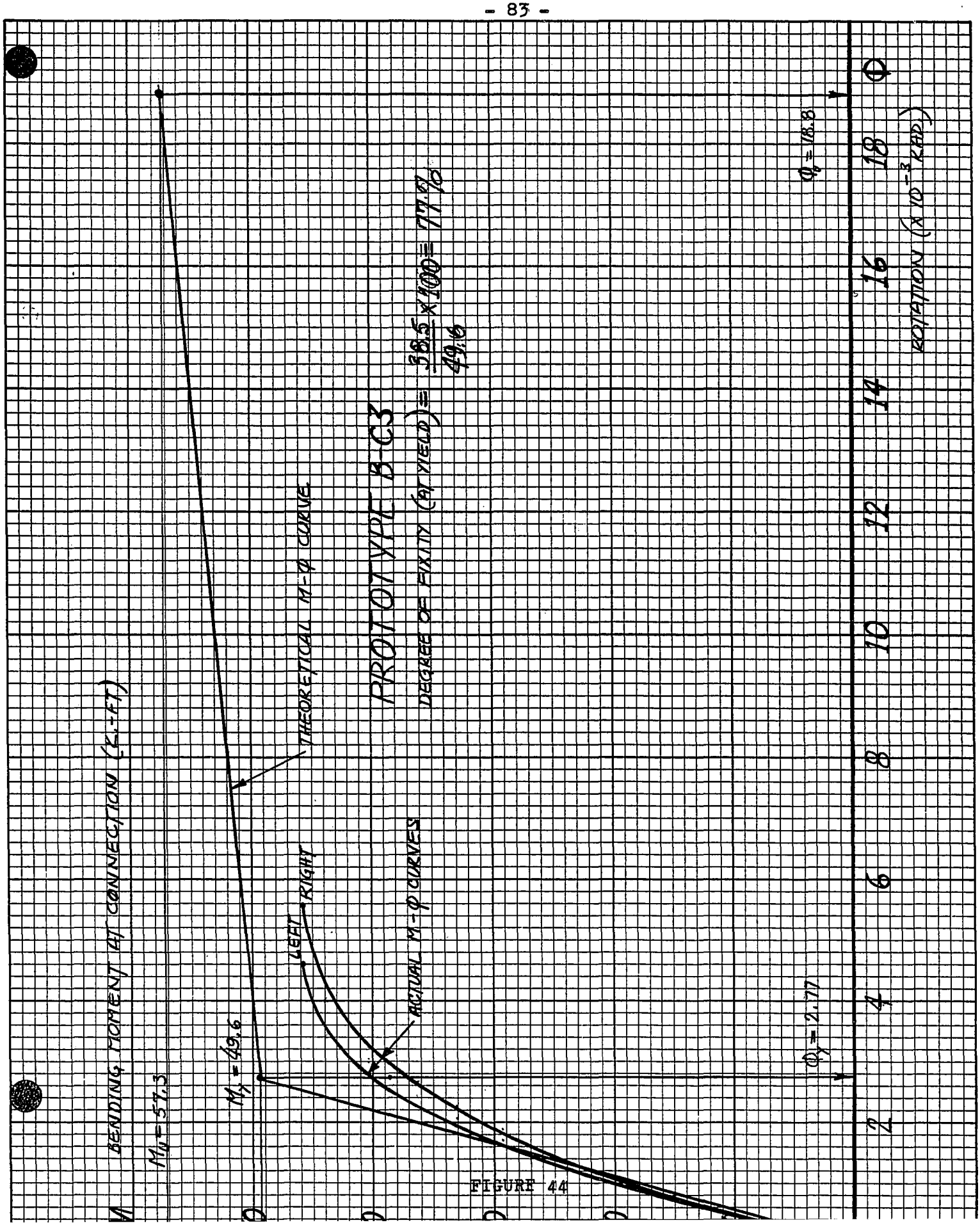
PROTOTYPE B-C3
DEGREE OF FIXITY (@ YIELD) = 36.5/49.6 × 100 = 77.1%
BENDING MOMENT AT CONNECTION (K.-FT.)
M_y = 57.3
M_1 = 49.6
THEORETICAL M-φ CURVE
ACTUAL M-φ CURVES
LEFT
RIGHT
ϕ_y = 2.77
ϕ_u = 18.8
ROTATION (X 10^{-3} RAD.)
0
2
4
6
8
10
12
14
16
18

FIGURE 44

degree of fixity equal to 96%. Values of 80% and 77% are obtained for BC2 and B-C3, respectively.

d) Applicability to design

This investigation has established the ultimate moment transfer capacity of three different sizes of a typical beam-to-column connection. With the same general arrangement, these three prototypes have shown to adequately resist moments that could be present in a precast reinforced concrete frame building.

In engineering practice, typical ultimate moments of 200 kips.-ft., 100 kips.-ft. and 50 kips.-ft. occurring at joints in a multi-story building could be resisted respectively by connections B-C1c, B-C2 and BC-3. As in the case of column-to-base, the designer who decides to use the connection arrangement studied in this thesis would be convinced of its structural efficiency, his choice being backed up by experimental data.

e) Material quantities and weights

For each connection, quantities and weights of the connecting hardware are given. For the sake of interest the cubic yardage of concrete per linear foot for each specimen is also presented. From these figures the fabricator can estimate his own labour time and various costs.

ITEM	B-C1c			B-C2			B-C3		
	Column	Beams	Total	Column	Beams	Total	Column	Beams	Total
1 - Steel Angle (lbs)	100		100	100		100	35		35
2 - Steel Plate (lbs)	27	131	158	27	70	97	119	35	54
3 - Anchor Bars (lbs) (No reinf. incl.)	71	18	89	71	13	84	12	6	18
4 - Total Hardware weight			367			301			107
5 - Fillet Weld (ins.) (3/8" Typ.) (Length, Ext. & Int.)	180	189	369	180	110	290	92	92	184
6 - Butt Weld (ins.)	(3/4") 22		22	(5/8") 16		16	(1/2") 12		12
7 - Concrete (Cu. Yd./lin. ft.)	0.26	0.26	0.52	0.26	0.19	0.45	0.17	0.09	0.26
8 - Rein. Steel (lbs) (Bars and Stir.)	89	142	231	89	100	189	50	84	134
9 - Total Spec. Weight (lbs)			2700			2310			1440

CHAPTER VII - CONCLUSIONS

Based on the test results obtained in this study, the following conclusions are drawn.

7.1 Column-to-Base Connections

a) The two column-to-base arrangements, Type I and Type II present the same moment-resisting characteristics. Both are shown to resist the ultimate design moment of 138 kips-ft. with a rigidity factor of approximately 70%. Significant ductility is displayed by both systems before collapse occurs.

b) Either system can be used in a building where such a moment is to be resisted at the column base. The choice of the arrangement is left to the designer and could be one of aesthetics.

7.2 Beam-to-Column Connections

a) This connection arrangement is proportioned following various design criteria pertaining to the precast concrete construction. The test results show that the arrangement adequately resists the ultimate design moment and displays some ductility, prior to failure.

b) The steel parts of the connection did not deform significantly under loading. In all cases, failure occurred after numerous cracks had developed and propagated in the connection region of the beams. The column stubs remained unaltered.

c) Degrees of fixity of 96%, 80% and 77% are obtained respectively for prototypes BC-1a, BC-2 and BC-3. The structural characteristics of each specimen are presented in the form of moment-rotation curves.

d) Ultimate design moments of the same magnitude as those considered and occurring at any joint in a building frame can be resisted by the appropriate connection. The experimental M-φ curve is a reliable proof of the structural adequacy of the connection under consideration.

e) Extensive welding between the units does not apparently affect the structural characteristics of the system. However care must be taken that the welding is performed after sufficient hydration has taken place. The assembly can be safely done after the time required for the complete development of the specified f'_c has elapsed.

f) Continuous and tackwelding performed on the reinforcing steel bars does not affect the yield stress but reduces the ultimate strain by about 65%.

This experimental work may constitute the basis of many complementary projects. The next chapter summarizes a few subjects toward which future work may be oriented.

CHAPTER VIII - FUTURE WORK

a) In current engineering practice, the hardware characterizing the connection is proportioned such that it transfers the ultimate loads, according to the ACI and NBC specifications. The research worker may be interested in knowing the stress distribution in the external and internal steel components of the joint. Such a study would permit to establish more definite design criteria and would subsequently lead to the dimensioning of a lighter and more economical connection. This would necessarily take the form of an experimental study since the theoretical considerations would be quite hard to handle.

b) A study of the stresses due to creep and shrinkage on the connected members once the ends are restrained will lead to some useful observations. This is an important aspect in design.

c) It may also be of interest to establish the amount of displacement of a typical joint and the deformation induced in the members of an actual building frame when the welding of the units is performed. It is easily visualized that the expansion of the steel parts due to welding brings about a stress distribution which could have some important secondary effects on the frame as a whole.

CHAPTER IX - BIBLIOGRAPHY

1 - Proceedings of the Symposium on design for earthquake Loadings. - McGill University, 1966.

2 - Eberbach, D.E., "An Investigation of Base Restraints of Precast Reinforced Concrete Columns", Unpublished Thesis, University of Toronto, (1959).

3 - LaFraugh, R. W. and Magure, D.D., "Connections in Precast Concrete Structures - "Column-Base Plates," Journal of the PCA, Vol. II, No. 6, Dec. 1966.

4 - Birkeland, P.W. and Birkeland, H.W., "Connections in Precast Concrete Construction", Journal of the ACI, title No. 63-15, March 1966.

5 - Holmes, H. and Bond, D., "Test on a Beam-to-column Connection for Precast Concrete", The Structural Engineer, Vol. 41, No. 9, Sept. 1963, pp.293-297.

6 - PCI Committee on Connection Details, "Connection Details for Precast-Prestressed Concrete Buildings", Prestressed Concrete Institute, Oct. 1963.

7 - ACI - ASCE Committee 512, "Suggested Design of Joints and Connections in Precast Structural Concrete", Journal of the ACI - Vol. 61, No. 8, Aug. 1964, pp. 921-937.

8 - Casaly, L. and Huggins, M. W., "Canadian Prestressed Concrete Institute Handbook", T. H. Best Printing Company Limited, Don Mills, Ontario - Apr. 1964.

9 - American Concrete Institute, "ACI Building Code", April 1963.

10 - National Research Council, "National Building Code", Canada, 1965.

11 - Mattock, H., Ferguson, P. M. and Thompson, J. N., "Damage Due to Welding Between Precast Concrete Units", U.S. Naval Civil Engineering Research and Evaluation Laboratory, Port Hueneme, California, Oct. 1953.

12 - Mattock, H., Toprac, A. A. and Thompson, J. N., "Evaluation of Damage Due to Welding Between Precast Concrete Units", U.S. Naval Civil Engineering Research and Evaluation Laboratory, Port Hueneme, California, Oct. 1953.

13 - Canadian Institute of Steel Construction, "Handbook of Steel Construction", CSA Standard S16, para. 23, 1967.

14 - Kriz, L. B. and Raths, C. H., "Connections in Precast Concrete Structures - Strength of Corbels", Journal of the Prestressed Concrete Institute, Vol. 10, No. 1, Feb. 1965, pp. 16-61; PCA Development Department Bulletin D85.

15 - Beedle, L.S., Editor, "Structural Steel Design", Ronald Press, N.Y., 1964.

16 - Mattock, A. H., "Rotational Capacity of Hinging Regions in Reinforced Concrete Beams", Proceedings of the International Symposium, Flexural Mechanics of Reinforced Concrete, ACI SP-12, Nov. 1965.

17 - Sloane, A., "Mechanics of Materials", Dover Publications Inc., New York, 1967.

18 - Galan, A., "Estimate of Concrete Strength by Ultrasonic Pulse Velocity and Damping Constant", ACI Journal, Title No. 64-59, October 1967.

19 - Richart, F.E. and Staehle, G. C., "Column Tests at University of Illinois", Journal ACI, 2, Feb., Mar. 1931; Proc., 27, pp. 731, 761; Journal ACI, 3, Nov. 1931, Jan. 1932; Proc. 28, pp. 167, 279.

20 - Hognestad, E., "A Study of Combined Bending and Axial Load in Reinforced Concrete Members", University of Illinois, Eng. Exp. Sta. Bull. No. 267, 1934.

APPENDIX A

MOMENT-ROTATION (M-φ) CALCULATIONS

1) Column-to-Base Connections

The rotation of the connection is computed from the horizontal deflections recorded by dial gages No. 2, 3 and 4, as shown on the following sketch. The average value of these three readings is taken as the rotation.

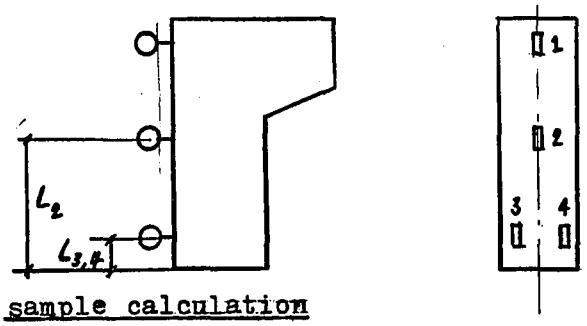

FIGURE A

sample calculation

from the table of readings, column-base type I.

a) for a moment of 20 k.-ft.

$$\Delta_2 = .008" \ , \quad L_2 = 24"$$

$$\tan \varphi_2 = \frac{\Delta_2}{L_2} = \frac{.008}{24} = .00033 \ ; \quad \varphi_2 = .00033$$

$$\Delta_{3,4} = .005" \ , \quad L_{3,4} = 8"$$

$$\varphi_{3,4} = \frac{\Delta_{3,4}}{L_{3,4}} = \frac{.005}{8} = .00062 \ ; \quad \varphi_{3,4} = .00062$$

$$\text{now average} \quad \varphi = \frac{\varphi_2 + \varphi_{3,4}}{2}$$

$$\varphi = \frac{.00033 + .00062}{2} = .000475 \text{ rad.}$$

COLUMN-BASE TYPE I - ECCENTRICITY = 8 INCHES								
Load (Kips)	Moment (K.-ft.)	Δ_1 (In.)	Φ_1 (rad.)	Δ_2 (in.)	Φ_2 (rad.)	$\Delta_{3,4}$ (in.)	$\Phi_{3,4}$ (rad.)	Av. Φ_2 & $\Phi_{3,4}$ (rad.)
0	0	.000	.0000	.000	.0000	.000	.0000	.0000
10	6.66	.014	.0003	.002	.00008	.001	.0001	.00009
20	13.33	.030	.0007	.005	.0002	.003	.0004	.0003
30	20.00	.046	.0010	.008	.0003	.005	.0006	.0005
40	26.66	.062	.0014	.014	.0006	.007	.0009	.0007
50	33.33	.077	.0017	.022	.0009	.010	.0013	.0011
60	40.00	.094	.0021	.030	.0013	.012	.0015	.0014
70	46.66	.114	.0026	.039	.0016	.015	.0019	.0018
80	53.33	.134	.0030	.049	.0020	.018	.0022	.0022
90	60.00	.155	.0035	.063	.0026	.018	.0022	.0024
100	66.66	.181	.0041	.074	.0031	.025	.0031	.0031
110	73.33	.202	.0046	.086	.0036	.029	.0036	.0036
120	80.00	.228	.0052	.098	.0041	.033	.0041	.0041
130	86.66	.254	.0058	.112	.0047	.038	.0043	.0045
140	93.33	.285	.0068	.127	.0053	.042	.0052	.0052
150	100.00	.317	.0072	.145	.0060	.047	.0059	.0060
160	106.66	.355	.0081	.164	.0068	.047	.0069	.0069
170	113.33	.394	.0090	.181	.0075	.060	.0075	.0075
180	120.00	.426	.0097	.205	.0085	.067	.0084	.0085
190	126.66	.475	.0108	.240	.0100	.078	.0097	.0099
200	133.33	.530	.0120	.267	.0121	.088	.0110	.0110
210	140.00	.595	.0135	.323	.0135	.096	.0120	.0127
220	146.66	.686	.0155	.380	.0158	-	-	.0158
230	153.33	.805	.0183	.466	.0194	-	-	.0194

COLUMN-BASE TYPE 11 – ECCENTRICITY = 10 INCHES

Load (Kips)	Moment (K.-ft.)	Δ_1 (In.)	Φ_1 (rad)	Δ_2 (in.)	Φ_2 (rad.)	$\Delta_{3,4}$ (in.)	$\Phi_{3,4}$ (rad.)
0	0	.000	.0000	.0000	.0000	.0000	.0000
10	8.33	.001	.0001	.0001	.00005	.001	.00004
20	16.66	.009	.0002	.002	.0001	.004	.00008
30	25.00	.016	.0004	.007	.0003	.007	.0003
40	33.33	.022	.0005	.012	.0005	.015	.0006
50	41.66	.035	.0008	.024	.0009	.023	.0009
60	50.00	.044	.0020	.036	.0015	.031	.0013
70	58.33	.185	.0042	.049	.0020	.036	.0015
80	66.66	.458	.0104	.055	.0023		
90	75.00	.633	.0144	.065	.0027		
100	83.33	.761	.0173	.086	.0036		
110	91.66	.844	.0192	.097	.0041	.037	.0016
120	100.00	.872	.0197	.122	.0051	.047	.0019
130	108.33	.880	.0200	.146	.0060	.059	.0025
140	116.66	.906	.0206	.167	.0070	.075	.0031
150	125.00	.915	.0208	.183	.0076	.094	.0039
160	133.33	.927	.0211	.223	.0093	.108	.0045
170	141.66	.990	.0225	.253	.0104	.121	.0050
180	150.00	1.108	.0246	.288	.0120	.135	.0056
190	158.33	1.149	.0261	.302	.0125	.159	.0066
200	166.66	1.189	.0271	.365	.0152	.179	.0075
210	175.00	1.211	.0275	.405	.0172	.204	

2) Beam-to-Column Connections

Figure B shows how the test assembly can deform and rotate through the angles shown when load is applied.

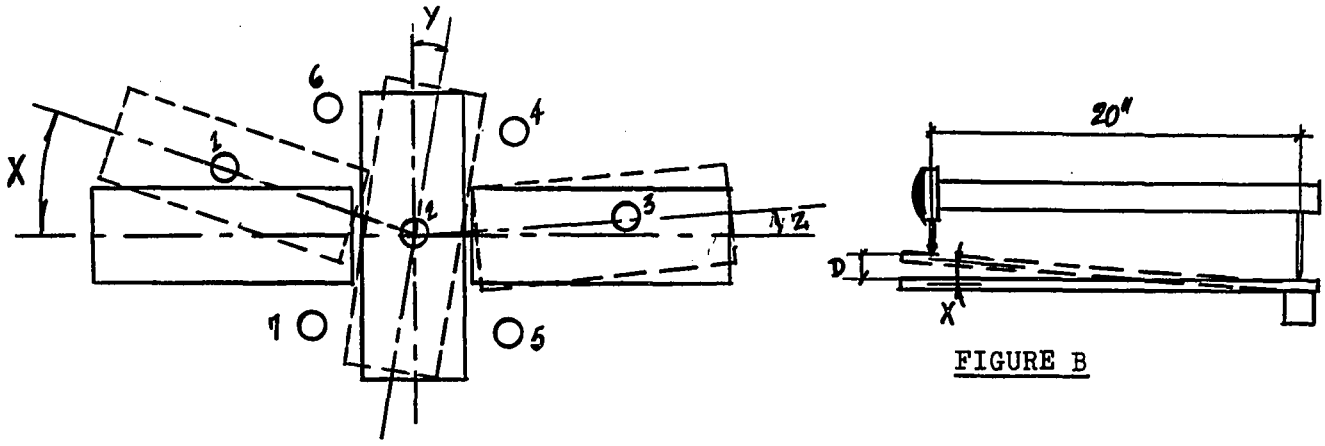

FIGURE B

O = dial identification

DLR = rotation of left beam with respect to the horizontal

DCR = rotation of column stub with respect to the vertical

DRR = rotation of right beam with respect to the horizontal

ROL = rotation of left beam with respect to column axis

ROR = rotation of right beam with respect to column axis

D = deflection recorded on dial gages

By interpreting the experimental readings from dial gages 1, 2 and 3, the rotation of the beams relative to the axis of the column can be computed.

Sample calculation

from the readings obtained for prototypes BC-1a for an applied moment of 44 k.ft.

Load	Moment	DL	DC	DR
0	0	0	0	0
24	44	.008	.004	.002

$\tan X = \frac{DL}{20"} = \frac{.008}{20} = 4.0 \times 10^{-4}$; DLR = 3.9999×10^{-4} rad.

$\tan Y = \frac{DC}{20"} = \frac{.004}{20} = 2.0 \times 10^{-4}$; DCR = 1.9999×10^{-4} rad.

$\tan Z = \frac{DR}{20"} = \frac{.002}{20} = 1.0 \times 10^{-4}$; DRR = $.9999 \times 10^{-4}$ rad.

Referring to figure B, the rotations ROL and ROR with respect to the column axis are expressed as:

$$ROL = DLR \pm DCR$$

$$ROR = DRR \pm DCR$$

for the case considered (BC-1a) ;

$$ROL = DLR - DCR$$

$$ROR = DRR + DCR$$

So $ROL \doteq (4 - 2) \times 10^{-4}$ rad $= 2.0 \times 10^{-4}$ rad

$ROR = (1 + 2) \times 10^{-4}$ rad $= 2.9999 \times 10^{-4}$ rad.

Another set of readings is also obtained from dial gages 4, 5, 6 and 7.

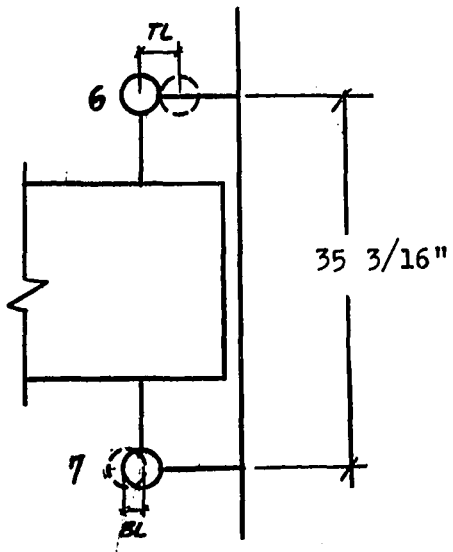

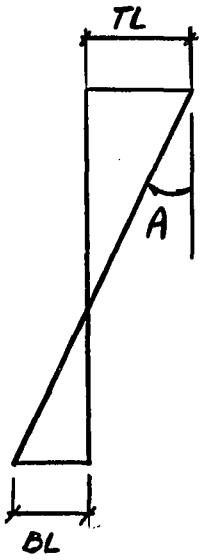

$$\tan A = \frac{TL + BL}{35\ 3/16"}$$

Sample calculation

From the readings obtained for prototype BC-1a ; for an applied moment of 44 K.-ft.

Load	Moment	TL	BL	TR	BR
0	0	0	0	0	0
24	44	.0020	.0020	.0010	.0020

$$\tan A = \frac{.0020 + .0020}{35\ 3/16"} = 1.40 \times 10^{-4} \text{ ; RLV} = 1.387 \times 10^{-4} \text{ rad}$$

similarly, from dial gages 4 and 5:

$$\tan B = \frac{.0010 + .0020}{35\ 3/16"} - 8.000 \times 10^{-5} \text{ ; RRV} = 8.5409 \times 10^{-5} \text{ rad.}$$

The final rotation of the connection is obtained by taking the average rotation computed from these two independent sets of readings:

(Applied moment : 44 k.ft.)

Angle of rotation of connection (left side)

from dial gages 1 and 2 : ROL = 1.9999×10^{-4} rad.

from dial gages 6 and 7 : RLV = 1.1387×10^{-4} rad

$$RML = \frac{ROL + RLV}{2} = \frac{1.9999 + 1.1387}{2} \times 10^{-4} = 1.3193 \times 10^{-4} \text{ rad}$$

Angle of rotation of connection (right side)

from dial gages 2 and 3 : ROR = 2.9999×10^{-4} rad.

from dial gages 4 and 5 : RRV = 8.5409×10^{-5} rad.

$$RMR = \frac{ROR + RRV}{2} = \frac{2.9999 + .85409}{2} \times 10^{-4}$$

$$RMR = 1.9270 \times 10^{-4} \text{ rad.}$$

The experimental results for the five beam-to-column prototypes are tabulated in the following pages.

```
/JOB GO,NOMAP
/FTC LIST
C      APPENDIX A
C      ROTATION CALCULATIONS
C      P IS THE VALUE OF LOAD (KIPS)
C      DL= DEFLECTIONS OF LEFT BEAM (IN.)
C      DC= DEFLECTIONS OF COLUMN (IN.)
C      DR= DEFLECTIONS OF RIGHT BEAM (IN.)
C      XM= MOMENT AT CONNECTION (KIPS-IN.)
C      DLR= ANGLE OF ROTATION OF LEFT BEAM (RAD)
C      DCR= ANGLE OF ROTATION OF COLUMN THROUGH VERTICAL (RAD.)
C      DRR= ANGLE OF ROTATION OF RIGHT BEAM (RAD.)
C      X= TAN OF ROTATION ANGLE (LEFT BEAM, RAD.)
C      Y= TAN OF ROTATION ANGLE (COLUMN, RAD.)
C      Z= TAN OF ROTATION ANGLE (RIGHT BEAM, RAD.)
C      ROL= ANGLE OF ROTATION OF LEFT BEAM, COLUMN VERTICAL (RAD.)
C      ROR= ANGLE OF ROTATION OF RIGHT BEAM, COLUMN VERTICAL (RAD.)
C      TL= DEFLECTIONS OF COLUMN REL. TO LEFT BEAM, RECORDED ON TOP LEFT
C      BL= DEFLECTIONS OF COL. REL. TO LEFT BEAM, RECORDED ON BOTTOM LEFT
C      TR= DEFLECTIONS OF COL. REL. TO RIGHT BEAM, RECORDED ON TOP RIGHT
C      BR= DEFLECTIONS  OF COL. REL. TO RIGHT BEAM, RECORDED ON BOTTOM RIGHT
C      A= TAN OF ROTATION ANGLE OF CONNECTION (LEFT SIDE)
C      B= TAN OF ROTATION ANGLE OF CONNECTION, (RIGHT SIDE)
C      RLV= ANGLE OF ROTATION OF CONNECTION, LEFT SIDE (RAD.)
C      RRV= ANGLE OF ROTATION OF CONNECTION, RIGHT SIDE (RAD.)
       DIMENSION P(50), DL(50), DC(50), DR(50), XM(50), X(50), Y(50)
       DIMENSION Z(50), DLR(50), DCR(50), DRR(50), ROL(50), ROR(50)
       DIMENSION TL(50), BL(50), TR(50), BR(50), RLV(50), A(50), B(50)
       DIMENSION RRV(50), RML(50), RMR(50)
C      READ AND WRITE LOAD AND DEFLECTION DATA
       READ (5,101) MM
  101  FORMAT (I2)
       NCOUNT=0
   35  READ (5,1) N, K, XL
    1  FORMAT (2I3, F8.3)
       WRITE (6,31)
   31  FORMAT (1H, 12HNO. OF VALUE, 5X, 4HLOAD, 5X, 2HDL, 9X, 2HDC, 9X, 2
      2HDR///)
       READ (5,2) (P(I), I=1,N)
    2  FORMAT (10F5.1)
       READ (5,3) (DL(I), I=1,N)
       READ (5,3) (DC(I), I=1,N)
       READ (5,3) (DR(I), I=1,N)
    3  FORMAT (10F5.3)
       WRITE (6,32)(I, P(I), DL(I), DC(I), DR(I), I=1,N)
   32  FORMAT (5X, I13, 9X, 1F6.1, 4X, 1F6.4, 4X, 1F6.4, 4X, 1F6.4)
C      COMPUTE MOMENTS, ANGLES OF ROTATION AT LEFT, CENTER, RIGHT
       WRITE (6,5)
    5  FORMAT (1H, 3X, 6HMOMENT, 9X, 13HLEFT BEAM ROT, 8X, 12HCOLUMN ROT,
      26X, 14HRIGHT BEAM ROT///)
       DO 4 I=1,N
       XM(I)= (P(I)*1.833)
       X(I)= DL(I)/20.0
       DLR(I)= ATAN(X(I))
       Y(I)= DC(I)/20.0
       DCR(I)= ATAN(Y(I))
       Z(I)= DR(I)/20.0
```

```
      WRITE (7, 25) XM(I), DLR(I), DCR(I), DRR(I)
   25 FORMAT ( 2X, 1F8.1, 6X, 1PE16.7, 5X, 1PE16.7, 2X, 1PE16.7)
    4 CONTINUE
      WRITE (6,7)
    7 FORMAT( 1H, 3X, 6HMOMENT, 8X, 13HABS. LEFT ROT, 6X, 14HABS. RIGHT
     2ROT///)
      IF (K-1) 6,9,12
C     COLUMN GOES RIGHT
    6 DO 8 I=1,N
      ROL(I)= DLR(I)+DCR(I)
      ROR(I)= DRR(I)-DCR(I)
      WRITE(6,26) XM(I),ROL(I), ROR(I)
      WRITE (7, 26) XM(I), ROL(I), ROR(I)
   26 FORMAT (1X, 1F8.1, 6X, 1PE16.7, 5X, 1PE16.7)
    8 CONTINUE
      GO TO 15
C     COLUMN STAYS VERTICAL
    9 DO 11 I=1,N
      ROL(I)= DLR(I)
      ROR(I)= DRR(I)
      WRITE (6,27) XM(I), ROL(I), ROR(I)
      WRITE (7, 27) XM(I), ROL(I), ROR(I)
   27 FORMAT (1X, 1F8.1, 6X, 1PE16.7, 5X, 1PE16.7)
   11 CONTINUE
      GO TO 15
C     COLUMN GOES LEFT
   12 DO 14 I=1,N
      ROL(I)= DLR(I)-DCR(I)
      ROR(I)= DRR(I)+DCR(I)
      WRITE(6,28) XM(I), ROL(I), ROR(I)
      WRITE (7,28) XM(I), ROL(I), ROR(I)
   28 FORMAT (1X, 1F8.1, 6X, 1PE16.7, 5X, 1PE16.7)
   14 CONTINUE
      GO TO 15
C     READ AND WRITE DEFLECTIONS OF BEAMS RELATIVE TO COLUMN
   15 READ (5,16) (TL(I), I=1,N)
      READ (5,16) (BL(I), I=1,N)
      READ (5,16) (TR(I), I=1,N)
      READ (5,16) (BR(I), I=1,N)
   16 FORMAT (10F5.3)
      WRITE (5,33)
   33 FORMAT (1H, 12HNO. OF VALUE, 5X, 4HLOAD, 5X, 2HTL, 9X, 2HBL, 10X,
     22HTR, 10X, 2HBR///)
      WRITE (6,34) (I, P(I), TL(I), BL(I), TR(I), BR(I), I=1,N)
   34 FORMAT (5X, 1I3, 9X, 1F6.1, 4X, 1F6.4, 4X, 1F6.4, 4X, 1F6.4, 4X, 1
     2F6.4)
C     COMPUTE ANGLES OF ROTATION OF CONNECTION
      WRITE (6,17)
   17 FORMAT( 1H, 3X, 6HMOMENT, 8X, 13HLEFT VERT ROT, 6X, 14HRIGHT VERT
     2ROT///)
      DO 18 I=1,N
      A(I)= (TL(I)+BL(I))/XL
      B(I)= (TR(I)+BR(I))/XL
      RLV(I)= ATAN(A(I))
      RRV(I)= ATAN(B(I))
      WRITE(6,29) XM(I), RLV(I), RRV(I)
      WRITE (7,29) XM(I), RLV(I), RRV(I)
   29 FORMAT (1X, 1F8.1, 6X, 1PE16.7, 5X, 1PE16.7)
   18 CONTINUE
```

```
      COMPUTE AVERAGE ROTATIONS
      WRITE (6,20)
   20 FORMAT (1H, 3X, 11HNO OF VALUE, 3X, 6HMOMENT, 9X, 13HMEAN ROT LEFT
     2, 8X, 14HMEAN ROT RIGHT///)
      DO 19 I=1,N
      RML(I)= (ROL(I)+RLV(I))/2.0
      RMR(I)= (ROR(I)+RRV(I))/2.0
      WRITE (6, 30) I , XM(I), RML(I), RMR(I)
   30 FORMAT (2X, 1I4, 9X, 1F8.1, 7X, 1PE16.7, 6X, 1PE16.7)
   19 CONTINUE
      NCOUNT= NCOUNT+1
      IF(NCOUNT-MM) 35,100,100
  100 STOP
      END
/DATA
```

C PROTOTYPE BC-1A

READING	LOAD	DL	DC	DR
1	4.0	0.0040	0.0020	0.0020
2	6.0	0.0040	0.0020	0.0020
3	8.0	0.0040	0.0020	0.0020
4	10.0	0.0040	0.0030	0.0020
5	12.0	0.0050	0.0030	0.0020
6	14.0	0.0050	0.0030	0.0020
7	16.0	0.0060	0.0040	0.0020
8	18.0	0.0060	0.0040	0.0020
9	20.0	0.0070	0.0040	0.0020
10	22.0	0.0070	0.0040	0.0020
11	24.0	0.0080	0.0040	0.0020
12	26.0	0.0080	0.0040	0.0020
13	30.0	0.0100	0.0040	0.0020
14	34.0	0.0100	0.0040	0.0020
15	38.0	0.0100	0.0040	0.0030
16	42.0	0.0100	0.0040	0.0050
17	46.0	0.0130	0.0050	0.0050
18	50.0	0.0140	0.0050	0.0060
19	54.0	0.0140	0.0050	0.0120
20	58.0	0.0150	0.0050	0.0130
21	62.0	0.0260	0.0050	0.0140
22	66.0	0.0290	0.0080	0.0170
23	70.0	0.0350	0.0130	0.0210

MOMENT	DLR	DCR	DRR
7.3	1.9999983E-04	9.9999990E-05	9.9999990E-05
11.0	1.9999983E-04	9.9999990E-05	9.9999990E-05
14.7	1.9999983E-04	9.9999990E-05	9.9999990E-05
18.3	1.9999983E-04	1.4999998E-04	9.9999990E-05
22.0	2.4999981E-04	1.4999998E-04	9.9999990E-05
25.7	2.4999981E-04	1.4999998E-04	9.9999990E-05
29.3	2.9999949E-04	1.9999983E-04	9.9999990E-05
33.0	2.9999949E-04	1.9999983E-04	9.9999990E-05
36.7	3.4999964E-04	1.9999983E-04	9.9999990E-05

44.0	3.9999955E-04	1.9999983E-04	9.9999990E-05
47.7	3.9999955E-04	1.9999983E-04	9.9999990E-05
55.0	4.9999962E-04	1.9999983E-04	9.9999990E-05
62.3	4.9999962E-04	1.9999983E-04	9.9999990E-05
69.7	4.9999962E-04	1.9999983E-04	1.4999998E-04
77.0	4.9999962E-04	1.9999983E-04	2.4999981E-04
84.3	6.4999959E-04	2.4999981E-04	2.4999981E-04
91.6	6.9999951E-04	2.4999981E-04	2.9999949E-04
99.0	6.9999951E-04	2.4999981E-04	5.9999968E-04
106.3	7.4999942E-04	2.4999981E-04	6.4999959E-04
113.6	1.2999992E-03	2.4999981E-04	6.9999951E-04
121.0	1.4499987E-03	3.9999955E-04	8.4999949E-04
128.3	1.7499980E-03	6.4999959E-04	1.0499994E-03

MOMENT	ROL	ROR
7.3	9.9999845E-05	1.9999998E-04
11.0	9.9999845E-05	1.9999998E-04
14.7	9.9999845E-05	1.9999998E-04
18.3	4.9999857E-05	2.4999981E-04
22.0	9.9999830E-05	2.4999981E-04
25.7	9.9999830E-05	2.4999981E-04
29.3	9.9999656E-05	2.9999972E-04
33.0	9.9999656E-05	2.9999972E-04
36.7	1.4999980E-04	2.9999972E-04
40.3	1.4999980E-04	2.9999972E-04
44.0	1.9999972E-04	2.9999972E-04
47.7	1.9999972E-04	2.9999972E-04
55.0	2.9999972E-04	2.9999972E-04
62.3	2.9999972E-04	2.9999972E-04
69.7	2.9999972E-04	3.4999964E-04
77.0	2.9999972E-04	4.4999947E-04
84.3	3.9999979E-04	4.9999962E-04
91.6	4.4999970E-04	5.4999930E-04
99.0	4.4999970E-04	8.4999949E-04
106.3	4.9999962E-04	8.9999940E-04
113.6	1.0499994E-03	9.4999932E-04
121.0	1.0499991E-03	1.2499990E-03
128.3	1.0999984E-03	1.6999990E-03

READING	MOMENT	TL	BL	TR	BR
1	4.0	0.0010	0.0010	0.0010	0.0010
2	6.0	0.0010	0.0010	0.0010	0.0010
3	8.0	0.0010	0.0010	0.0010	0.0010
4	10.0	0.0010	0.0010	0.0010	0.0010
5	12.0	0.0010	0.0020	0.0010	0.0010
6	14.0	0.0020	0.0020	0.0010	0.0010
7	16.0	0.0020	0.0020	0.0010	0.0020
8	18.0	0.0020	0.0020	0.0010	0.0020
9	20.0	0.0020	0.0020	0.0010	0.0020
10	22.0	0.0020	0.0020	0.0010	0.0020
11	24.0	0.0020	0.0020	0.0010	0.0020
12	26.0	0.0030	0.0030	0.0020	0.0020
13	30.0	0.0030	0.0030	0.0020	0.0030
14	34.0	0.0030	0.0040	0.0020	0.0030
15	38.0	0.0040	0.0040	0.0030	0.0030

16	42.0	0.0040	0.0050	0.0030	0.0040
17	46.0	0.0050	0.0050	0.0040	0.0040
18	50.0	0.0050	0.0050	0.0040	0.0040
19	54.0	0.0070	0.0020	0.0040	0.0050
20	58.0	0.0080	0.0020	0.0050	0.0050
21	62.0	0.0090	0.0020	0.0090	0.0050
22	66.0	0.0110	0.0020	0.0110	0.0070
23	70.0	0.0150	0.0020	0.0150	0.0130

MOMENT	A	B
7.3	5.6939491E-05	5.6939491E-05
11.0	5.6939491E-05	5.6939491E-05
14.7	5.6939491E-05	5.6939491E-05
18.3	5.6939491E-05	5.6939491E-05
22.0	8.5409236E-05	5.6939491E-05
25.7	1.1387891E-04	5.6939491E-05
29.3	1.1387891E-04	8.5409236E-05
33.0	1.1387891E-04	8.5409236E-05
36.7	1.1387891E-04	8.5409236E-05
40.3	1.1387891E-04	8.5409236E-05
44.0	1.1387891E-04	8.5409236E-05
47.7	1.7081841E-04	1.1387891E-04
55.0	1.7081841E-04	1.4234871E-04
62.3	1.9928813E-04	1.4234871E-04
69.7	2.2775783E-04	1.7081841E-04
77.0	2.5622756E-04	1.9928813E-04
84.3	2.8469716E-04	2.2775783E-04
91.6	2.8469716E-04	2.2775783E-04
99.0	2.5622756E-04	2.5622756E-04
106.3	2.8469693E-04	2.8469716E-04
113.6	3.1316676E-04	3.9857603E-04
121.0	3.7010643E-04	5.1245512E-04
128.3	4.8398529E-04	7.9715252E-04

READING	MOMENT	RLV	RRV
1	7.3	7.8469660E-05	1.2846966E-04
2	11.0	7.8469660E-05	1.2846966E-04
3	14.7	7.8469660E-05	1.2846966E-04
4	18.3	5.3469674E-05	1.5346962E-04
5	22.0	9.2704533E-05	1.5346962E-04
6	25.7	1.0693936E-04	1.5346962E-04
7	29.3	1.0693927E-04	1.9270438E-04
8	33.0	1.0693927E-04	1.9270438E-04
9	36.7	1.3193930E-04	1.9270438E-04
10	40.3	1.3193930E-04	1.9270438E-04
11	44.0	1.5693926E-04	1.9270438E-04
12	47.7	1.8540898E-04	2.0693929E-04
13	55.0	2.3540901E-04	2.2117421E-04
14	62.3	2.4964381E-04	2.2117421E-04
15	69.7	2.6387861E-04	2.6040897E-04
16	77.0	2.7811364E-04	3.2464368E-04
17	84.3	3.4234836E-04	3.6387867E-04
18	91.6	3.6734832E-04	3.8887840E-04
19	99.0	3.5311352E-04	5.5311341E-04
20	106.3	3.9234827E-04	5.9234817E-04

21	113.6	6.8158307E-04	6.7428756E-04
22	121.0	7.1005267E-04	8.8122697E-04
23	128.3	7.9199183E-04	1.2485757E-03

C PROTOTYPE BC-1B

READING	LOAD	DL	DC	DR
1	4.0	0.0010	0.0010	0.0030
2	8.0	0.0010	0.0010	0.0040
3	12.0	0.0020	0.0030	0.0050
4	16.0	0.0020	0.0030	0.0070
5	20.0	0.0030	0.0030	0.0080
6	24.0	0.0040	0.0030	0.0100
7	28.0	0.0050	0.0040	0.0120
8	32.0	0.0050	0.0040	0.0130
9	36.0	0.0050	0.0050	0.0130
10	40.0	0.0060	0.0050	0.0130
11	44.0	0.0070	0.0060	0.0150
12	48.0	0.0100	0.0060	0.0150
13	52.0	0.0180	0.0180	0.0170
14	56.0	0.0270	0.0310	0.0410
15	60.0	0.0400	0.0430	0.0520
16	64.0	0.0520	0.0600	0.0640
17	68.0	0.0630	0.0690	0.0770
18	72.0	0.0690	0.0740	0.0820
19	76.0	0.0830	0.0860	0.0940
20	80.0	0.1030	0.1130	0.1190
21	84.0	0.1150	0.1260	0.1350

MOMENT	DLR	DCR	DRR
7.3	4.9999988E-05	4.9999988E-05	1.4999998E-04
14.7	4.9999988E-05	4.9999988E-05	1.9999983E-04
22.0	9.9999990E-05	1.4999998E-04	2.4999981E-04
29.3	9.9999990E-05	1.4999998E-04	3.4999964E-04
36.7	1.4999998E-04	1.4999998E-04	3.9999955E-04
44.0	1.9999983E-04	1.4999998E-04	4.9999962E-04
51.3	2.4999981E-04	1.9999983E-04	5.9999968E-04
58.7	2.4999981E-04	1.9999983E-04	6.4999959E-04
66.0	2.4999981E-04	2.4999981E-04	6.4999959E-04
73.3	2.9999949E-04	2.4999981E-04	6.4999959E-04
80.7	3.4999964E-04	2.9999949E-04	7.4999942E-04
88.0	4.9999962E-04	2.9999949E-04	7.4999942E-04
95.3	8.9999964E-04	8.9999964E-04	8.4999949E-04
102.6	1.3499991E-03	1.5499988E-03	2.0499970E-03
110.0	1.9999971E-03	2.1499968E-03	2.5999940E-03
117.3	2.5999940E-03	2.9999912E-03	3.1999869E-03
124.6	3.1499879E-03	3.4499837E-03	3.8499797E-03
132.0	3.4499837E-03	3.6999802E-03	4.0999725E-03
139.3	4.1499697E-03	4.2999722E-03	4.6999604E-03
146.6	5.1499531E-03	5.6499355E-03	5.9499256E-03
154.0	5.7499334E-03	6.2999129E-03	6.7498945E-03

MOMENT	ROL	ROR
7.3	9.9999976E-05	9.9999990E-05
14.7	9.9999976E-05	1.4999985E-04
22.0	2.4999981E-04	9.9999830E-05
29.3	2.4999981E-04	1.9999966E-04
36.7	2.9999996E-04	2.4999958E-04
44.0	3.4999964E-04	3.4999964E-04
51.3	4.4999947E-04	3.9999979E-04
58.7	4.4999947E-04	4.4999970E-04
66.0	4.9999962E-04	3.9999979E-04
73.3	5.4999930E-04	3.9999979E-04
80.7	6.4999913E-04	4.4999993E-04
88.0	7.9999911E-04	4.4999993E-04
95.3	1.7999993E-03	-5.0000148E-05
102.6	2.8999979E-03	4.9999822E-04
110.0	4.1499920E-03	4.4999714E-04
117.3	5.5999830E-03	1.9999570E-04
124.6	6.5999702E-03	3.9999606E-04
132.0	7.1499608E-03	3.9999234E-04
139.3	8.4499419E-03	3.9998814E-04
146.6	1.0799889E-02	2.9999018E-04
154.0	1.2049846E-02	4.4998154E-04

READING	MOMENT	TL	BL	TR	BR
1	4.0	0.0	0.0	0.0010	0.0
2	8.0	0.0010	0.0010	0.0020	0.0010
3	12.0	0.0010	0.0010	0.0030	0.0010
4	16.0	0.0010	0.0010	0.0030	0.0010
5	20.0	0.0010	0.0010	0.0040	0.0010
6	24.0	0.0020	0.0010	0.0050	0.0020
7	28.0	0.0030	0.0010	0.0060	0.0020
8	32.0	0.0030	0.0020	0.0070	0.0020
9	36.0	0.0040	0.0020	0.0090	0.0020
10	40.0	0.0050	0.0020	0.0100	0.0020
11	44.0	0.0070	0.0020	0.0120	0.0020
12	48.0	0.0080	0.0020	0.0140	0.0020
13	52.0	0.0100	0.0020	0.0160	0.0020
14	56.0	0.0120	0.0020	0.0180	0.0020
15	60.0	0.0130	0.0020	0.0210	0.0020
16	64.0	0.0150	0.0020	0.0240	0.0020
17	68.0	0.0160	0.0020	0.0280	0.0020
18	72.0	0.0220	0.0020	0.0320	0.0020
19	76.0	0.0220	0.0020	0.0360	0.0020
20	80.0	0.0220	0.0020	0.0410	0.0020
21	84.0	0.0220	0.0020	0.0450	0.0020

MOMENT	A	B
7.3	0.0	2.8469745E-05
14.7	5.6939491E-05	8.5409236E-05
22.0	5.6939491E-05	1.1387891E-04
29.3	5.6939491E-05	1.1387891E-04
36.7	5.6939491E-05	1.4234861E-04
44.0	8.5409236E-05	1.9928813E-04
51.3	1.1387891E-04	2.2775783E-04

58.7	1.4234871E-04	2.5622756E-04
66.0	1.7081831E-04	3.1316676E-04
73.3	1.9928813E-04	3.4163659E-04
80.7	2.5622756E-04	3.9857603E-04
88.0	2.8469693E-04	4.5551546E-04
95.3	3.4163659E-04	5.1245512E-04
102.6	3.9857603E-04	5.6939456E-04
110.0	4.2704563E-04	6.5480382E-04
117.3	4.8398529E-04	7.4021309E-04
124.6	5.1245512E-04	8.5409195E-04
132.0	6.8327365E-04	9.6797105E-04
139.3	6.8327365E-04	1.0818499E-03
146.6	6.8327365E-04	1.2241986E-03
154.0	6.8327365E-04	1.3380772E-03

READING	MOMENT	RLV	RRV
1	7.3	4.9999988E-05	6.4234860E-05
2	14.7	7.8469733E-05	1.1770453E-04
3	22.0	1.5346962E-04	1.0693936E-04
4	29.3	1.5346962E-04	1.5693926E-04
5	36.7	1.7846969E-04	1.9617402E-04
6	44.0	2.1770434E-04	2.7464377E-04
7	51.3	2.8193905E-04	3.1387876E-04
8	58.7	2.9617408E-04	3.5311352E-04
9	66.0	3.3540884E-04	3.5658316E-04
10	73.3	3.7464360E-04	3.7081819E-04
11	80.7	4.5311335E-04	4.2428798E-04
12	88.0	5.4234802E-04	4.5275758E-04
13	95.3	1.0708179E-03	2.3122749E-04
14	102.6	1.6492868E-03	5.3469627E-04
15	110.0	2.2885185E-03	5.5240048E-04
16	117.3	3.0419827E-03	4.7010439E-04
17	124.6	3.5562124E-03	6.2704389E-04
18	132.0	3.9166138E-03	6.8398169E-04
19	139.3	4.5666061E-03	7.4091903E-04
20	146.6	5.7415776E-03	7.6209428E-04
21	154.0	6.3665584E-03	8.9402939E-04

C PROTOTYPE BC-1C

READING	LOAD	DL	DC	DR
1	4.0	0.0	0.0	0.0010
2	8.0	0.0010	0.0020	0.0030
3	12.0	0.0010	0.0020	0.0050
4	16.0	0.0020	0.0050	0.0070
5	20.0	0.0020	0.0050	0.0090
6	24.0	0.0020	0.0060	0.0110
7	28.0	0.0020	0.0070	0.0130
8	32.0	0.0020	0.0070	0.0140
9	36.0	0.0020	0.0080	0.0160
10	40.0	0.0030	0.0090	0.0190
11	44.0	0.0030	0.0100	0.0190
12	48.0	0.0030	0.0100	0.0210

14	56.0	0.0050	0.0100	0.0240
15	60.0	0.0060	0.0110	0.0260
16	64.0	0.0080	0.0110	0.0270
17	68.0	0.0100	0.0110	0.0290
18	72.0	0.0110	0.0110	0.0310
19	76.0	0.0130	0.0110	0.0330
20	80.0	0.0140	0.0110	0.0360
21	84.0	0.0150	0.0110	0.0380
22	88.0	0.0180	0.0110	0.0410
23	92.0	0.0200	0.0110	0.0420
24	96.0	0.0230	0.0110	0.0450
25	100.0	0.0290	0.0110	0.0510
26	104.0	0.0330	0.0110	0.0550
27	108.0	0.0370	0.0110	0.0590
28	112.0	0.0430	0.0110	0.0650
29	116.0	0.0500	0.0110	0.0700
30	120.0	0.0800	0.0150	0.0980

MOMENT	DLR	DCR	DRR
7.3	0.0	0.0	4.9999988E-05
14.7	4.9999988E-05	9.9999990E-05	1.4999998E-04
22.0	4.9999988E-05	9.9999990E-05	2.4999981E-04
29.3	9.9999990E-05	2.4999981E-04	3.4999964E-04
36.7	9.9999990E-05	2.4999981E-04	4.4999970E-04
44.0	9.9999990E-05	2.9999949E-04	5.4999976E-04
51.3	9.9999990E-05	3.4999964E-04	6.4999959E-04
58.7	9.9999990E-05	3.4999964E-04	6.9999951E-04
66.0	9.9999990E-05	3.9999955E-04	7.9999957E-04
73.3	1.4999998E-04	4.4999970E-04	9.4999955E-04
80.7	1.4999998E-04	4.9999962E-04	9.4999955E-04
88.0	1.4999998E-04	4.9999962E-04	1.0499994E-03
95.3	1.9999983E-04	4.9999962E-04	1.0999995E-03
102.6	2.4999981E-04	4.9999962E-04	1.1999994E-03
110.0	2.9999949E-04	5.4999976E-04	1.2999992E-03
117.3	3.9999955E-04	5.4999976E-04	1.3499991E-03
124.6	4.9999962E-04	5.4999976E-04	1.4499987E-03
132.0	5.4999976E-04	5.4999976E-04	1.5499988E-03
139.3	6.4999959E-04	5.4999976E-04	1.6499986E-03
146.6	6.9999951E-04	5.4999976E-04	1.7999979E-03
154.0	7.4999942E-04	5.4999976E-04	1.8999977E-03
161.3	8.9999964E-04	5.4999976E-04	2.0499970E-03
168.6	9.9999947E-04	5.4999976E-04	2.0999971E-03
176.0	1.1499994E-03	5.4999976E-04	2.2499962E-03
183.3	1.4499987E-03	5.4999976E-04	2.5499947E-03
190.6	1.6499986E-03	5.4999976E-04	2.7499937E-03
198.0	1.8499978E-03	5.4999976E-04	2.9499910E-03
205.3	2.1499968E-03	5.4999976E-04	3.2499882E-03
212.6	2.4999946E-03	5.4999976E-04	3.4999859E-03
220.0	3.9999746E-03	7.4999942E-04	4.8999563E-03

MOMENT	ROL	ROR
7.3	0.0	4.9999988E-05
14.7	1.4999998E-04	4.9999988E-05
22.0	1.4999998E-04	1.4999982E-04

36.7	3.4999964E-04	1.9999989E-04
44.0	3.9999932E-04	2.5000027E-04
51.3	4.4999947E-04	2.9999996E-04
58.7	4.4999947E-04	3.4999987E-04
66.0	4.9999938E-04	4.0000002E-04
73.3	5.9999968E-04	4.9999985E-04
80.7	6.4999959E-04	4.4999993E-04
88.0	6.4999959E-04	5.4999976E-04
95.3	6.9999928E-04	5.9999991E-04
102.6	7.4999942E-04	6.9999974E-04
110.0	8.4999925E-04	7.4999942E-04
117.3	9.4999932E-04	7.9999934E-04
124.6	1.0499994E-03	8.9999894E-04
132.0	1.0999995E-03	9.9999900E-04
139.3	1.1999994E-03	1.0999988E-03
146.6	1.2499993E-03	1.2499981E-03
154.0	1.2999992E-03	1.3499979E-03
161.3	1.4499994E-03	1.4999972E-03
168.6	1.5499992E-03	1.5499974E-03
176.0	1.6999992E-03	1.6999964E-03
183.3	1.9999985E-03	1.9999950E-03
190.6	2.1999984E-03	2.1999939E-03
198.0	2.3999976E-03	2.3999913E-03
205.3	2.6999966E-03	2.6999884E-03
212.6	3.0499944E-03	2.9499861E-03
220.0	4.7499724E-03	4.1499548E-03

READING	MOMENT	TL	BL	TR	BR
1	4.0	0.0	0.0	0.0	0.0
2	8.0	0.0	0.0	0.0010	0.0
3	12.0	0.0	0.0	0.0010	0.0010
4	16.0	0.0	0.0	0.0020	0.0010
5	20.0	0.0	0.0	0.0020	0.0010
6	24.0	0.0010	0.0	0.0030	0.0010
7	28.0	0.0010	0.0010	0.0030	0.0020
8	32.0	0.0010	0.0010	0.0040	0.0020
9	36.0	0.0010	0.0010	0.0040	0.0020
10	40.0	0.0020	0.0010	0.0050	0.0020
11	44.0	0.0030	0.0010	0.0060	0.0020
12	48.0	0.0030	0.0010	0.0070	0.0020
13	52.0	0.0050	0.0020	0.0070	0.0020
14	56.0	0.0050	0.0020	0.0080	0.0020
15	60.0	0.0070	0.0030	0.0100	0.0020
16	64.0	0.0080	0.0040	0.0100	0.0020
17	68.0	0.0090	0.0050	0.0120	0.0020
18	72.0	0.0100	0.0050	0.0130	0.0020
19	76.0	0.0120	0.0060	0.0140	0.0020
20	80.0	0.0140	0.0070	0.0160	0.0020
21	84.0	0.0150	0.0080	0.0170	0.0030
22	88.0	0.0170	0.0080	0.0190	0.0030
23	92.0	0.0190	0.0100	0.0210	0.0030
24	96.0	0.0210	0.0110	0.0230	0.0030
25	100.0	0.0250	0.0130	0.0280	0.0030
26	104.0	0.0270	0.0140	0.0300	0.0030
27	108.0	0.0290	0.0150	0.0320	0.0040
28	112.0	0.0320	0.0170	0.0350	0.0060
29	116.0	0.0350	0.0200	0.0380	0.0080

30	120.0	0.0930	0.0700	0.0850	0.0450

MOMENT	A	B
7.3	0.0	0.0
14.7	0.0	2.8469745E-05
22.0	0.0	5.6939491E-05
29.3	0.0	8.5409236E-05
36.7	0.0	8.5409236E-05
44.0	2.8469745E-05	1.1387891E-04
51.3	5.6939491E-05	1.4234871E-04
58.7	5.6939491E-05	1.7081831E-04
66.0	5.6939491E-05	1.7081831E-04
73.3	8.5409236E-05	1.9928813E-04
80.7	1.1387891E-04	2.2775783E-04
88.0	1.1387891E-04	2.5622756E-04
95.3	1.9928813E-04	2.5622756E-04
102.6	1.9928813E-04	2.8469693E-04
110.0	2.8469716E-04	3.4163659E-04
117.3	3.4163659E-04	3.4163659E-04
124.6	3.9857603E-04	3.9857603E-04
132.0	4.2704586E-04	4.2704563E-04
139.3	5.1245512E-04	4.5551546E-04
146.6	5.9786439E-04	5.1245512E-04
154.0	6.5480382E-04	5.6939456E-04
161.3	7.1174325E-04	6.2633399E-04
168.6	8.2562235E-04	6.8327365E-04
176.0	9.1103162E-04	7.4021309E-04
183.3	1.0818499E-03	8.8256178E-04
190.6	1.1672592E-03	9.3950122E-04
198.0	1.2526684E-03	1.0249102E-03
205.3	1.3950167E-03	1.1672589E-03
212.6	1.5658350E-03	1.3096076E-03
220.0	4.6405345E-03	3.7010489E-03

READING	MOMENT	RLV	RRV
1	7.3	0.0	2.4999987E-05
2	14.7	7.4999989E-05	3.9234859E-05
3	22.0	7.4999989E-05	1.0346965E-04
4	29.3	1.7499982E-04	9.2704533E-05
5	36.7	1.7499982E-04	1.4270446E-04
6	44.0	2.1423446E-04	1.8193957E-04
7	51.3	2.5346945E-04	2.2117433E-04
8	58.7	2.5346945E-04	2.6040897E-04
9	66.0	2.7846941E-04	2.8540916E-04
10	73.3	3.4270436E-04	3.4964387E-04
11	80.7	3.8193911E-04	3.3887872E-04
12	88.0	3.8193911E-04	4.0311366E-04
13	95.3	4.4964370E-04	4.2811362E-04
14	102.6	4.7464366E-04	4.9234834E-04
15	110.0	5.6734821E-04	5.4581789E-04
16	117.3	6.4581796E-04	5.7081785E-04
17	124.6	7.2428770E-04	6.4928737E-04
18	132.0	7.6352269E-04	7.1352231E-04
19	139.3	8.5622724E-04	7.7775703E-04
20	146.6	9.2393183E-04	8.8122650E-04

21	154.0	9.7740139E-04	9.5969625E-04
22	161.3	1.0808713E-03	1.0631655E-03
23	168.6	1.1878107E-03	1.1166355E-03
24	176.0	1.3055154E-03	1.2201048E-03
25	183.3	1.5409242E-03	1.4412783E-03
26	190.6	1.6836287E-03	1.5697475E-03
27	198.0	1.8263329E-03	1.7124508E-03
28	205.3	2.0475052E-03	1.9336236E-03
29	212.6	2.3079142E-03	2.1297969E-03
30	220.0	4.6952516E-03	3.9254986E-03

C PROTOTYPE BC-2

READING	LOAD	DL	DC	DR
1	2.0	0.0	0.0	0.0
2	4.0	0.0010	0.0	0.0030
3	6.0	0.0030	0.0	0.0040
4	8.0	0.0050	0.0010	0.0050
5	10.0	0.0060	0.0010	0.0070
6	12.0	0.0080	0.0010	0.0070
7	14.0	0.0090	0.0010	0.0100
8	16.0	0.0100	0.0010	0.0120
9	18.0	0.0120	0.0010	0.0140
10	20.0	0.0130	0.0010	0.0150
11	22.0	0.0150	0.0010	0.0150
12	24.0	0.0180	0.0010	0.0190
13	26.0	0.0190	0.0010	0.0210
14	28.0	0.0210	0.0010	0.0220
15	30.0	0.0230	0.0010	0.0240
16	32.0	0.0250	0.0010	0.0260
17	34.0	0.0280	0.0010	0.0290
18	36.0	0.0310	0.0010	0.0320
19	38.0	0.0340	0.0010	0.0350
20	40.0	0.0380	0.0020	0.0380
21	42.0	0.0420	0.0020	0.0410
22	44.0	0.0470	0.0030	0.0460
23	46.0	0.0510	0.0040	0.0500
24	48.0	0.0560	0.0040	0.0560
25	50.0	0.0620	0.0050	0.0590
26	52.0	0.0690	0.0050	0.0660

MOMENT	DLR	DCR	DRR
3.7	0.0	0.0	0.0
7.3	4.9999988E-05	0.0	1.4999998E-04
11.0	1.4999998E-04	0.0	1.9999983E-04
14.7	2.4999981E-04	4.9999988E-05	2.4999981E-04
18.3	2.9999949E-04	4.9999988E-05	3.4999964E-04
22.0	3.9999955E-04	4.9999988E-05	3.4999964E-04
25.7	4.4999970E-04	4.9999988E-05	4.9999962E-04
29.3	4.9999962E-04	4.9999988E-05	5.9999968E-04
33.0	5.9999968E-04	4.9999988E-05	6.9999951E-04
36.7	6.4999959E-04	4.9999988E-05	7.4999942E-04
40.3	7.4999942E-04	4.9999988E-05	7.4999942E-04
44.0	8.9999964E-04	4.9999988E-05	9.4999955E-04

47.7	9.4999955E-04	4.9999988E-05	1.0499994E-03
51.3	1.0499994E-03	4.9999988E-05	1.0999995E-03
55.0	1.1499994E-03	4.9999988E-05	1.1999994E-03
58.7	1.2499993E-03	4.9999988E-05	1.2999992E-03
62.3	1.3999988E-03	4.9999988E-05	1.4499987E-03
66.0	1.5499988E-03	4.9999988E-05	1.5999987E-03
69.7	1.6999983E-03	4.9999988E-05	1.7499980E-03
73.3	1.8999977E-03	9.9999990E-05	1.8999977E-03
77.0	2.0999971E-03	9.9999990E-05	2.0499970E-03
80.7	2.3499958E-03	1.4999998E-04	2.2999961E-03
84.3	2.5499947E-03	1.9999983E-04	2.4999946E-03
88.0	2.7999927E-03	1.9999983E-04	2.7999927E-03
91.6	3.0999898E-03	2.4999981E-04	2.9499910E-03
95.3	3.4499837E-03	2.4999981E-04	3.2999874E-03

MOMENT	ROL	ROR
3.7	0.0	0.0
7.3	4.9999988E-05	1.4999998E-04
11.0	1.4999998E-04	1.9999983E-04
14.7	2.9999972E-04	1.9999982E-04
18.3	3.4999941E-04	2.9999949E-04
22.0	4.4999947E-04	2.9999949E-04
25.7	4.9999962E-04	4.4999947E-04
29.3	5.4999953E-04	5.4999953E-04
33.0	6.4999959E-04	6.4999936E-04
36.7	6.9999951E-04	6.9999928E-04
40.3	7.9999934E-04	6.9999928E-04
44.0	9.4999955E-04	8.9999940E-04
47.7	9.9999947E-04	9.9999923E-04
51.3	1.0999993E-03	1.0499994E-03
55.0	1.1999994E-03	1.1499992E-03
58.7	1.2999992E-03	1.2499990E-03
62.3	1.4499987E-03	1.3999986E-03
66.0	1.5999987E-03	1.5499985E-03
69.7	1.7499982E-03	1.6999978E-03
73.3	1.9999975E-03	1.7999976E-03
77.0	2.1999970E-03	1.9499969E-03
80.7	2.4999958E-03	2.1499961E-03
84.3	2.7499944E-03	2.2999947E-03
88.0	2.9999923E-03	2.5999928E-03
91.6	3.3499897E-03	2.6999912E-03
95.3	3.6999835E-03	3.0499876E-03

READING	MOMENT	TL	BL	TR	BR
1	2.0	0.0	0.0010	0.0010	0.0010
2	4.0	0.0010	0.0010	0.0020	0.0010
3	6.0	0.0010	0.0020	0.0030	0.0010
4	8.0	0.0020	0.0020	0.0040	0.0010
5	10.0	0.0030	0.0020	0.0050	0.0020
6	12.0	0.0040	0.0030	0.0060	0.0020
7	14.0	0.0050	0.0030	0.0080	0.0020
8	16.0	0.0060	0.0040	0.0110	0.0020
9	18.0	0.0080	0.0040	0.0110	0.0030
10	20.0	0.0090	0.0040	0.0120	0.0030
11	22.0	0.0100	0.0040	0.0130	0.0030

12	24.0	0.0120	0.0050	0.0150	0.0030
13	26.0	0.0130	0.0050	0.0160	0.0030
14	28.0	0.0150	0.0050	0.0170	0.0030
15	30.0	0.0160	0.0050	0.0190	0.0030
16	32.0	0.0180	0.0060	0.0190	0.0030
17	34.0	0.0200	0.0060	0.0230	0.0040
18	36.0	0.0220	0.0060	0.0250	0.0040
19	38.0	0.0240	0.0070	0.0270	0.0040
20	40.0	0.0270	0.0070	0.2900	0.0060
21	42.0	0.0290	0.0070	0.0310	0.0060
22	44.0	0.0330	0.0100	0.0340	0.0070
23	46.0	0.0350	0.0120	0.0360	0.0090
24	48.0	0.0390	0.0130	0.0390	0.0110
25	50.0	0.0420	0.0150	0.0420	0.0120
26	52.0	0.0450	0.0190	0.0460	0.0150

MOMENT	A	B
3.7	4.3243228E-05	8.6486471E-05
7.3	8.6486471E-05	1.2972971E-04
11.0	1.2972971E-04	1.7297284E-04
14.7	1.7297284E-04	2.1621601E-04
18.3	2.1621617E-04	3.0270219E-04
22.0	3.0270219E-04	3.4594536E-04
25.7	3.4594559E-04	4.3243193E-04
29.3	4.3243193E-04	5.6216167E-04
33.0	5.1891827E-04	6.0540508E-04
36.7	5.6216167E-04	6.4864825E-04
40.3	6.0540484E-04	6.9189142E-04
44.0	7.3513458E-04	7.7837775E-04
47.7	7.7837775E-04	8.2162116E-04
51.3	8.6486433E-04	8.6486433E-04
55.0	9.0810773E-04	9.5135090E-04
58.7	1.0378370E-03	9.5135090E-04
62.3	1.1243236E-03	1.1675667E-03
66.0	1.2108102E-03	1.2540533E-03
69.7	1.3405394E-03	1.3405394E-03
73.3	1.4702689E-03	1.2799300E-02
77.0	1.5567555E-03	1.5999987E-03
80.7	1.8594575E-03	1.7729709E-03
84.3	2.0324292E-03	1.9459436E-03
88.0	2.2486446E-03	2.1621590E-03
91.6	2.4648597E-03	2.3351309E-03
95.3	2.7675582E-03	2.6378315E-03

READING	MOMENT	RLV	RRV
1	3.7	2.1621614E-05	4.3243228E-05
2	7.3	6.8243229E-05	1.3986474E-04
3	11.0	1.3986474E-04	1.8648629E-04
4	14.7	2.3648620E-04	2.0810787E-04
5	18.3	2.8310763E-04	3.0135084E-04
6	22.0	3.7635071E-04	3.2297242E-04
7	25.7	4.2297249E-04	4.4121570E-04
8	29.3	4.9121561E-04	5.5608060E-04
9	33.0	5.8445893E-04	6.2770210E-04
10	36.7	6.3108047E-04	6.7432364E-04

11	40.3	7.0270197E-04	6.9594523E-04
12	44.0	8.4256707E-04	8.3918846E-04
13	47.7	8.8918861E-04	9.1081019E-04
14	51.3	9.8243169E-04	9.5743174E-04
15	55.0	1.0540534E-03	1.0506751E-03
16	58.7	1.1689181E-03	1.1006750E-03
17	62.3	1.2871611E-03	1.2837825E-03
18	66.0	1.4054044E-03	1.4020258E-03
19	69.7	1.5452688E-03	1.5202686E-03
20	73.3	1.7351331E-03	7.2996467E-03
21	77.0	1.8783761E-03	1.7749977E-03
22	80.7	2.1797251E-03	1.9614827E-03
23	84.3	2.3912117E-03	2.1229684E-03
24	88.0	2.6243180E-03	2.3810752E-03
25	91.6	2.9074233E-03	2.5175605E-03
26	95.3	3.2337699E-03	2.8439090E-03

C PROTOTYPE BC-3

READING	LOAD	DL	DC	DR
1	2.0	0.0030	0.0	0.0030
2	4.0	0.0080	0.0	0.0080
3	6.0	0.0130	0.0010	0.0130
4	8.0	0.0170	0.0010	0.0180
5	10.0	0.0220	0.0010	0.0250
6	12.0	0.0280	0.0010	0.0320
7	14.0	0.0350	0.0010	0.0410
8	16.0	0.0420	0.0020	0.0490
9	18.0	0.0500	0.0030	0.0580
10	20.0	0.0580	0.0040	0.0680
11	22.0	0.0680	0.0060	0.0800
12	24.0	0.0820	0.0080	0.0980

MOMENT	DLR	DCR	DRR
3.7	1.4999998E-04	0.0	1.4999998E-04
7.3	3.9999955E-04	0.0	3.9999955E-04
11.0	6.4999959E-04	4.9999988E-05	6.4999959E-04
14.7	8.4999949E-04	4.9999988E-05	8.9999964E-04
18.3	1.0999995E-03	4.9999988E-05	1.2499993E-03
22.0	1.3999988E-03	4.9999988E-05	1.5999987E-03
25.7	1.7499980E-03	4.9999988E-05	2.0499970E-03
29.3	2.0999971E-03	9.9999990E-05	2.4499949E-03
33.0	2.4999946E-03	1.4999998E-04	2.8999920E-03
36.7	2.8999920E-03	1.9999983E-04	3.3999849E-03
40.3	3.3999849E-03	2.9999949E-04	3.9999746E-03
44.0	4.0999725E-03	3.9999955E-04	4.8999563E-03

MOMENT	ROL	ROR
3.7	1.4999998E-04	1.4999998E-04
7.3	3.9999955E-04	3.9999955E-04
11.0	6.9999951E-04	5.9999945E-04
14.7	8.9999940E-04	8.4999949E-04
18.3	1.1499994E-03	1.1999991E-03

22.0	1.4499987E-03	1.5499985E-03
25.7	1.7999979E-03	1.9999968E-03
29.3	2.1999970E-03	2.3499948E-03
33.0	2.6499946E-03	2.7499921E-03
36.7	3.0999917E-03	3.1999850E-03
40.3	3.6999844E-03	3.6999751E-03
44.0	4.4999719E-03	4.4999532E-03

READING	MOMENT	TL	BL	TR	BR
1	2.0	0.0020	0.0010	0.0020	0.0010
2	4.0	0.0050	0.0020	0.0050	0.0010
3	6.0	0.0070	0.0030	0.0070	0.0020
4	8.0	0.0100	0.0030	0.0100	0.0030
5	10.0	0.0140	0.0040	0.0120	0.0030
6	12.0	0.0170	0.0060	0.0150	0.0040
7	14.0	0.0210	0.0090	0.0180	0.0050
8	16.0	0.0250	0.0110	0.0210	0.0070
9	18.0	0.0300	0.0150	0.0250	0.0080
10	20.0	0.0360	0.0190	0.0280	0.0100
11	22.0	0.0410	0.0230	0.0320	0.0110
12	24.0	0.0500	0.0300	0.0430	0.0130

MOMENT	A	B
3.7	1.2972971E-04	1.2972971E-04
7.3	3.0270219E-04	2.5945925E-04
11.0	4.3243193E-04	3.8918876E-04
14.7	5.6216167E-04	5.6216167E-04
18.3	7.7837775E-04	6.4864825E-04
22.0	9.9459384E-04	8.2162092E-04
25.7	1.2972965E-03	9.9459384E-04
29.3	1.5567555E-03	1.2108102E-03
33.0	1.9459436E-03	1.4270255E-03
36.7	2.3783741E-03	1.6432416E-03
40.3	2.7675582E-03	1.8594575E-03
44.0	3.4594452E-03	2.4216163E-03

READING	MOMENT	RLV	RRV
1	3.7	1.3986474E-04	1.3986474E-04
2	7.3	3.5135075E-04	3.2972940E-04
3	11.0	5.6621572E-04	4.9459399E-04
4	14.7	7.3108054E-04	7.0608058E-04
5	18.3	9.6418848E-04	9.2432369E-04
6	22.0	1.2222962E-03	1.1858097E-03
7	25.7	1.5486472E-03	1.4972952E-03
8	29.3	1.8783761E-03	1.7804024E-03
9	33.0	2.2979677E-03	2.0885076E-03
10	36.7	2.7391817E-03	2.4216119E-03
11	40.3	3.2337699E-03	2.7797148E-03
12	44.0	3.9797053E-03	3.4607835E-03

/END READ---NO MORE DATA CARDS

APPENDIX B

CALCULATIONS OF THEORETICAL MOMENT-ROTATION RELATIONSHIPS

1. Column-to-Base Connections

a) Conditions at yield and ultimate

In order to obtain the degree of fixity of the base arrangement at yield, the yield moment (M_y) of the column must be determined. The problem consists in finding the load, applied at an actual eccentricity of 10 inches, that will make the column yield. The calculations involved are cumbersome and lengthy. Moreover, the terms "yield point load" and "ultimate load" in the case of tied columns are not quite distinct. Previous tests[19,20] have shown that when a tied column is yielding, it means that its ultimate capacity is attained. A more representative estimate of the base fixity would be obtained by comparing the theoretical rotation occurring at the base of the column (when pinned) with the actual column having its base fixed by means of either connection arrangement, at the ultimate design moment level. In any case, the degree of fixity will be referred to as "degree of fixity at yield".

b) Ultimate capacity of the column (USD)

i) Properties of the materials

$f'_c = 4500$ psi

$f_y = 50000$ psi

$w = 145$ lbs./ft.^{3}

$m = f_y / .45\, f'_c = 13.08$

$E_c = w^{1.5} \times 33 \sqrt{f'_c} = 3.87 \times 10^6$ psi

$E_s = 30 \times 10^6$ psi

$n = E_s / E_c = 7.75$

ii) Balanced eccentricity : 8.65 in.

Since actual e = 10 in., tension controls.

iii) Determine P_u

ACI Code formula (19-5):

Ultimate load = P_u = 235 kips

Ultimate moment = $M_u = \frac{235 \times 10}{12}$ = 196 k.-ft.

Ultimate design load = $P_u^i = \quad P_u = .70 \times 235 = 165$ kips.

Ultimate design moment = $M_u^i = \frac{165 \times 10}{12}$ = 138 k.-ft..

c) Corresponding rotations

i) The theoretical rotation at yield (at ultimate design value) is obtained by the Euler formula:

$$d = e \left(\sec \frac{aL}{2} - 1\right)$$

where $a = \frac{P}{EI_t}$

where I_t = moment of inertia (transformed, uncracked section)

The term d is the mid-height horizontal deflection for a pinned-ends column acted on by an eccentric load (eccentricity : e). The formula is applicable in this case under the condition that the stresses in both materials (concrete and steel) are still in their respective range of linear proportionality. (In other words, we are in the region just prior to yield).

for $e = 10$ in., $P = 165$ kips, $I_{tu} = 5675$ in^4.

$d = .550$ in.

And the rotation at the ends = .0046 rad.

ii) The rotation at ultimate is obtained from the compatibility of strains diagram[16]

$$\psi_u = \frac{E_{cu} + E_y}{d} = .000362$$

As the curvature is actually measured over a length of 44 in.

$$\phi_u = \psi_u \times 44" = .01159 \text{ rad.}$$

2. Beam-to-Column Connections

a) Assumptions

i) At yield, the stress in the tension reinforcement equals the yield stress, ($f_s = f_y$).

ii) The compression reinforcement is neglected in the calculations.

b) Conditions at yield and ultimate

The moments at yield and ultimate are obtained by using Mattock's analysis.[16]

i) Properties of the materials

$f'_c = 4000$ psi ; $w = 145$ lbs./ft.^{3} ; $E_c = 3.65 \times 10^6$ psi

$f_y = 50000$ psi ; $E_s = 30 \times 10^6$ psi

$n = E_s/E_c = 8.22$

$$M_y = \frac{1}{2} f_c \, kbd \, (1 - k/3)$$

$$M_u = bd^2 \left[p f_s \left(1 - \frac{k_2 \, p f_s}{k_1 k_3 f'_c} \right) \right]$$

c) Rotations at yield

The rotations at yield are computed by the conjugate beam method.[17] The rotation at 40 in. from the support (where it is measured in the laboratory) is obtained by computing the shear force at the same distance, in the conjugate system.

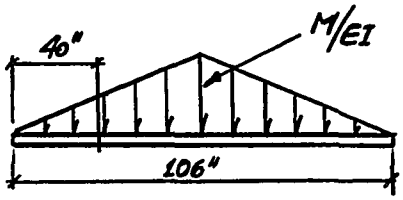

$$T_{40} = \frac{11.4 \, M}{EI} \, (x \, 12 \, x \, 10^3)$$

d) The rotations at ultimate

The rotations at ultimate are obtained from the compatibility of strains diagram

$$\psi_u = \frac{E_{cu} + E_y}{d}$$

$$\phi_u = \psi_u \, x \, 40"$$

e) Sample calculation

for the case of BC-1a

i) Yield

$$M_y = 189 \text{ k. ft.}$$

$$\phi_y \, (40") = 14.26 \, x \, 10^{-4} \text{ rad}$$

ii) Ultimate

$$M_u = 213 \text{ k. ft.}$$

$$\Phi_u = \psi_u \times 40'' = 10.2 \times 10^{-3} \text{ rad.}$$

A table summarizing all the calculations follow.

THEORETICAL M- CALCULATIONS			
f_y = 48900 psi ; f'_c = 4000 psi ; E_s = 30 x 10^6 psi ; E_c = 3.65 x 10^6 psi			
k_1 = .85 ; k_2 = .425; k_3 = .85	BC-1c	BC - 2	BC - 3
b x d	12" x 18.5"	9" x 14"	7.5" x 10"
A_s	3.14 in^2	2.37 in^2	1.67 in^2
I_{tu}	4968 in^4	1780 in^4	670 in^4
f_c	2260 psi	2490 psi	2680 psi
k	.613	.734	.815
M_y	189 k.-ft.	100 k.-ft.	49.6 k.-ft.
M_u	213 k.-ft.	116 k.-ft.	57.3 k.-ft.
$\Phi_{y(40")}$	14.3×10^{-4}	21×10^{-4}	27.7×10^{-4}
Φ_u	102×10^{-4}	134×10^{-4}	188×10^{-4}

APPENDIX C

ULTRASONIC PULSE TEST

The ultrasonic pulse test was developed in an attempt to measure, in a non-destructive manner, some physical properties of concrete. The method is particularly effective in estimating the quality of concrete and in detecting the development of cracks in structures and to check deterioration due to frost or chemical action.

The apparatus consists of a transmitter driver and of a piezo-electric crystal transducer emitting vibrations at its fundamental frequency. The transducer is in contact with the concrete, so that the vibrations travel through it and are picked up by another transducer in contact with the opposite face of the specimen under test. The wave velocity is determined directly from the time taken by a pulse to travel a measured distance ; in our case, one foot, the thickness of the specimen.

The purpose of this test was to evaluate the damage due to welding of embedded steel elements between precast concrete units. It was expected that the heat produced by the welding would result in the development of cracks in the concrete, both on the surface and in the volume of the specimen. The ultrasonic test will detect the cracks by a decrease in the velocity of sound propagation.

Welding was performed on three specimens; fillet size of 1/4", 3/8" and 1/2" were applied, each fillet resulting in a different temperature gradient that had to be dissipated throughout the section. A fourth cube was used as a control specimen and had no welds.

It is observed from the curve that a 8% variation in the ultrasonic velocities were obtained between the most severely heated specimen and control. The results show that the physical properties of concrete have been altered to an extent which is negligible.

Furthermore, inspection of the beam-to-column connections after failure did not reveal any apparent damage due to the heat developed during welding..

ULTRASONIC PULSE TEST

SPECIMENS : 12" x 12" x 12" CONCRETE CUBES (4)

12" x 4" x 1/2" STEEL PLATES

EMBEDDED IN SECTION

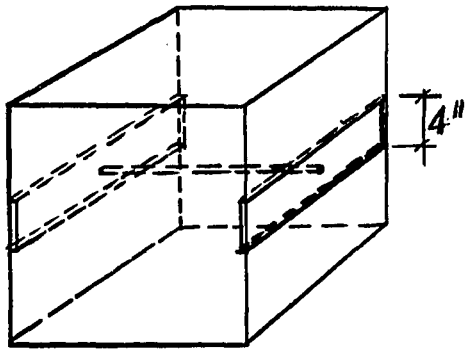

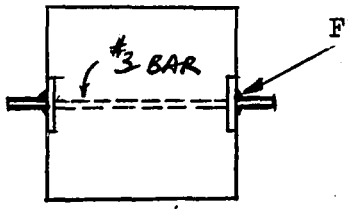

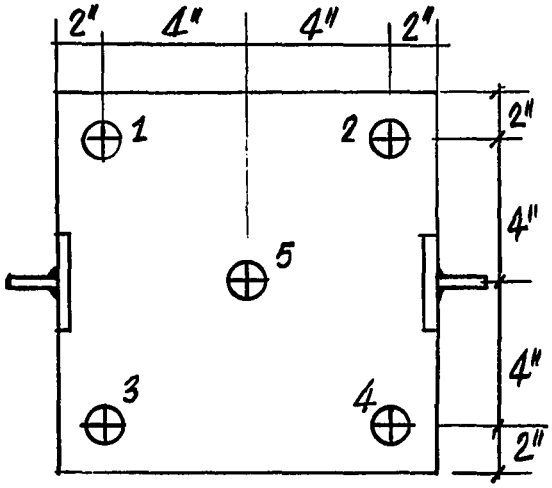

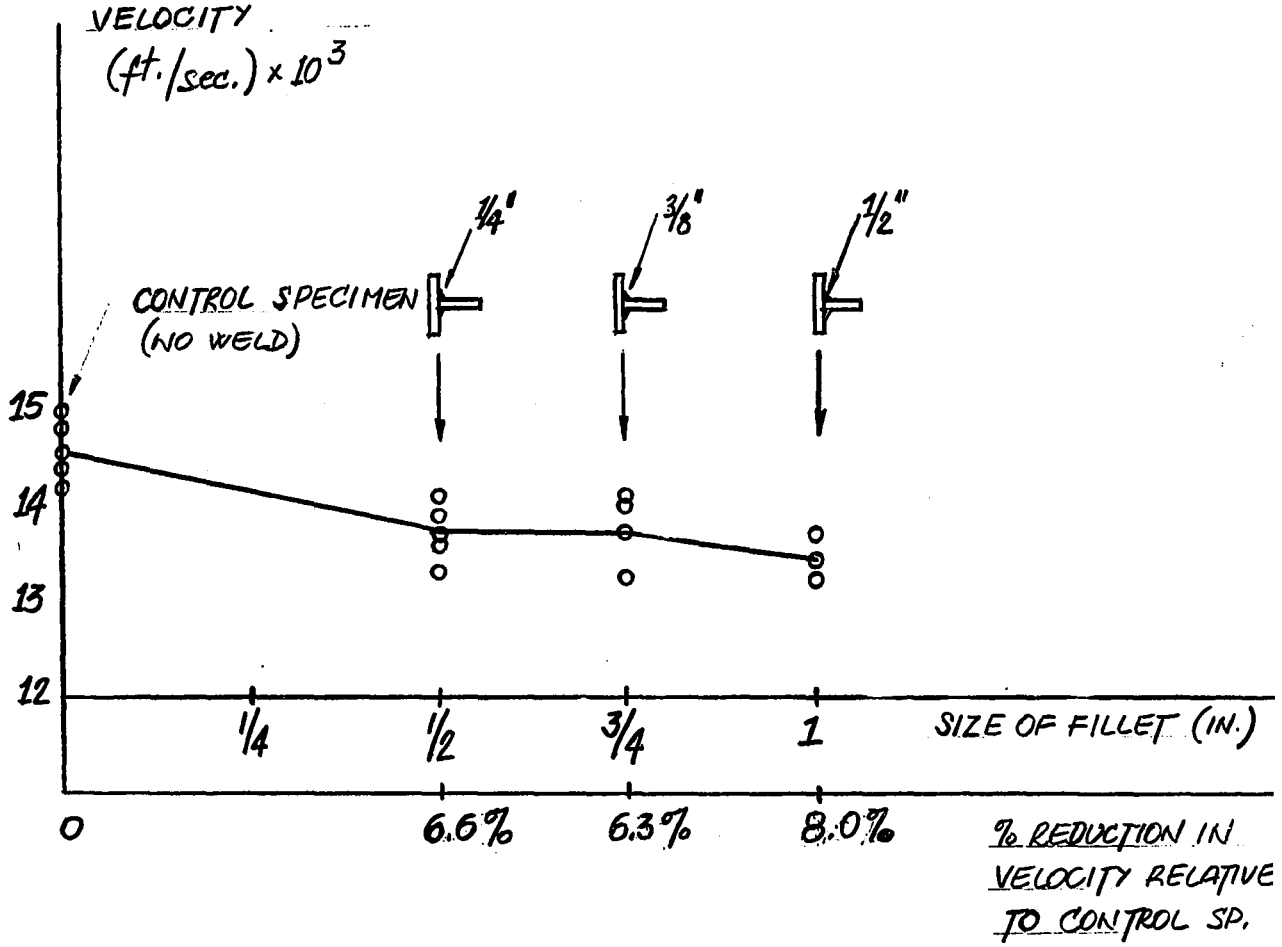
VELOCITY
(ft./sec.) x 10^3
1/4"
3/8"
1/2"
CONTROL SPECIMEN
(NO WELD)
15
14
13
12
1/4
1/2
3/4
1
SIZE OF FILLET (IN.)
0
6.6%
6.3%
8.0%
% REDUCTION IN VELOCITY RELATIVE TO CONTROL SP.

APPENDIX D

MATERIAL PROPERTIES

1. Tension Tests

Within the welding test program, tension tests were conducted on a number of 3/4" diameter deformed bars (50,000 psi) on which different welding intensities were applied. The purpose of this investigation was to detect any structural deficiencies in the material resulting from the heat developed by the welding.

Tension tests were performed on two bars without welds, two bars on which continuous welding was performed and two bars subjected to spotwelding only. The measurements were taken over a 8 in. gage length, on which the welding was applied. The results are presented in the following table and stress-strain curves are plotted using the average of the two readings. It is noticed that while the yield stress is approximately the same for the three cases, the ultimate strain is reduced by 40% in the case of continuous welding and by 65% for spotwelding application.

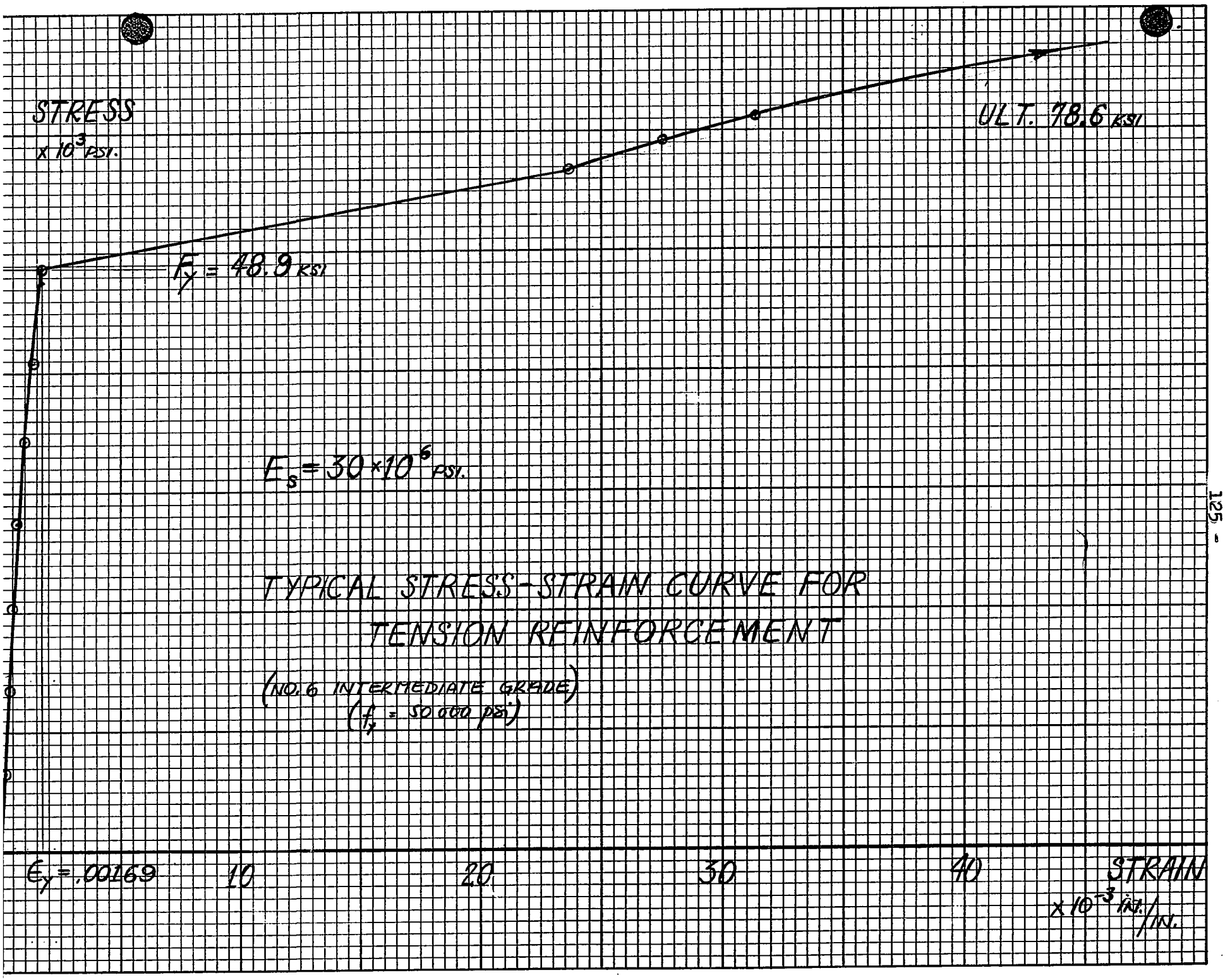
STRESS
x 10³ PSI.
ULT. 78.6 KSI
F_y = 48.9 KSI
E_s = 30 x 10⁶ PSI.
TYPICAL STRESS-STRAIN CURVE FOR
TENSION REINFORCEMENT
(NO. 6 INTERMEDIATE GRADE)
(f_y = 50 000 psi)
ε_y = .00169
10
20
30
40
STRAIN
x 10⁻³ in./in.

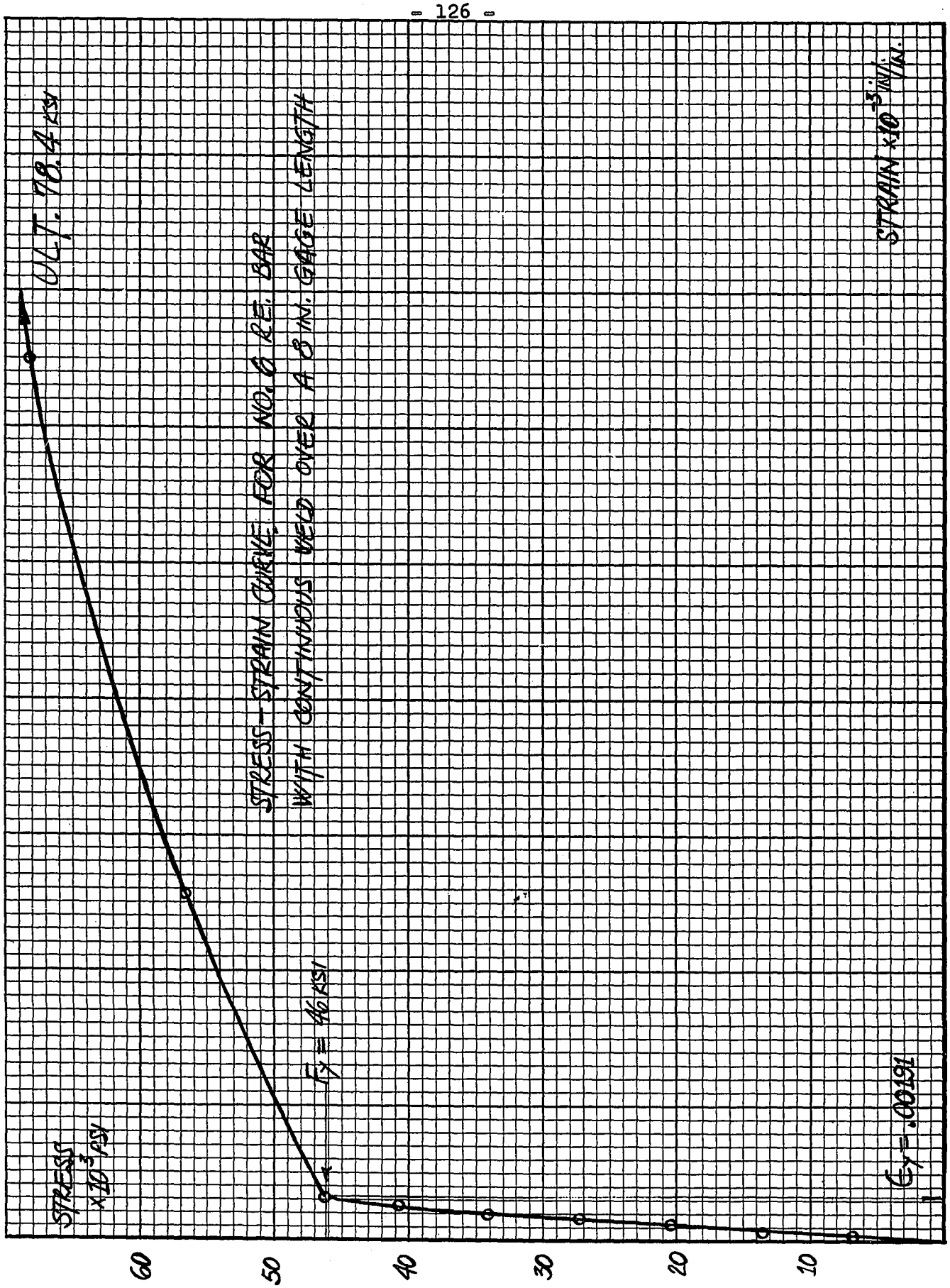
STRESS-STRAIN CURVE FOR NO. 6 RE. BAR
WITH CONTINUOUS WELD OVER A 8 IN. GAGE LENGTH
F_y = 46 KSI
U.T. 78.4 KSI
ϵ_y = .0021
STRESS x 10^3 PSI
STRAIN x 10^{-3} IN/IN.
60
50
40
30
20
10
10
20
30
40

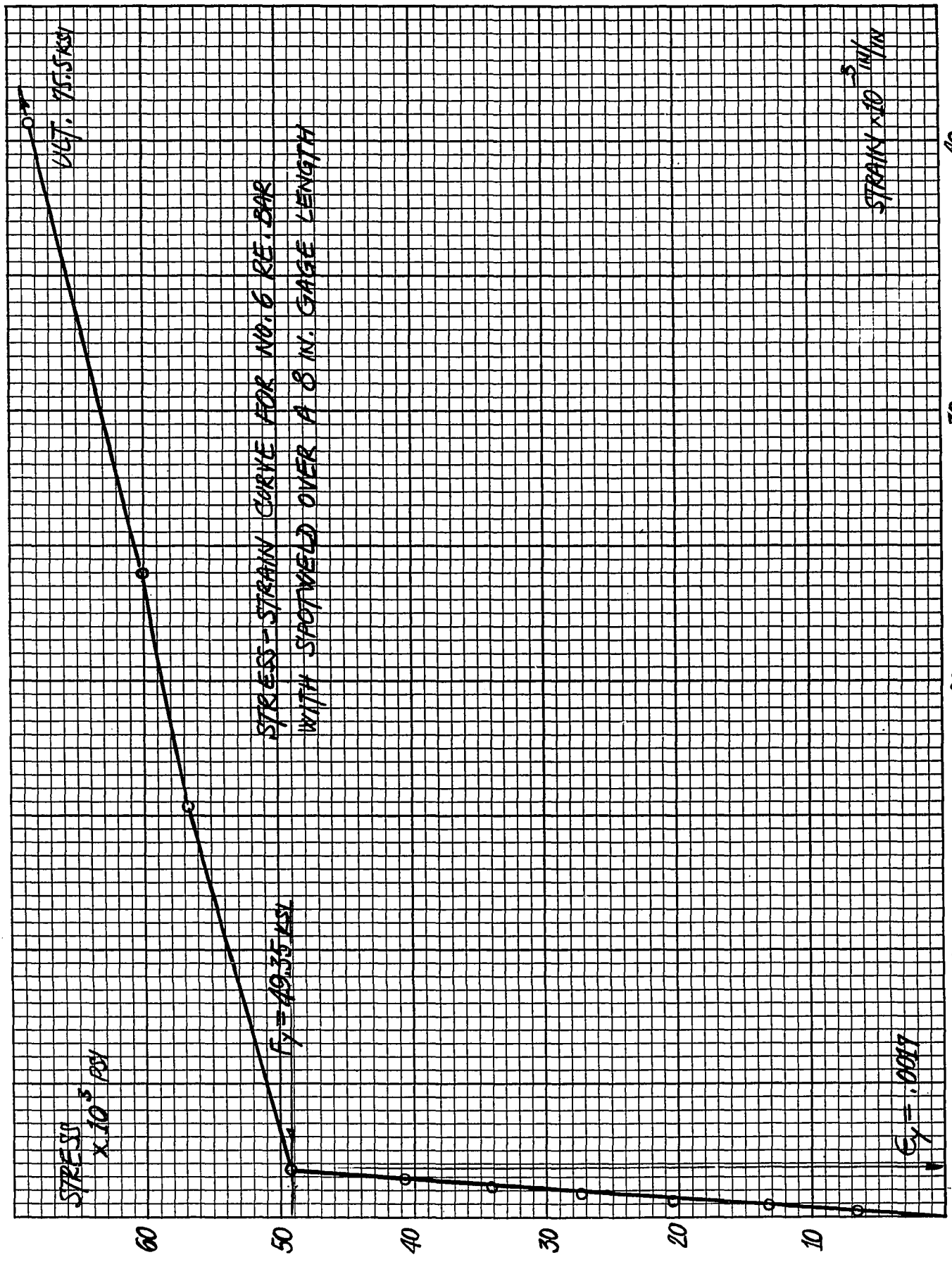
STRESS-STRAIN CURVE FOR NO. 6 RE. BAR
WITH STOTMEID OVER A 8 IN. GAGE LENGTH
f_y = 49.35 KSI
ULT. 75.5 KSI
ϵ_y = .0017
STRESS x 10^3 psi
STRAIN x 10^{-3} in/in
60
50
40
30
20
10
10
20
30
40

2. Compression Tests on Concrete Cylinders

For each prototype tested, the value of the compressive strength was obtained by taking the average crushing force of three 6 in. x 12 in. cylinders. The results are tabulated below.

COMPRESSIVE STRENGTH (f'_c = psi)							
	C.-B. TYPE I	C.-B. TYPE II	B-C1a	B-C1b	B-C1c	B-C2	B-C3
CYLINDER NO. (6" x 12")	(28 Days)	(28 days)	(28 days)	(7 days)	(7 days)	(7 days)	(7 days)
No. 1	4060	5060	2800	5150	2180	2700	3820
No. 2	4175	5835	3330	4950	3900	3500	3890
No. 3	5200	4525	3500	5100	3070	3600	3960
Av.	4480	5140	3210	5070	3350	3600	3900
	GROUT CYLINDERS PAD	(3"x6")					
No. 1	4700	4850					
No. 2	4900	4600					
No. 3	5925	5450					
Av.	5170	4970					